UNIVERSITY OF CALIFORNIA
RIVERSIDE

Gene Regulatory Machinery and Proteomics of Sexual Reproduction in *Phytophthora infestans*

A Dissertation submitted in partial satisfaction
of the requirements for the degree of

Doctor of Philosophy

in

Plant Pathology

by

Xiaofan Niu

December 2010

Dissertation Committee:
Dr. Howard Judelson, Chairperson
Dr. Katherine Borkovich
Dr. Thomas Eulgem

The Dissertation of Xiaofan Niu is approved:

_____

_____

_____

Committee Chairperson

University of California, Riverside

Acknowledgements

I would like to express my greatest appreciation to my major advisor, Dr. Howard Judelson, for his guidance, support and endless patience. His adventurous and rigorous scholarship has reshaped my viewpoint in regard to both research and social life. Without his guidance and persistent help, this dissertation would not have been possible.

I would also like to thank my committee members, Dr. Katherine Borkovich and Dr. Thomas Eulgem, for their valuable advice, encouragement and support in the course of completing this dissertation. I would like to give my special thanks to Dr. Sonqin Pan, the academic coordinator of CEPCEB W.M. Keck Proteomics Core Facility, for his effort in helping me in the proteomics study.

I am grateful to all the past and current members of the Judelson lab for sharing their experience and knowledge, and their unforgettable friendship. My gratitude also goes to all the faculty, staffs and fellow students in the department for their help, encouragement and friendship.

A huge thank you is going to my beloved parents for their infinite love, support and patience. Without them, I would not have been able to accomplish what I did. Last but least, I want to thank to other my family members and friends their help and moral support.

ABSTRACT OF THE DISSERTATION

Gene Regulatory Machinery and Proteomics of Sexual Reproduction in *Phytophthora infestans*

by

Xiaofan Niu

Doctor of Philosophy, Graduate Program in Plant Pathology
University of California, Riverside, December 2010
Dr. Howard Judelson, Chairperson

Mating is important for the survival of *Phytophthora infestans*, the causal agent of potato and tomato late blight. The mating process increases population fitness and produces thick-walled oospores that can survive harsh environmental conditions. To better understand the mechanisms that regulate of sexual reproduction in *P. infestans*, the promoters of two mating-induced genes, PITG_002525 and PITG_00483, were studied in order to identify their *cis*-regulatory elements. PITG_02525 encodes an elicitin-like protein, and PITG_00483 encodes a PUMILIO (Pum) protein. The promoter of PITG_02525 was sequentially deleted and fused with a β-glucuronidase reporter gene to identify its regulatory motifs. The full length promoter was found to be active in young and mature, and male and female, structures. The deletion analysis identified a potential repressor element and an activator. Similar studies of the *pum* promoter showed expression both during oosporogenesis and sporulation. One promoter element was found to be essential for the expression of the gene in both stages. Fusing this element with a

minimal promoter indicated that it was sufficient for gene expression during sporulation, but not in mating. The RNA binding domain (RBD) of Pum then was used as a model to develop a system for *P. infestans* protein interaction studies. Expression of the RBD with a tandem affinity purification tag designed with *P. infestans* codon bias, allowed the successful purification of the Pum RBD with a potential binding partner. This system is adaptable for future studies of other protein interactions. A MudPIT global proteomics comparison of oospores with nonsporulating hyphae (NSH) was then conducted to profile the protein composition of oospores and identify important proteins for germination. It was proposed that the proteins detected in dormant oospores were synthesized during early oosporogenesis and stored for germination. Our study identified proteins that are more abundant in oospores belonging to several functional groups. These included enzymes involved in carbohydrate and fatty acid oxidation to produce energy, and anti-oxidant and anti-stress proteins that may protect the germ tubes, and secreted proteins that could be involved in host infection. This revealed that *P. infestans* has a very well designed life cycle.

Table of Contents

List of Figures

CHAPTER I Characterization of regulatory elements determining the expression pattern of two mating-induced genes in *Phytophthora infestans*

CHAPTER II Developing the tandem affinity purification system for protein interaction studies using a translational regulator, PUMILIO

CHAPTER III Comparative proteomics study of oospores and nonsporulating hyphae of *Phytophthora infestans*

List of Tables

Introduction

The Oomycetes

Oomycetes are referred to as water mold due to their general preference for high humidity and free water. They constitute a large collection of species that include saprophytes and important pathogens of plants, vertebrates, insects, fish and microbes. The most important morphological feature of the group is the production of sexual spores, known as oospores, by the union of two gametangia, oogonium and antheridium, in which meiosis occurs before fertilization (Erwin & Ribeiro, 1996). Despite having other similar morphological features to true fungi, such as hyphae and spores, oomycetes are classified as heterokonts, a group which includes brown algae and diatoms (Hawsworth et al., 1995). This taxonomic relatedness is supported by both genetic and biochemical evidence (Gunderson et al., 1987). Oomycetes are diploid during the vegetative stage while true fungi are haploid. The cell wall of oomycetes is primarily composed of cellulose instead of chitin, and generally does not have septations. Oomycota and fungi have different metabolic pathways, distinct rRNA sequences, storage compounds, and ultrastructural characteristics (Bartnicki-Garcia & Wang, 1983; Alexopoulos et al., 1996; Forster et al., 2000). These differences are the reasons why many fungicides are effective against true fungi but not oomycetes. Crop protection from oomycetes is usually accomplished by integrating environmental manipulation, cultural practices, and fungicide treatments together (Inglis, 2004). Cultivation strategies including selecting

resistant cultivars, using healthy seed and transplants as well as soil managements to ensure vigorous plant growth are important. These strategies are incorporated into other cultural practices, which include arranging plant spacing, avoiding mechanical damage, and controlling weeds and wound-causing insects. Chemical use is also one of the most commonly applied strategies, especially in fruit and vegetable production (Inglis, 2004). Pesticides are most likely to succeed if used for seed treatment or on foliage before infection. Currently, there are very few oomycete pesticides that have curative effects, for example mefenoxam and dimethomorph, and oomycetes are reported to have quickly developed resistance against those that are available (Gisi & Cohen, 1996;DeMuth et al., 1995).

Phytophthora and *Phytophthora infestans*

The genus *Phytophthora,* the "plant destroyer", is one of the most important groups of oomycetes. It contains over 100 species and all are plant pathogens causing serious damage. Major diseases caused by *Phytophthora* consist of: leaf blights, damping off, fruit rots, root rots, and stem rots (also known as foot, crown, collar, or trunk rots). Some of the species have narrow host ranges, such as *P. infestans,* pathogenic only to Solanaceae family, and *P. sojae,* which only infects soybean plants. Some other species have a very broad host range. For example, *P. cinnamomi* has been reportedly identified from over 900 hosts (Zentmyer, 1980), and *P. palmivora* (Chee, 1969) is capable of infecting more than 130 different hosts. Due to the economic significance of

Phytophthora, and the needs for developing tools for model organisms, the genomes of several of the best studied species have already been sequenced. *P. sojae* and *P. ramorum* were sequenced by JGI (http://genome.jgi-psf.org/Physo1_1/Physo1_1.home.html, and http://genome.jgi-psf.org/Phyra1_1/Phyra1_1.home.html), and *P. infestans* sequencing was completed by the Broad Institute of MIT and Harvard (http://www.broadinstitute.org/annotation/genome/phytophthora_infestans/MultiHome.html). Genome assemblies and annotation of *P. capsici* and *Hyaloperonospora arabidopsidis* are also being completed.

Phytophthora infestans is arguably the most notorious plant pathogen in history. *P. infestans*, the first member identified in the oomycete group, was given its name by Heinrich Anton de Bary in 1876 (Erwin & Ribeiro, 1996). It is the causal agent of potato late blight. In the field, pale green water soaked lesions start showing at the margins and tips of leaves, and grow into a brown or purple-black leisons. In favorable weather with high humidity, a white layer of mycelia can be seen on the underside of the leaves. Lesions can also appear on the stem and these eventually kill the plant foliage above the lesions. Infected tubers are shrunken outside with brown or purplish lesions and reddish dry rot inside. These tubers often have secondary infections. Diseased tubers are completely inedible and cannot be used as seeds.

P. infestans is best known for being responsible for causing the Irish potato famine in 1846-1847 (Bourke, 1964). It was hypothesized that a single clonal line of *P. infestans* migrated from Mexico to the northeastern United States in 1842 to 1843 and from there to Europe in 1845 and became an international problem (Goodwin et al.,

1994b). The disease epidemic in Ireland resulted in approximately one million deaths and a million emigrants. It has remained one of the most economically important plant diseases ever since that time by causing significant losses of yield, the need for extensive fungicide usage, and postharvest loss. The cost of the damage caused by *P. infestans* annually is estimated to be five billion dollars (Erwin & Ribeiro, 1996; Smart & Fry, 2001).

P. infestans serves as a model organism for oomycetes because of its experimental accessibility. Since the release of its complete genome sequence, studies of the pathogen have been significantly accelerated. A genome database with eight-fold sequencing coverage and over 100 k of expressed sequence tags (ESTs) generated from different developmental stages can be accessed via the Broad Institute website (Kamoun et al., 1999; Randall & Judelson, 1999; Haas et al., 2009). The *P. infestans* genome is about 240 Mb in size, and 17,797 protein coding sequences have been identified. The majority of the genome (~74%) consists of repetitive DNA that probably results from the diverse families of effector proteins. Studies have revealed the conservation of the core proteome that consists of genes involved in DNA replication, transcription and protein translation among the three published *Phytophthora* genomes, *P. infestans*, *P. sojae* and *P. ramorum* (Ebstrup et al., 2005; Savidor et al., 2008).

Transcriptome profiles of asexual and sexual developmental stages of *P. infestans* using Affymetrix GeneChips and NimbleGen chips are available for screening genes that are significant for each stage (Haas et al., 2009; Judelson et al., 2008; Prakob & Judelson, 2007). Expression of 8,509 genes in hyphae, 8,975 in sporangia, 8,484 in

cleaving sporangia, 7,295 in zoospores, and 7,856 in germinated cysts and appressoria were detected. About half the *P. infestans* genes showed significant differential expression during the transitions between developmental stages, with approximately 10% being stage-specific and most changes occurring during zoosporogenesis (Judelson et al., 2008). 87 genes were found to be up-regulated more than 10-fold during mating, with 28 of them induced over 100-fold (Pracob & Judelson, 2007). Potential crosstalk between asexual and sexual reproduction was suggested by genes present in both groups. Comparison with a homothallic species *P. phaseoli* revealed that part of the sexual pathway is active constitutively in homothallics (Pracob & Judelson, 2007). During infection of the host, 494 genes were induced at least two-fold. The most highly upregulated of these included 79 RXLR proteins, apoplastic effecter genes including protease inhibitors, cysteine-rich secreted proteins, and NPP1-family members (Haas,et al., 2009).

Sexual reproduction in *P. infestans*

Both asexual and sexual reproduction stages of *P. infestans* have been observed and described in the natural environment and in research laboratories (Erwin & Ribeiro, 1996). *P. infestans* is heterothallic, which means that it needs two compatible mating types to sexually reproduce. These mating types are referred to as A1 and A2 (Brasier, 1992). Formation of gametangia can be triggered by the hormones from the opposite mating type. Aged cultures, physical damage, and *Trichoderma viride* were also shown to

be effective in stimulating oospore production (Braisier, 1971; Reeves & Jackson, 1974; Smart et al., 2000). In addition, some self-fertile strains have been identified, with lower oospore production than from a traditional A1/A2 cross (Fyfe & Shaw, 1992), and it has been reported that the first germinating oospores more commonly arise from parental hybrids (Fry, 2008). Both A1 and A2 mating types can act as male and female, and there is a tendency for one strain to be either male or female (Judelson, 1997). Oospore production has been successfully induced using the opposite mating type from a different species (Skidmore et al., 1984) and purified mating hormones from other species (Qi et al., 2005).

When sexual reproduction is triggered, differentiation starts with tissue swelling, which will further develop into male or female gametangia (antheridia and oogonia), followed by the occurrence of meiosis in those structures (Elliott, 1983). Antheridia of *P. infestans* are amphigynous. Oogonia are 35-45 µm in diameter, antheria are 12-20 µm in length and oospores measure from 24 to 56 µm in diameter (Ho, 1981). Oospore wall formation initiates in the periplasm where cisternae condense to form a thin outer wall when the periplasmic cytoplasm degenerates. The outer wall is composed of several 20 nm-thick dense layers and the number of layers varies from one to five. Inside the outer wall, there is a thick inner oospore wall (0.7 to 1 µm). The inner wall consists mainly of 1, 3-beta glucan rather than cellulose (Beakers & Bartnicki-Garcia, 1989). The thick walls of oospores play important roles not only in resistance to unfavorable environmental conditions, but also in energy storage for the germination process. The metabolism of mature oospores is slowed down to a very low level.

The viability of the oospore can be affected by many factors including genetics and nutritional status (Elliott, 1983; Rutherford and Ward 1985). The percentage of oospore germination is consistently low, so viability tests are usually done before germinating oospores in the laboratory. Viability can be evaluated by tetrazolium bromide stain (MTT) (Sutherland & Cohen, 1983). Viable oospores were stained in a rosy-pink color, and non-viable ones were stained black.

Oospores germinate erratically or stay dormant (Sussman, 1966). Dormancy was distinguished by Sussman into two types: constitutive dormancy and exogenous dormancy. Constitutive dormancy is due to innate properties such as metabolic pathway blockage or production of a self-inhibitor. This type of dormancy can be broken by cold or alternating warm and cold treatments, short heat shock, or treating with chemicals such as detergents and organic acids (Griffin, 1981). Exogenous dormancy is usually caused by unfavorable chemical or physical environmental factors. Some microbes in the soil may also play a role in dormancy.

After receiving the appropriate stimuli, oospores usually germinate and form single or multiple germ tubes, and develop into either diploid A1 or A2 hyphae (Kronstad & Staben, 1997), which then enter the asexual cycle. Germination is usually affected by physical, chemical, and biological factors.

The role of sexual reproduction in the historical distribution of *P. infestans*

It was discovered that the populations of *P. infestans* in the Toluca Valley of Mexico were significantly different from those in other locations. Also, unlike elsewhere, the A1 and A2 mating types existed in equal frequencies in the Toluca Valley, which is thought to be the origin of all *P. infestans* seen throughout the world today (Goodwin et al., 1992), and no clonal lineage dominated the population (Flier et al., 2003). In contrast, until the mid 20th century, the population of *P. infestans* across Europe, Asia, South America, and North America was dominated by a single clonal lineage—the US-1 lineage (Goodwin et al., 1994b), which was the A1 mating type.

After detection of the A2 mating type outside of Mexico in the 1950s, the sexual stage of *P. infestans* was observed in most European countries and in North America by the 1980s (Hohl & Iselin, 1984; Shattock et al., 1990). This has led to changes in the global *P. infestans* population structure. The switch of the European *P. infestans* population was explained by a massive shipment of infected potato tubers from Mexico in the winter of 1976/77 (Niederhauser, 1991), and the North American population most likely changed during the 1980s to early 1990s due to shipments of infected tomatoes (Goodwin et al., 1994a). These changes were illustrated in studies of isozyme variation (Spielman et al., 1991) and RLFP DNA fingerprinting (RG-57) (Drenth et al., 1994) that showed a marked increase in variation when comparing isolates sampled before and after the early 1980s. This change was also evident in a shift in the frequency of virulence factors (Drenth et al.. 1994).

In locations where sexual reproduction occurs, oospores clearly contribute to survival through the winter or under stressful conditions. Sexual reproduction also increases the population diversity of the pathogen. Oospores contain thick multilayered cell walls and are rich in lipids, proteins, and vacuoles, and persist much longer than asexual spores. By allowing the exchange of the genetic traits, sexual reproduction diversifies the population and produces more competitive and aggressive strains, as the pathogen's fitness is enhanced. Disease epidemics in some parts of northern Europe were reported to begin earlier in the season when initiated by oospores (Andersson et al., 1998; Flier et al., 2007). In North America, oospores were found to have viabilities greater than 50% when exposed to temperatures of -20 and -50 ℃ for up to 90 days, whereas viabilities ranged from 23 to 36% with exposure to 0, 4, or 15 ℃. When the temperature rose to 36 ℃, the lowest viability, 22%, was observed (Medina & Platt, 1999). This finding demonstrated that oospores not only can survive the winter conditions in northeastern North America but can also germinate and infect new potato tissue in the following growing season.

Asexual reproduction cycles of *P. infestans*

Asexual spores are the major means of disease epidemic initiation and also serve as secondary infection during the disease season. The asexual life cycle of *P. infestans* usually starts from deciduous sporangia carried by wind or free water to available hosts. Sporangia contain multiple nuclei, and remain metabolically active. Sporangia have two

pathways for germination, which is a common feature in oomycetes. In cool, damp conditions, when the temperature is below 12 ℃, sporangia germinate indirectly. The sporangial cytoplasm cleaves into 8 to 12 biflagellated uninucleate zoospores. This process is also called zoosporogenesis. Zoospores are able to swim to nearby hosts with the aid of chemotaxis and/or electrotaxis (Deacon & Donaldson, 1993; Hill et al., 1998). In response to physical or chemical stimuli, zoospores can lose their flagella and encyst. Cysts produce adhesive proteins to help themselves attach to the host. A germ tube will be produced by the cyst and an appresorium will be developed at the tip of the germ tube to penetrate the host cell walls. Mycelia grow intercellularly, and produce haustoria to absorb the nutrients from the cell without breaking the cell membrane. If the temperature is above 14 ℃, then sporangia primarily undergo the other pathway, which is direct germination. After landing on the host, sporangia produce germination tubes without being cleaved into zoospores, and mycelia will grow inside the host tissue.

Sporulation of *P. infestans* can be affected by many factors, including aeration, nutrients, light, temperature, pH, ions, humidity, and other microorganisms present in the environment (Mitchell & Zentmyer, 1971; Ribeiro, 1983).

P. infestans as an experimental model

P. infestans has several advantages as a model for studying oomycete biology and their genetic and molecular interactions with host plants. *P. infestans* has a well defined life cycle, and is easily cultured *in vitro*. Both the asexual and sexual stages can

occur on agar culture plates. The asexual spores, which are the main inocula for disease epidemics, can be easily purified. Many molecular tools for this microorganism have also been developed. Stable transformants of *P. infestans* can be obtained using protoplast, microprojectile bombardment, electroporation, or *Agrobacterium* (Judelson, 1993; Van West et al., 1999; Cvitanich & Judelson, 2003; Vijn & Govers, 2003). Together with another five published or soon to be released genome sequence databases of related species, *P. ramorum*, *P. sojae*, *P. capsici*, *H. arabidopsidis*, and *Pythium ultimum*, molecular genetics studies of *P. infestans* have been accelerated significantly.

Aims of the study

In the long term, we aim to use *P. infestans* as our model to find ways to control oomycetes, a group of economically significant pathogens, and protect crops from them in financially and environmentally friendly ways. In order to do that, knowledge of the biology, genetics, and regulatory pathways of the pathogen is required. However, much is yet to be known about the biology of oomycetes despite their importance. In many true fungi regulatory proteins such as transcription factors, enzymes, and kinases have been well studied and many signal transduction pathways have been identified, however in oomycetes these are still poorly understood. Improved knowledge of oomycete molecular biology may provide us with potential targets to develop pesticides or resistant cultivars to manage the pathogens. It was reported that sexual reproduction of *P. infestans* has negative cross-talk with the asexual reproduction stage, which provides the major

inoculum for disease epidemics (Bonde, 1982; Fabritius et al., 2002). With the variable dormancy and low germination rate of oospores, the stimulation of sexual reproduction may reduce the amount of asexual spores in the field and significantly lower the viable inoculum. Disease cycles may thus be interrupted or manipulated by encouraging sexual reproduction.

In order to decipher the mechanisms involved in the regulation of sexual reproduction in *P. infestans*, understanding the temporal and spatial expression patterns of some genes that are activated or induced specifically at this stage, and the transcription factors that regulate the expression of these genes, is essential. Understanding the function of proteins that are present during the sexual reproduction stage also provides knowledge of the pathways and factors necessary to enter the sexual stage. My dissertation focuses on the regulation of gene expression and the proteomics of the sexual reproduction stage.

Chapter I describes the characterization of the transcriptional regulatory components in the promoters of two mating-induced genes, PITG_02525 and PITG_00483. PITG_002525 encodes an elicitin-like protein. Its expression is up-regulated by 100-fold during mating, and is defined as mating specific. PITG_00483 encodes a PUMILIO (Pum) protein, which belongs to the Puf family of RNA binding proteins. This gene is expressed in both oospores and asexual sporangia, thus it might be an essential gene for the reproduction of *P. infestans*. Sequential promoter deletions, and sequence fusions with a non-functional minimal promoter were employed to identify the

functional motifs of these mating-induced genes. This study was planned to improve our understanding of the regulatory machinery involved n sexual reproduction.

Chapter II focuses on developing tools for protein interaction assays using the Pum RNA-binding-domain (RBD). To identify the RNA substrates and the protein binding partners of this RNA-binding protein, cloning constructs for *in vitro* and *in vivo* binding assays were generated and transformed into *P. infestans*. The *in vitro* binding assay was performed using maltose-binding protein-tagged RBD and total RNA *in vitro*. The purified RNA was analyzed by the differential display method and cDNA library construction. The *in vivo* binding assay was accomplished by fusing the RBD with a tandem affinity purification (TAP) and transformating the construct into *P. infestans*. The binding of RBD and its target RNAs would occur *in vivo*, and then the whole RBD-RNA complex was purified. The TAP-tag was designed according to *P. infestans* codon bias, and contains one calmodulin-binding domain and two protein A domains. These expression systems will provide valuable tools for future studies of protein interactions in *P. infestans*.

Chapter III presents a global comparative protein profiling study of the proteomes of oospores and nonsporulating hyphae. Proteins extracted from oospores and nonsporulating hyphae of mating type A1 and A2 were analyzed by multidimensional protein identification technology (MuDPIT), and iTRAQ labeling was used for protein quantification. By identifying stage-specific proteins or proteins upregulated or downregulated in oospores, this comparative proteomics study brings us insights into candidate proteins that are important for oospore survival and germination.

References

Alexopoulos, C. J., C. W. Mims, and M. Blackwell (1996). Introductory Mycology. Wiley, New York.

Andersson, B., M. Sandstrom, and A. Stromberg (1998). "Indications of soil borne inoculum of *Phytophthora infestans*." Potato Res **41**: 305-310.

Bartnicki-Garcia, S. and M. C. Wang (1983). Biochemical aspects of morphogenesis in *Phytophthora*. *Phytophthora*, its biology, txonomy, ecology, and pathology. D. C. Erwin, S. Bartnicki-Garcia and P. H. Tsao. St. Paul, Minnesota, APS Press**:** 121-137.

Beakers, G. W. and S. Bartnicki-Garcia (1989). "Ultrastructure of mature oogonium-oospore wall complexes in *Phytophthora megasperma*: a comparison of *in vivo* and *in vitro* dissolution of the oospore wall." Mycol Res **93**: 321-334.

Bourke, P. M. A. (1964). "Emergence of potato blight, 1843-46." Nature **203**: 805-808.

Braisier, C. M. (1971). "Induction of sexual reproduction in single A2 isolates of *Phytophthora* species by *Trichoderma viride*." Nat New Biol **231**: 283.

Brasier, C. M. (1992). "Evolutionary biology of *Phytophthora* Part I. Genetic system sexuality and the generation of variation." Annu Rev Phytopathol **30**: 153-171.

Chee, K. H. (1969). "Hosts of *Phytophthora palmivora*." Rev Apple Mycol **48**: 337-344.

Cvitanich, C. and H. S. Judelson (2003). "Stable transformation of the oomycete, *Phytophthora infestans*, using microprojectile bombardment." Curr Genet **42**: 228-235.

Deacon, J. W. and S. P. Donaldson (1993). "Molecular recognition in the homing responses of zoosporic fungi, with special reference to *Pythium* and *Phytophthora*." Mycol Res **97**: 1153-1171.

Drenth, A., I. C. Q. Tas, and F. Govers (1994). "DNA fingerprinting uncovers a new sexually reproducing population of *Phytophthora infestans* in the Netherlands." Eur J Plant Pathol **100**: 97-107.

Ebstrup, T., G. Saalbach, and H. Egsgaard (2005). "A proteomics study of in vitro cyst germination and appressoria formation in *Phytophthora infestans*." Proteomics **5**: 2839-2848.

Elliott, C. G. (1983). Physiology of sexual reproduction in *Phytophthora*. *Phytophthora*, its biology, taxonomy, ecology, and pathology, APS Press**:** 71-80.

Erwin, D. C. and O. K. Ribeiro (1996). *Phytophthora* diseases worldwide. St. Paul, Minn., APS Press.

Flier, W. G., N. J. Grunwald, L. P. N. M. Kroon, A. K. Sturbaum, T. B. van den Bosch, E. Garay-Serrano, et al. (2003). "The population structure of *Phytophthora infestans* from the Toluca valley of central Mexico suggests genetic differentiation between populations from cultivated Potato and wild *Solanum* spp." Phytopathology **93**: 382-390.

Flier, W. G., L. P. N. M. Kroon, A. Hermansen, H. M. G. van Raaij, B. Speiser, L. Tamm, et al. (2007). "Genetic struture and pathogenicity of populations of *Phytophthora infestans* from organic potato crops in France, Norway, Switzerland, and the United Kingdom." Plant Pathol **56**: 562-572.

Forster, H., M. P. Cummings, and D. Coffey (2000). "Phylogenetic relationships of *Phytophthora* species based on ribosomal ITS1 DNA sequence analysis with emhpasis on Waterhouse groups V and VI." Mycol Res **104**: 1055-1061.

Fry, W. (2008). "*Phytophthora infestans*: the plant (and R gene) destroyer." Mol Plant Pathol **9**: 385-402.

Fyfe, A. M. and D. S. Shaw (1992). "An analysis of self-fertility in field isolates of *Phytophthora infestans*." Mycol Res **96**: 390-394.

Gisi, U. and Y. Cohen (1996). "Resistance to phenylamide fungicides: a case study with *Phytophthora infestans* involving mating type and race structure." Annu Rev Phytopathol **34**: 549-572.

Goodwin, S. B., B. A. Cohen, K. L. Deahl, and W. E. Fry (1994a). "Migration from northern Mexico as the probable cause of recent genetic changes in populations of *Phytophthora infestans* in the United States and Canada." Phytopathology **84**: 553-558.

Goodwin, S. B., B. A. Cohen, and W. E. Fry (1994b). "Panglobal distribution of a single clonal lineage of the Irish potato famine fungus." Proc Natl Acad Sci **91**: 11591-11595.

Goodwin, S. B. and A. Drenth (1997). "Origin of the A2 mating type of *Phytophthora infestans* outside Mexico." Phytopathology **87**(10): 992-999.

Goodwin, S. B., L. J. Spielman, J. M. Matuszak, S. N. Bergeron, and W. E. Fry (1992). "Clonal diversity and genetic differentiation of *Phytophthora infestans* populations in northern and central Mexico." Phytopathology **82**: 955-961.

Griffin, D. H. (1981). Fungal physiology, John Wiley and Sons.

Gunderson, J. H., H. Elwood, A. Ingold, K. Kindle, and M. L. Sogin (1987). "Phylogenetic relationships between chlorophytes, chrysophytes, and oomycetes." Proc Natl Acad Sci **84**: 5823-5827.

Haas, B. J., S. Kamoun, M. C. Zody, R. H. Y. Jiang, R. E. Handsaker, L. M. Cano, et al. (2009). "Genome sequence and analysis of the Irish potato famine pathogen *Phytophthora infestans*." Nature **461**: 393-398.

Hawsworth, D. L., P. M. Kirk, P. F. Cannon, J. C. David and J. A. Staplers (1995). Ainsworth and Bisby's dictionary of the fungi. Wallingford, United Kingdom, CBA International.

Hill, A. E., D. E. Grayson, and J. W. Deacon (1998). "Surpressed germination and early death of *Phytophthora infestans* sporangia caused by pectin, inorganic phophate,

ion chelators and calcium-modulating treatments. " Eur J Plant Pathol **104**: 367-376.

Hohl, H. R. and K. Iselin (1984). "Strains of *Phytophthora infestans* from Switzerland with A2 mating behavior. " Trans Br Mycol Soc **83**: 529-531.

Judelson, H. S. (1993). "Intermolecular ligation mediates efficient cotransformation in *Phytophthora infestans*." Mol Gen Genet **239**: 241-250.

Judelson, H. S. (1997). "Expression and inheritance of sexual preference and selfing potential in *Phytophthora infestans*." Fungal Genet Biol **21**: 188-197.

Judelson, H. S., A. M. V. Ah-Fong, G. Aux, A. O. Avrova, C. Bruce, C. Cakir, et al. (2008). "Gene expression profiling during asexual development of the late blight pathogen *Phytophthora infestans* reveals a highly dynamic transcriptome." Mol Plant Microbe Interact **21**: 433-447.

Kamoun, S., P. Hraber, B. Sobral, D. Nuss, F. Govers (1999). "Initial assessment of gene diversity for the oomycete pathogen *Phytophthora infestans* based on expressed sequences." Fungal Genet Biol **28**: 94-106.

Kronstad, J. W. and C. Staben (1997). "Mating type in filamentous fungi." Annual Review of Genetics **31**: 245-276.

Mitchell, D. J. and G. A. Zentmyer (1971). "Effects of oxygen and carbon dioxide tensions on sporangium and oospore formation by *Phytophthora* spp. ." Phytopathology **61**: 807-811.

Niederhauser, J. S. (1991). *Phytophthora infestans*: the Mexican connection. *Phytophthora*. J. A. Lucas, R. C. Shattock, D. S. Shaw and L. R. Cooke. Cambridge, Cambridge University Press**:** 25-45.

Prakob, W. and H. S. Judelson (2007). "Gene expression during oosporogenesis in heterothallic and homothallic *Phytophthora*." Fungal Genet Biol **44**: 726-739.

Qi, J., T. Asano, T. Asano, M. Jinno, K. Matsui, K Atsumi, Y. Sakagami, et al. (2005). "Characterization of a *Phytophthora* mating hormone." Science **309**: 1828.

Randall, T. A. and H. S. Judelson (1999). "Construction of a bacterial artificial chromosome library of *Phytophthora infestans* and transformation of clones into *P. infestans*." Fungal Genet Biol **28**: 160-170.

Reeves, R. J. and R. M. Jackson (1974). "Stimulation of sexual preproduction in *Phytophthora* by damage." J Gen Microbiol **84**: 303-310.

Ribeiro, O. K. (1983). Physiology and asexual sporulation and spore germination in *Phytophthora*. *Phytophthora*, its biology, taxonomy, ecology and pathology. D. C. Erwin, S. Bartnicki-Garcia and P. H. Tsao. St. Paul, Minnesota, APS Press**:** 55-70.

Rutherford, F. S. and E. W. B. Ward (1985). "Evidence for genetic control of oospore aborton in *Phytophthora megasperma* f. sp. *glycinea*." Can J Bot **63**: 1671-1673.

Savidor, A., R. S. Donahoo, O. Hurtado-Gonzales, M. L. Land, M. B. Shah, K. H. Lamour, et al. (2008). "Cross-species global proteomics reveals conserved and unique processes in *Phytophthora sojae* and *Phytophthora ramorum*." Mol Cell Proteomics **7**: 1501-1516.

Shattock, R. C., D. S. Shaw, A. M. Fyfe, J. R. Dunn, K. H. Loney, and J. A. Shattock (1990). "Phenotypes of *Phytophthora infestans* collected in England and Wales from 1985 to 1988: mating type, response to metalaxyl and isoenzyme analysis." Plant Pathol **39**: 242-248.

Skidmore, D. I., R. C. Shattock, and D. S. Shaw (1984). "Oospores in cultures of *Phytophthora infestans* resulting from selfing induced by the presence of *P. drechsleri* isolated from blighted potato foliage. " Plant Pathol **33**: 173-183.

Smart, C. D. and W. E. Fry (2001). "Invasions by the late blight pathogen: renewed sex and enhanced fitness." Biol Invasions **3**: 235-243.

Smart, C. D., H. Mayton, E. S. Mizubuti, M. R. Willmann, W. E. Fry (2000). "Environmental and genetic factors influencing self-fertility in *Phytophthora infestans*." Phytopathology **90**: 987-994.

Spielman, L. J., A. Drenth, L. C. Davidse, L. J. Sujkowski, W. Gu, P. W. Tooley, et al. (1991). "A second world-wide migration and population displacement of *Phytophthora infestans*?" Plant Pathol **40**: 422-430.

Sussman, A. S. (1966). Dormancy and spore germination. The Fungi. C. G. Ainsworth and A. S. Sussman. New York, Academic Press. **II:** 733-764.

Sutherland, E. D. and S. D. Cohen (1983). "Evaluation of tetrazolium bromide as a vital stain for fungal oospores." Phytopathology **73**: 1532-1535.

van West, P., S. Kamoun, J. W. van't Klooster, and F. Govers (1999). "Internuclear gene silencing in *Phytophthora infestans*." Mol Cell **3**: 339-348.

Vijn, I. and F. Govers (2003). "*Agrobacterium tumefaciens* mediated transformation of the oomycete plant pathogen *Phytophthora infestans*." Mol Plant Pathol **4**: 459-467.

Zentmyer, G. A. (1980). *Phytophthora cinnamomi* and the diseases it causes. St. Paul, Minnesota, American Phytopathology Society.

Chapter I

Characterization of regulatory elements determining the expression pattern of two mating-induced genes in *Phytophthora infestans*

Abstract

The regulatory components of two mating-induced promoters were characterized in this study. PITG_02525 encodes an elicitin-like protein that is expressed only during the mating stage. Elicitins are a group of extracellular elicitor proteins that cause a hypersensitive response in hosts and believed to play important roles such as sterol or lipid binding during infection. Gene PITG_00483 was identified as pumilio, encoding an RNA-binding protein that functions as a post-transcriptional repressor, which is induced both during asexual sporulation and the development of sexual spores. To identify the *cis*-elements regulating the temporal and spatial expression of these genes, sequentially deleted promoters were fused with a β-glucuronidase (GUS) reporter gene. Transformants of *P. infestans* expressing GUS under the control of the full length PITG_02525 promoter revealed that GUS transcripts started accumulating from the early stage of mating, sexual structure formation, and continued to the maturation of sexual spores, oospores, based on histochemical staining. GUS expression was also observed in mycelia that are initiating to form either the male or female sexual structures. A potential repressor element and an activator were identified by deletion analysis. Expression of GUS driven by the PITG_00483 promoter during mating was first detected in male and

female gametangial initials and persisted in mature oospores. Expression was also observed in hyphal tips just prior to asexual sporulation, in sporangiophores, and in mature sporangia. An element was found to be essential for the expression of the gene in both stages, and shown to be able to drive transcription during sporulation, but not in sexual reproduction.

Introduction

Sexual reproduction is important for the survival of many lower eukaryotic microbes including oomycetes because the process increases population fitness and diversity by generating recombinant genotypes that are more virulent or resistant, in response to natural selective pressure. The sexual spores of oomycetes are usually thick-walled structures that provide robust protection against unfavorable environmental conditions such as cold, degradation by microbes, or even chemical fumigation (Agrios, 2004). In some places in Europe, these sexual spores, oospores, have been reported to serve as the initial inocula for disease epidemics at the beginning of the growing season (Andersson et al., 1998; Flier et al., 2007)

Many of the most important oomycetes belong to the genus *Phytophthora* (Erwin & Ribeiro, 1996), which contain economically significant plant and animal pathogens. For example, the notorious *P. infestans* caused the great Irish famine in the 1840s and continues to be responsible for billions of dollars of yield looses per year on potato and tomato (Smart & Fry, 2001).

The physiology of sexual reproduction in *P. infestans* has been well studied, however, little is known at the molecular level. Even though a few studies have been done on profiling the transcriptome of the sexual stage, and a group of genes were shown to be expressed during the early stages of sexual reproduction, how these genes are regulated remains unknown. With the aid of DNA-mediated transformation approaches for *Phytophthora*, knowledge of the molecular biology of each developmental stage of these microbes has been accumulating rapidly (Judelson et al.. 1991; Cvitanich & Judelson, 2003; Ah-Fong et al., 2008). With the advancement of molecular tools and technologies and the completion of genome sequencing, large scale gene expression studies of *Phytophthora* have provided invaluable insight into the signaling pathways involved in each stage (Kamoun et al., 1999; Kim & Judelson, 2003; Škalamera et al., 2004; Tani et al., 2004; Prakob & Judelson, 2007).

When transcription factors bind to regulatory elements in promoter regions of a gene, the basal transcriptional machinery is then recruited to the core promoter to initiate transcription (Stargell & Struhl, 1996). A core promoter is generally defined as the genomic region that surrounds a transcription start site (TSS) and/or the segment of DNA that is required to recruit the transcription initiation complex and initiate transcription (Sandelin et al., 2007). Several kinds of core promoters have been identified in eukaryotic organisms. One type is called the TATA-box, with the consensus TATAAA sequence. It resides about 30 bp upstream of the TSS, and is commonly found in humans and true fungi, but not in oomycetes (Wobbe & Struhl, 1990; Smale & Kadonaga, 2003). In oomycetes, the commonly found core promoter is called Inr (initiator), which was often

found located near the TSS. In *P. infestans*, most of the genes were found to contain an Inr element (CTCCTTCT), and a downstream flanking promoter region (FPR) was often found together with Inr (McLeod et al., 2004).

To enhance our understanding of sexual development, especially the gene regulation mechanisms that are used during the early stage of sexual reproduction, this study focused on characterizing the transcription factor binding sites and core promoter regions of the promoters of selected mating-induced genes of *P. infestans*.

Five mating-specific genes (mating-specific is defined as 100-fold induction during mating comparing to vegetative stages according to microarray data (Prakob & Judelson, 2007)) were selected for promoter studies. These genes were PITG_02525, PITG_17302, PITG_01958, PITG_11454, and PITG_01038. Another gene, PITG_00483, up-regulated 100-fold during mating and 10-fold up-regulated in sporulating hyphae was added later. In this study, promoters of PITG_00483 and PITG_02525 were subjected to detailed examination of their transcription regulatory components.

PITG_02525 encodes a mating-specific elicitin-like protein called M25 identified in a prior study (Fabritius et al., 2002). The elicitins and elicitin-like proteins are extracellular proteins that occur in oomycete species, such as *Phytophthora* and *Pythium*, some of which induce the hypersensitive response (HR) in hosts. Elicitins and elicitin-like proteins have very diverse expression patterns, and many of them were found to be down-regulated during infection (Kamoun et al., 1997; Qutob et al., 2003; Haas et al., 2009), probably due to the plant immune response. The functions of most elicitins and elicitin-like proteins remain unknown, but some discoveries have shed light on the

potential roles of this protein family. Certain elicitins (Kamoun et al., 1997) bind lipids or sterols, and it has been suggested that these proteins function as sterol carriers and lipid transfer proteins (Mikes et al., 1997; Osman et al., 2001; Blein et al., 2002). Dissecting the promoter of PITG_02525 would help us better understand the regulatory mechanisms that regulate the expression of this important gene family.

A pumilio (*pum*) gene, PITG_00483, was first identified in *P. infestans* by Fabritius and Cvitanich (2002), and the gene structure and localization was described later by Cvitanich and Judelson (2003). It belongs to the Puf family of genes, named after the first two members identified in the family: *Drosophila* Pumilio and *Caenorhabditis elegans* FBF mRNA binding factor (Murata & Wharton, 1995; Jobson et al., 1999). All members of this family have a conserved functional domain consisting of eight repeat motifs with the ability to bind mRNA 3' untranslated regions (UTR), and they share the general function of repressing the translation of target mRNAs by accelerating mRNA turnover or recruiting targets to different locations to prevent them from being translated (Wharton et al., 1998; Souza et al., 1999; Goodwin, 2001; White et al., 2001; Wickens et al., 2002). In the oomycete *Saprolegnia parasitica*, *pum* is specifically expressed in asexual spores, is present only in cysts, and decays as soon as cysts germinate (Andersson & Cerenius, 2002). In *P. infestans*, *pum* is present in both male and female structures, and in sporangia and young sporangiophores (Cvitanich & Judelson, 2003). The promoter of this gene holds special interest since the gene participates in two distinct life stages and the regulatory components might not be the same for each stage, or one component could act differently in different stages.

In this study, gene features such as the TSS, 5' UTR, and the functional promoters of the selected genes were identified. Temporal and spatial expression patterns of the chosen genes and their sexual preferences were characterized, and their transcription regulatory components during sexual reproduction were identified through examining the effects of partial deletions of the promoters fused with a β-glucuronidase reporter gene. Fusions of portions of the potential regulatory motifs with a minimal promoter were used to confirm the activity of the elements.

Materials and methods

Culture conditions and strains of *Phytophthora infestans*

P. infestans isolate 88069 (A1, The Netherlands) and its transformants were cultured on rye A agar at 18 ℃ as described (Judelson et al., 1991). Sporulating hyphae were obtained from 10-day-old rye cultures. Transformation was carried out by electroporation to generate stable transformants and performed as previously described (Judelson & Michelmore, 1991). Strain 618 (A2, Mexico) was used for setting up mating cultures.

Matings were performed at 18 ℃ in the dark by placing 3 mm wide agar strips containing the parents in the center of a rye agar plate, 1.7 cm from each other. The inocula were placed on polycarbonate membranes (0.4 micron; Osmonics). All the mating tissues examined in this study were 10 days old.

Sequence analysis

Partial cDNA sequences of five target genes were obtained from libraries constructed by two previous studies of mating-induced genes (Fabritius et al., 2002; Prakob & Judelson, 2007). Gene-specific nested primers were designed to perform GenomeWalker (Clontech) analysis to acquire upstream genomic sequence information of PITG_02525, PITG_01958, and PITG_17302 using DNA from strain 8811 (A1, UK). The sequences obtained were assembled and aligned together with the partial cDNA sequences using the DNAstar Seqman sequence analysis program for Macintosh. The assemblies were then compared with the sizes of their homologs in *P. sojae* and *P. ramorum* genome databases (http://genome.jgi-psf.org/Physo1_1/Physo1_1.info.html and http://genome.jgi-psf.org/Phyra1_1/Phyra1_1.home.html, respectively) and the estimation of transcripts from Northern analysis to predict their ORF sizes. The gene models were later compared with Broad Institute of MIT and Harvard *P. infestans* genome annotation (http://www.broadinstitute.org/annotation/genome/phytophthora_infestans/MultiHome.html).

PITG_11454 and PITG_01038 models were established by searching their cDNA sequences against the *P. infestans* ESTs in dbEST, assembling the resulting sequences, and comparing them with their *P. sojae* and *P. ramorum* homolog gene models. 5' RACE was used to determine the TSS positions of each gene with strain 8811, and the resulting bands were sequenced to identify the exact TSS (Table 1.1. and Fig. 1.1.A). The length of

the 5’ untranslated region (5’ UTR) was defined as the distance between the predicted start codon of the ORF and the TSS. The intergenic region between the stop codon of the upstream gene and start codon of the target gene was defined as the promoter region of the target gene.

Table 1. 1. Gene specific primers (GSP) designed to perform 5' RACE analysis on selected mating-induced genes with strain 8811 (A1) of *P. infestans*. The distance between the last GSP and the predicted translation start site (ATG) is also listed. PITG numbers are the official accession number of the Broad Institute of MIT and Harvard *P. infestans* database, and Pi numbers are cDNA numbers from the microarray study of Prakob and Judelson (2007). Primers were named after the Pi numbers.

PITG	Pi	GSP for 5' RACE (5'-3')	Distance of last GSP to ATG
01038	015704	1. GCTCGGAGTGGTTGTCGTGTAGAT 2. ACCATTACTCGCTGCAACTGTGA 3. GCAGCCTTCCTCTCGGTTCTTGTG	228
01958	011132	1. GCCAGGAACGAACGCAACGACATCT 2. AGCTCCATTTGCCGAACCGAACAGG 3. GTGCGCTCTGCAAGAAGGTCAA	193
02525	000192	1. GCGGTTGAGTGGTGCTTGTCGTCTT 2. GCACCGCATTCATAAGAAGCACACA	221
11454	015281	1. GCAGGCAACCGACTCCAGTATTCAT 2. TCTGGCCTTCATCGACGAGTTTCT 3. GTTGGGTGGGACATCTAGTTGTGAG	298
17302	004496	1. CTTGCGTACCGAGCTGTTTCA 2. GCAGCGCCGAGCAGCAAAAGACCC	44

Promoter:GUS plasmid construction

Promoter fragments were generated by polymerase chain reaction (PCR) using Taq DNA polymerase and specific primers, and cloned into pNPGUS, which contains a promoterless GUS gene along with neomycin phosphotransferase (nptII) for G418 selection. For both PITG_00483 and PITG_02525 promoter 5' deletion constructs, plasmids are named based on the size of the promoter as counted upstream from the ATG. Two 3' deletion constructs were also made for PITG_02525 promoters. Their names are based on the beginning and ending nucleotide. For instance, Del119-70 contained promoter sequences 119 nt to 70 nt upstream of ATG.

Promoter 5' deletion sequences of PITG_02525 were also amplified by PCR from 88069 genomic DNA using forward primers 192 PMRT F: 5;-TTGCATTTCTTAACATTGAGTAT (full length promoter), 192promdel215: 5'-GTCTCTTCTAAAGTTGTG, 192promdel196: 5'-TTGCAAGAGAATCGAGGG, 192promdel162: 5'-CTTTCTCGAAGAAAGCCT, 192promdel154: 5'-GGATTCATAGCTCATACAGATCAAA, 192promdel131: 5'-GAATTCCAAAGCGAGAAGCTCTCG, 192promdel119: 5'-GAATTCGCTCTCGCTGTCAGCTTC, 192promdel101: 5'-CCTCATTCCTCAATTTGCTC, and 192promdel70: 5'-CCAGTCCCAGACACCGTCTC. A single reverse primer was used for amplifying these fragments, 192 prmt R: 5'-ACGGGGCTTGGAAGTGCTCGGA. Promoter 3' deletion fragments were amplified with forward primers 192-delR119-52: 5'-

AGACGGTGTCTGGGACTGGA and 192-delR70-119: 5'-TTACCAGCTAGAGAGCAAAT, with 192promdel119. All of these amplicons were cloned into pNPGUS. Using XN1921-2rpsrF: 5'-CTAGATCTTCTAAT and XN1921-2rpsrR: 5'-CTAGATTAGAAGAT, a motif (TCTTCTAA) was generated and fused with a chimeric construct containing a sporulation-induced promoter motif (SPIP), *NIFS* minimal promoter, and the GUS reporter gene. The resulting construct was called (1-2)-SPIP-*NIFS*. This SPIP-*NIFS*-GUS chimeric construct was developed by Roy and Judelson (unpublished data) by fusing a motif that is overrepresentitive in sporulating induced genes of *P. infestans* with the *NIFS* minimal promoter and GUS reporter gene. This SPIP-*NIFS*-GUS chimerci construct itself was shown to be able to induce GUS expression in sporangia, sporagiaphores and sporulating hyphae (Roy and Judelson, unpublished data). Sequence orientations of all the constructs were confirmed by sequencing.

Sequences for serial deletions of the PITG_00483 promoter were amplified by PCR from strain 88069 genomic DNA using the following set of forward primers: PumPromdel644: 5'-CCGAGGAAACCCCAGGCAATCT, PumPromdel406: 5'-AGTCCCACAGTTTTGAGCAGTC, PumPromdel328: 5'-GAATTCCAGACGCGCCGACACGGG, Pumpromdel279: 5'-GAATTCTGGCAAGCCATTGCTAAA, Pumpromdel256: 5'-GAATTCTGGCAAGCCATTGCTAAA, Pum197F: 5'-CCGGCGTGGGTGGGTCCTTT, Pum162F: 5'-CGGCAACCTGTCACATAGCC, Pum120F: 5'-CCCACCCGCCCGCATGCACA, Pum93F: 5'-CATTCTCCAAATTGCCGTCT, and

Pum50F: 5'-ATCTGGAGAGGTTTCAGCGG. A single reverse primer was used to amplify all the deletion fragments, PumPromdelR29: 5'-GGCGGTTGCTGGGTGTCGAGTG. These fragments were cloned into pNPGUS. The fragment amplified using Pum120F and PumPromdelR29 was also inserted into a chimeric construct which consists of a 74-nt minimal promoter from the nuclear LIM interactor-interacting factors *NIFS* gene of *P. infestans* followed by GUS (Ah-Fong et al., 2007). This minimal promoter construct was developed by removing sequences upstream of *NIFS* TSS so the minimal promoter cannot trigger the expression of the GUS gene by itself. However, when the *NIFS* minimal promoter was fused after a transcription activator, the chimeric promoter construct was proved to be able to initiate the expression of the GUS reporter gene (Ah-Fong et al., 2007). Sequence orientations were confirmed by sequencing.

PITG_ 17302 full length promoter was amplified with primers 4496 PRMT F: 5'-TGACGCGACTTTGTTGAAGGCAA and 4496 PRMT R: 5'-TTGGACACGGCAGATGGAGTACC. PITG_01958 full length promoter was amplified with primers 11132 PRMT F: 5'-TCCTGCGAGTTGAAGTGATACG and 11132 PRMT R: 5'-GGACCTGTCGCTTTCAAGTTGC.

Blot analysis

Northern blots were performed as described (Judelson & Roberts, 2002), and 18S rRNA was used as a loading control. Five micrograms of total RNA was separated on 1.2%

agarose/6.6% formaldehyde gels, transferred to nylon membranes by capillary blotting in 10 X SSPE (1.8 M NaCl, 0.1 M $NaHPO_4$, 0.01 M EDTA, pH 7.7). The membranes were then fixed by UV crosslinking, and hybridized with ^{32}P-labeled randomly primed probes made from amplified fragments of the targeted genes. High-stringency washes were carried out in 0.2 X SSPE (1.8 M NaCl, 0.1 M $NaHPO_4$, 0.01 M EDTA, pH 7.7), 0.2% sodium dodecyl sulfate (w/v), and 0.1% sodium pyrophosphate at 65 ℃. Low-stringency washes were in 1 X SSPE, 0.2% sodium dodecyl sulfate (w/v), and 0.1% sodium pyrophosphate at 65 ℃. Signals were detected by phosphorimager analysis using Quantity One software.

Results

TSS, 5' UTR and promoter identification of selected mating-induced genes

Five predicted genes that were predicted to be mating-induced based on a microarray study (Prakob & Judelson, 2007) were subjected to further characterization ((Fig. 1.1.A). Northern blot was used to confirm the mating specific expression of PITG_01958, PITG_02525, and PITG_17302, and calculate the approximate transcript sizes (data not shown). At the beginning of this study, the *P. infestans* genome sequencing project from the Broad Institute of MIT and Harvard was not finished. Only a 96 k EST database was available from dbEST. In order to extract the promoter regions of each gene, the start codon of each ORF was manually identified using the

GenomeWalker method. PITG_1145 and PITG_01038 promoters were extracted by searching their cDNA sequences against the dbEST *P. infestans* database, and start codon positions were estimated based on their homologs in *P. sojae* and *P. ramorum* databases, When the *P. infestans* sequencing project was finished later, all five identified translation start sites were compared with the Broad Institute genome annotations and found to be consistent. To determine their TSS and 5' UTR sizes, 5' RACE was employed (Fig. 1.1.B). A summary of the characters of these genes is listed in Fig. 1.1.A. Previous studies suggested that the 5' UTR of *P. infestans* genes range from 35 to 150 bp (McLeod et al., 2004; Xiang et al., 2009), and most of the 5' UTRs identified in this study also fell into this range, with one exception, PITG_11454, which has a longer 5' UTR, 250 bp in length.

The average intergenic region of *P. infestans* is 603 bp, similar to that seen in *P. sojae* and *P. ramorum*, which are 804 bp and 633 bp, respectively (Haas et al., 2009). Therefore, most of the promoter regions tested for function in this study contained intergenic regions smaller than 600 bp, with the exception being PITG_01958, whose intergenic region was 2200 bp (Fig. 1.1.A).

Figure 1.1. Characterization of the structure of selected mating-induced genes. (A) List of tested mating-induced genes and their promoter, 5' UTR, and ORF sizes, and their predicted functions. ORF sizes were estimated by Northern analysis and the sizes of their homologs in *P. sojae* and *P. ramorum*, and later confirmed with Broad Institute of MIT and Harvard *P. infestans* annotations. The length of the 5' UTR of each gene was defined by the distance between the predicted TSS and the beginning of the ORF determined by 5' RACE. Promoters are defined as the intergenic region between the stop codon of the upstream genes and the start codon of the targeted genes. PITG_01038 and PITG_11454 promoters were not subjected to GUS assay (N/A). (B) 5' RACE analysis of the five selected mating-induced genes to determine their 5' UTR and TSS (TSS of PITG_00483, pumilio, was defined previously in Cvitanich and Judelson (2003))

A

PITG	Promoter region used in GUS assay (end at ATG)	5' UTR size (bp from ATG)	Predicted ORF size (bp)	Predicted gene function
00483	700	30*	2771	Pumilio
01038	N/A	20	1227	Conserved hypothetical protein
01958	2200	100	1266	Conserved hypothetical protein
02525	254	97	967	Elicitin-like mating protein M25
11454	N/A	260	2202	Dynamin
17302	550	150	1814	Multicopper oxidase

B

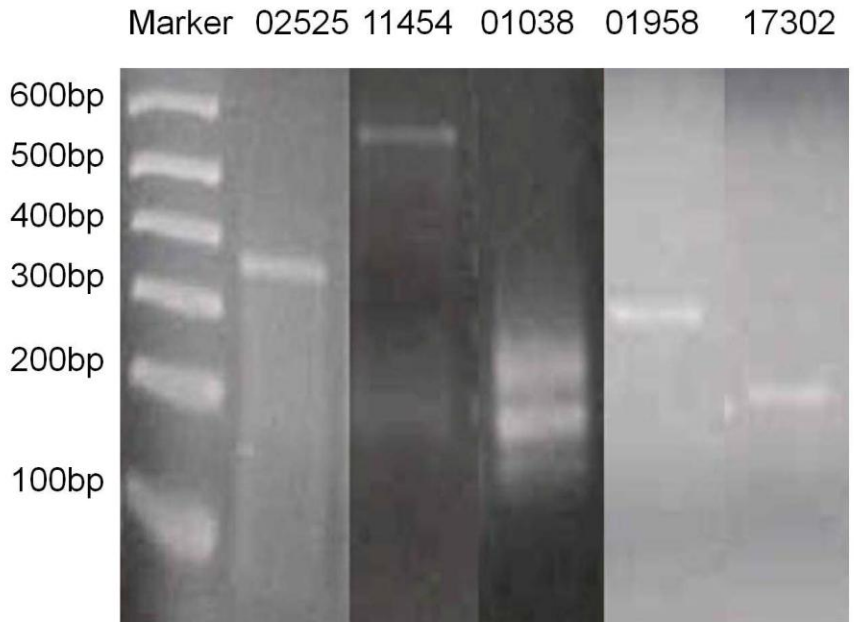

PITG_02525, 00483, 01958 and 17302 transcripts are induced at a relatively early stage of oosporogenesis

Promoters of four genes, PITG_02525, 00483, 01958 and 17302, were cloned into pNPGUS upstream of a GUS reporter gene. The constructs were transformed into *P. infestans* by zoospore electroporation, and the transformants were grown on G418-containing rye media to confirm the intake of the plasmids. The transformants were then mated with 618 (A2) as described in Materials and Methods for 10 days. The mating tissues and the asexual tissues of the transformants outside of the mating zone were subjected to histochemical staining to examine the temporal and spatial patterns of GUS expression.

Out of 40 transformants examined for PITG_17302, 22 showed GUS activity. GUS expression could be observed as soon as the sexual structures began initiating, and a fragment of hyphal tissue near the sexual structures also exhibited GUS staining in addition to the sexual structures (Fig. 1.2.A. lower panel). The GUS activity persisted in 10 day old oospores, and was observed both in male structures (antheridia, Fig. 1.2.A. upper left panel) and female structures (oogonia, Fig. 1.2.A. upper right panel). Among the oospores that showed GUS expression, about 60% of the time the expression was observed in antheridia, 20% in oogonia, and 20% in both structures. No GUS activity was detected in other regions of hyphae, indicating the promoter of PITG_17302 was turned on specifically during the production of oospores, starting from the initiation to the maturation of oospores, with a preference for expression in male structures.

Histochemical staining of 40 transformants from PITG_01958 showed similar patterns as the previous gene (Fig. 1.2.B). Twenty eight transformants were GUS positive. GUS expression was also seen in initiating young sexual structures and the fragments of hyphae attached to them, and in relatively mature oospores. Both antheridia and oogonia showed GUS activity. Approximately 50-55% of the time GUS was seen in antheridia, and 20% in oogonia, and 20-25% in both structures.

Four transformants of the PITG_02525 promoter were examined and 3 were found to be expressing GUS. The patterns followed those of the previously described genes, in that the GUS activity was present both in young and mature mating tissues and both male and female tissues (Fig. 1.5, "Full length" row). GUS expression was detected in male structures 50% of the time. The chances of detecting expression in oogonia and in both structures were equal.

Full length promoter-GUS expression patterns of PITG_00483, *pum*, have been described in Cvitanich and Judelson (2003) and confirmed during this study (not shown). Not only was the promoter of this gene turned on during oosporogenesis, it was also up-regulated in sporulation. The GUS activity of the full length Pum promoter was seen in mating tissues with the same patterns as the previous three genes. In addition, it was detected in sporangiophores, young and mature sporangia, and even in zoospores.

Figure 1.2. Mating-specific in histochemical staining of transformants expressing GUS under the control of PITG_17302 and PITG_01958 promoters. A. GUS activity driven by the PITG_17032 promoter was located exclusively in relatively mature sexual structures, oogonia (female structure, upper right panel) or antheridia (male structure, upper left panel), and in hyphae-bearing young initiating sexual structures (lower panel). B. GUS activity of PITG_01958 promoters was also detected exclusively in sexual structures, both in young initiating sexual structures (upper panel) and mature oospores (lower panel).

A

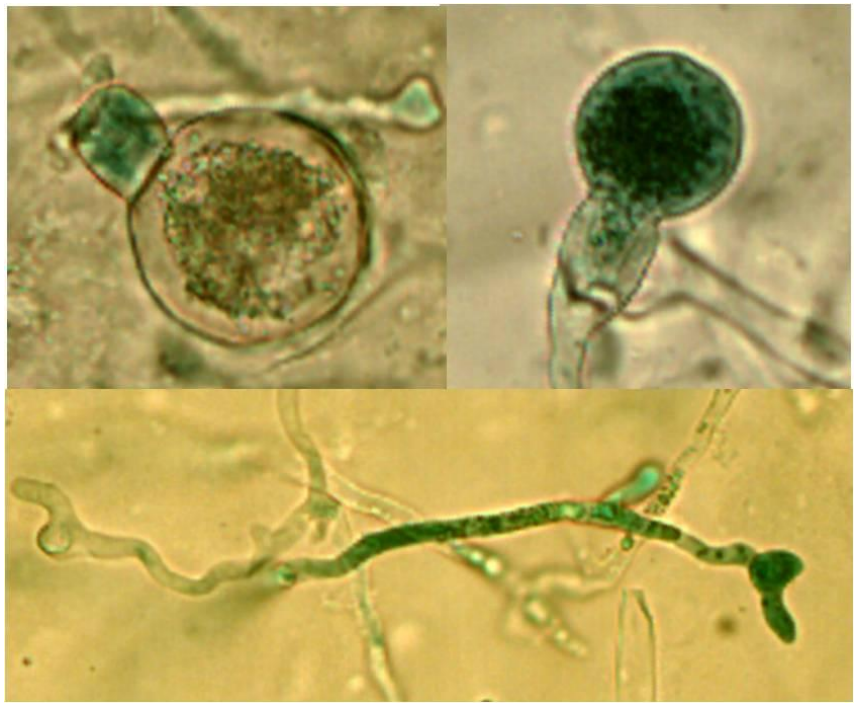

B

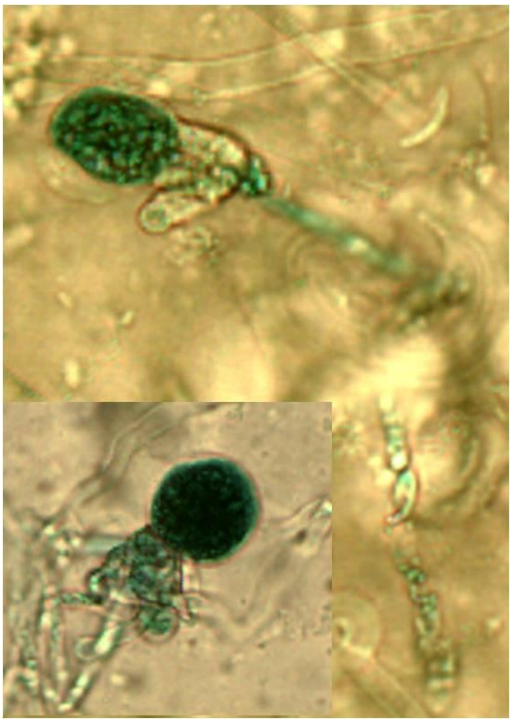

Sequential deletions of the promoters of PITG_02525

The promoters of PITG_02525 and PITG_00483 were subjected to detailed analysis. Sequential deletion analysis was used to locate the regulatory elements for stage specific transcription (Fig. 1.3, Fig. 1.4, Fig. 1.7, and Fig. 1.8).

PITG_02525 has a relatively short promoter and a long 5' UTR, which constitutes about 30% of the promoter region. Its promoter was compared with the homologues in *P. sojae* and *P. ramorum* and appeared to be highly conserved among species (Fig. 1.3). Residing near the TSS were the core promoter elements Inr, FPR, and SAAS (a (C/G)AA(C/G) core promoter element identified by Roy and Judelson, unpublished data). A total of eight 5' deletion constructs were made for PITG_02525 (Fig. 1.3, Fig. 1.4, and Fig. 1.5). When the promoter was shortened from full length (244 bp) to 215 bp (Del215), and then to 196 bp (Del196), the expression patterns in mating tissue remained the same as with the full-length promoter. However, only the full-length promoter appeared to be mating specific, since starting from Del215, transformants began to exhibit GUS staining in hyphal tips and sporangia. Approximately 2-3% of hyphal tips and sporangia in only two of the 20 Del215 transformants were stained, so the staining was probably due to the leakage of the cleaved GUS substrate and was not considered as true GUS expression. The staining increased to 10% of the hyphae and sporangia in 8 out of 12 Del196 transformants, and 30% sporangia and 20% hyphae in half of the Del162 (162 bp promoter remaining) transformants. In mating tissues of Del162, about 35% of the vegetative hyphae started to have GUS expression in addition to mating structures. Since

mating tissues were a mixture of GUS-positive A1 and GUS-negative A2, about 70% of hyphae in the transformants gave GUS signals. It was considered to represent constitutive expression in the mating tissues of Del162. During the process of trimming the promoter from 154 bp (Del154) to 101 bp (Del101), transformants all showed constitutive GUS expression both in mating tissues and in asexualtissues. When the promoter was trimmed to 70 bp upstream of ATG, GUS expression in all tissues stopped. Del70 was the construct in which the TSS and the core promoter elements (between 97-70 bp upstream of ATG) were completely removed, so it was not surprising that Del70 no longer allowed GUS expression. Meanwhile, two 3' deletion constructs were developed to test if there were regulatory components in the 5' UTR region of the promoter. Promoter regions between 119 and 70 bp, and 119 and 50 bp, were cloned into the pNPGUS vector and transformed into *P. infestans*. These showed the same constitutive expression both in mating and asexual tissues as Del154-Del101 (Fig. 1.5).

By examining the general trend of GUS expression in deletion construct transformants, it appeared that after the first deletion, the transformants started to have non-mating-specific GUS expression. An 8-nt motif between Del215 and Del196, TCTTCTAA, was found to be highly conserved among species. It is possible that the motif is responsible for suppressing gene expression in non mating tissues. Therefore, this motif was fused with a chimeric construct containing a sporulation-induced promoter motif (SPIP), *NIFS* minimal promoter, and the GUS reporter gene to examine its repressor ability. The resulting construct was called (1-2)-SPIP-*NIFS*. However, three out of four transformants obtained using this construct still showed GUS expression in

sporangia and sporangiophores. So the TCTTCTAA motif itself was not solely responsible for the repression of PITG_02525 in sporulation.

In spite of the GUS results, Northern analysis showed the GUS expression remained to be mating-exclusive from full length promoter to Del154 (Fig. 1.6). This is in partial conflict with the GUS staining results since constitutive expression in asexual hyphae of the transformants should have provided enough GUS transcripts to be detected. Maybe there were technical issues in the Northern analysis and the experiment needed to be repeated.

Figure 1.3. Promoter alignments of PITG_02525 homologs using ClustalW and BOXSHADE. These alignments include the regions upstream of ATG of PITG_02525 (Pi02525) and its homologues from *P. ramorum* (Pr02525) and *P. sojae* (Ps02525). Numbers with arrows at the top of the panels indicate 5' sequential deletion points from the ATG used in promoter studies of this gene. Numbers with arrows below the panels indicate the starting and ending points of two 3' deletions. TSS and core promoter elements, INR, FPR and SAAS positions were labeled. Black shading represents the conserved regions among the three homologs.

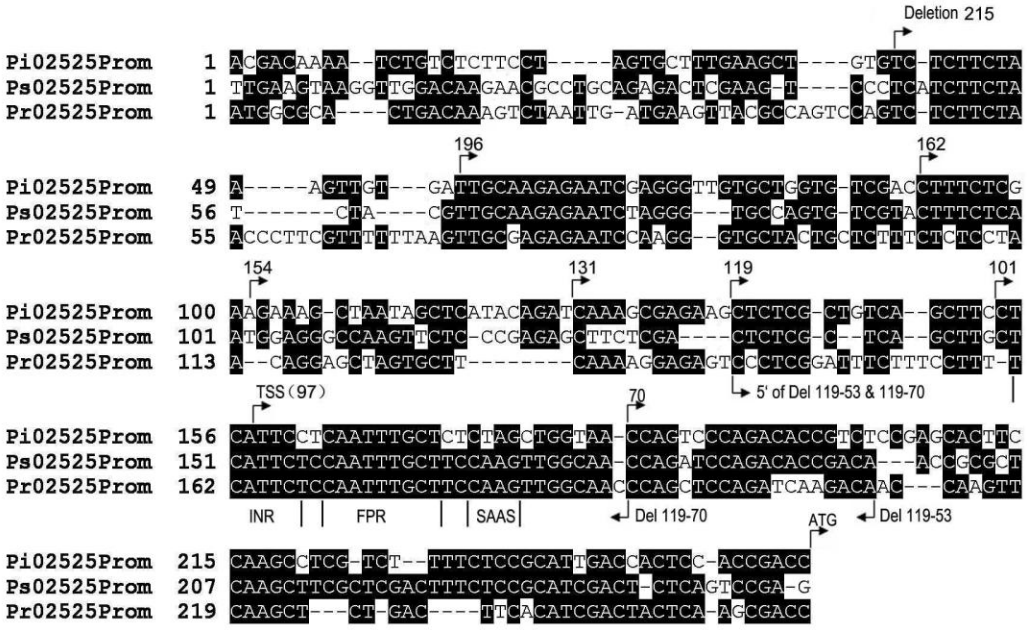
Deletion 215
Pi02525Prom 1 ACGACAAAA--TCTGTCTCTTCCT-----AGTGCTTTGAAGCT----GTGTC-TCTTCTA
Ps02525Prom 1 TTGAAGTAAGGTTGGACAAGAACGCCTGCAGAGACTCGAAG-T----CCCTCATCTTCTA
Pr02525Prom 1 ATGGCGCA----CTGACAAAGTCTAATTG-ATGAAGTTACGCCAGTCCAGTC-TCTTCTA
196
162
Pi02525Prom 49 A-----AGTTGT---GATTGCAAGAGAATCGAGGGTTGTGCTGGTG-TCGACCTTTCTCG
Ps02525Prom 56 T-------CTA----CGTTGCAAGAGAATCTAGGG---TGCCAGTG-TCGTACTTTCTCA
Pr02525Prom 55 ACCCTTCGTTTTTTAAGTTGCGAGAGAATCCAAGG--GTGCTACTGCTCTTTCTCTCCTA
154
131
119
101
Pi02525Prom 100 AACAAAG-CTAATAGCTCATACAGATCAAAGCGAGAAGCTCTCG-CTGTCA--GCTTCCT
Ps02525Prom 101 ATGCAGGGCCAAGTTCTC-CCGAGAGCTTCTCGA---CTCTCG-C--TCA--GCTTGCT
Pr02525Prom 113 A--CAGGAGCTAGTGCTT--------CAAAAGGAGAGTCCCTCGGATTTCTTTCCTTT-T
TSS(97)
70
5' of Del 119-53 & 119-70
Pi02525Prom 156 CATTCCTCAATTTGCTCTCTAGCTGGTAA-CCAGTCCCAGACACCGTCTCCGAGCACTTC
Ps02525Prom 151 CATTCTCCAATTTGCTTCCAAGTTGGCAA-CCAGATCCAGACACCGACA---ACCCCGCT
Pr02525Prom 162 CATTCTCCAATTTGCTTCCAAGTTGGCAACCCAGCTCCAGATCAAGACAAC---CAAGTT
INR
FPR
SAAS
Del 119-70
Del 119-53
ATG
Pi02525Prom 215 CAAGCCTCG-TCT--TTTCTCCGCATTGACCACTCC-ACCGACC
Ps02525Prom 207 CAAGCTTCGCTCGACTTTCTCCGCATCGACT-CTCAGTCCGA-G
Pr02525Prom 219 CAAGCT---CT-GAC----TTCACATCGACTACTCA-AGCGACC

Figure 1.4. Schematic diagrams of truncated promoters used to test the transcriptional activity of the promoter of PITG_02525. Truncated promoters were fused with a GUS reporter gene in the pNPGUS vector, generating one full length promoter and eight 5' deletion constructs, Del215 to Del70, and two 3' deletion constructs containing promoter regions 119-70 bp and 119-53 bp upstream of the start codon (ATG). Whether the plasmids confer GUS activity in mating and sporulating hyphae (SPH) or not is indicated by plus and minus signs. Plus, "+", stands for expression, "-" stands for no expression, "++" indicates constitutive expression, and "+/-" means more than 1 of the transformants were GUS-positive, but the expression was not convincing because less than 5% of the tissues were stained. An 8 nt conserved motif as shown was cloned upstream of a sporulation-induced promoter motif (SPIP) followed by the Nifs minimal promoter and the GUS reporter gene to test its function in transcription regulation.

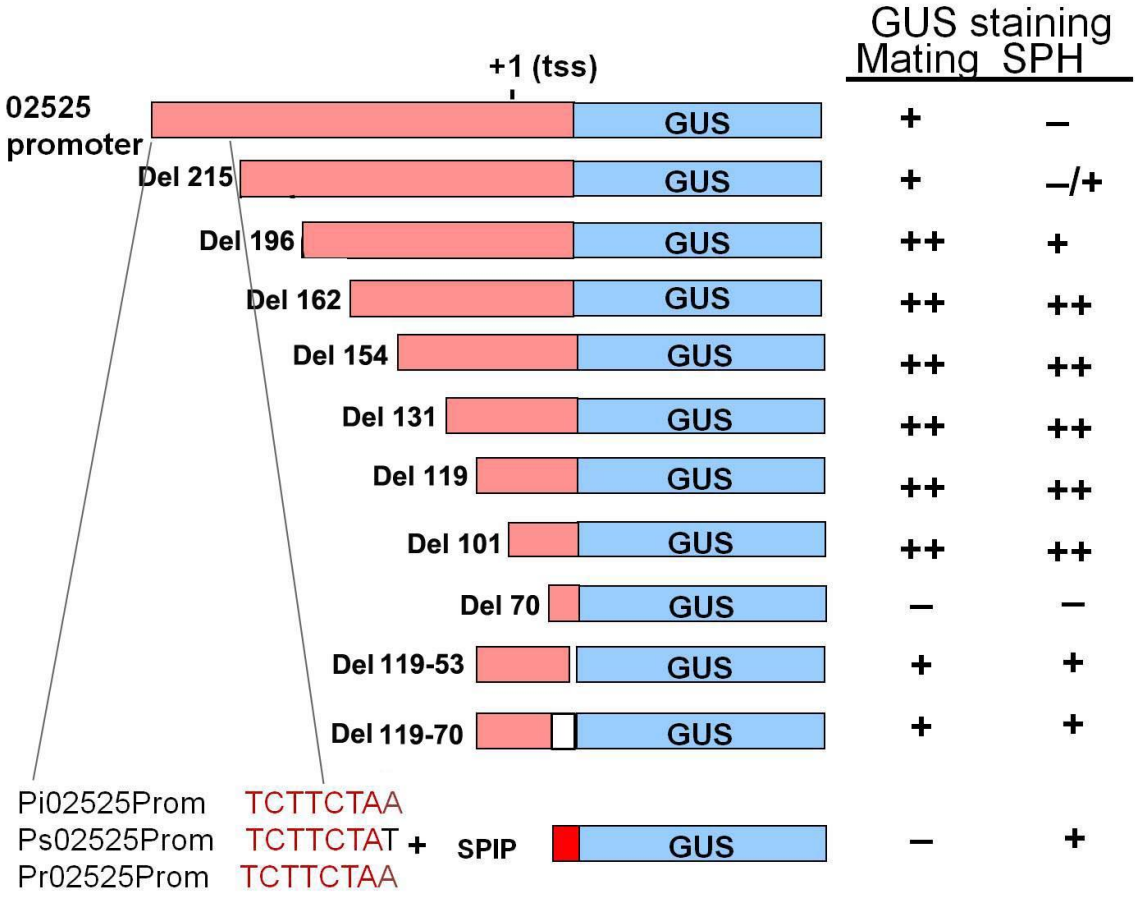
GUS staining
Mating SPH
+1 (tss)
02525
promoter
GUS
+ –
Del 215
GUS
+ –/+
Del 196
GUS
++ +
Del 162
GUS
++ ++
Del 154
GUS
++ ++
Del 131
GUS
++ ++
Del 119
GUS
++ ++
Del 101
GUS
++ ++
Del 70
GUS
– –
Del 119-53
GUS
+ +
Del 119-70
GUS
+ +
Pi02525Prom TCTTCTAA
Ps02525Prom TCTTCTAT
Pr02525Prom TCTTCTAA
+
SPIP
GUS
– +

Figure 1.5. GUS expression in transformants containing serial deletions of the PITG_02525 promoter. Each row of panels represents the GUS expression patterns of one deletion construct, whose number is indicated at the left of the row. “M” indicates mating tissue and “A” indicates asexual tissue. The fractions at the bottom of each panel are the number of GUS-positive transformants versus the total number of transformants obtained with that particular construct.

	M	A
Full length	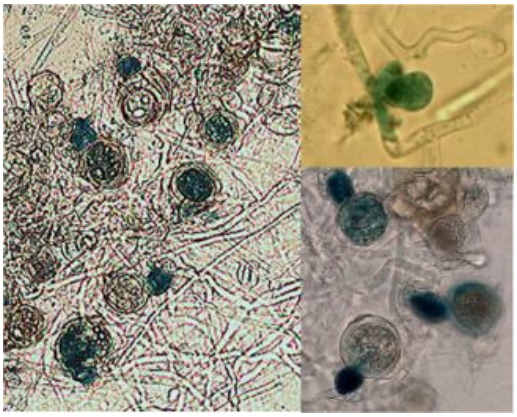	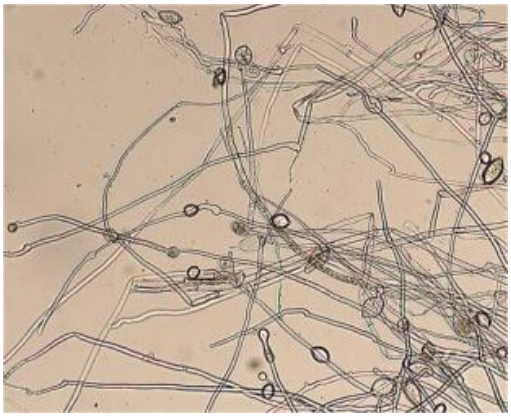
	3/4	0/4
Del 215	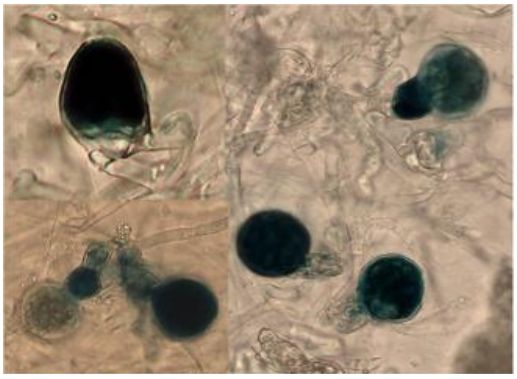	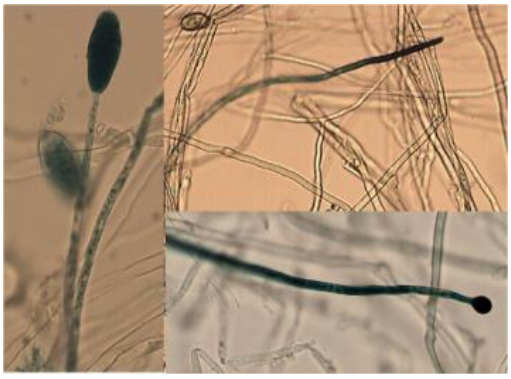
	11/20	2/20
Del 196	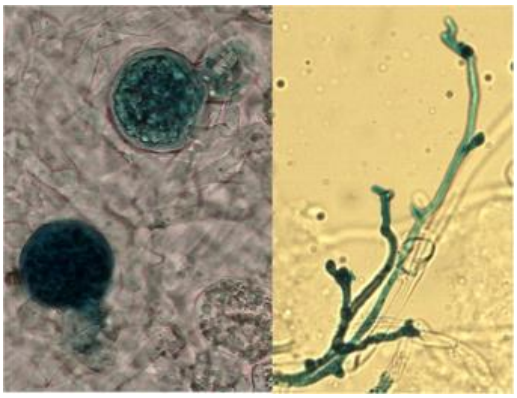	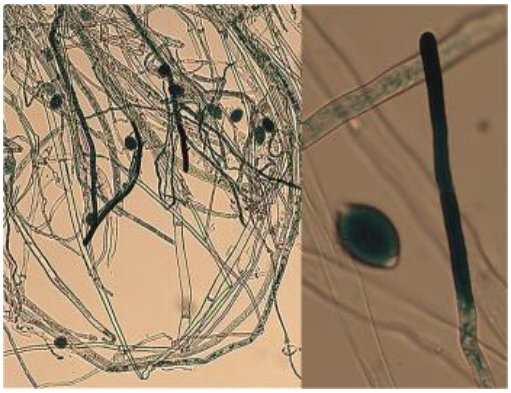
	9/13	8/12

Continue from figure 1.5

	M	A
Del 162	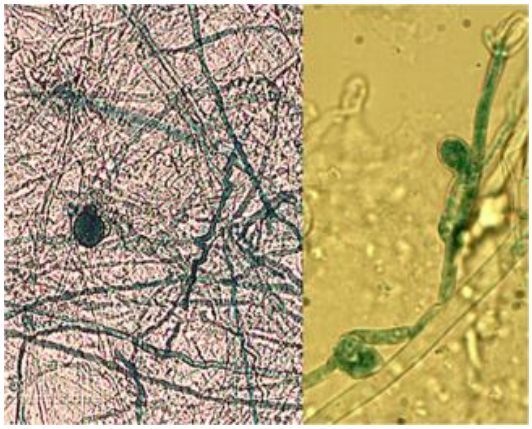	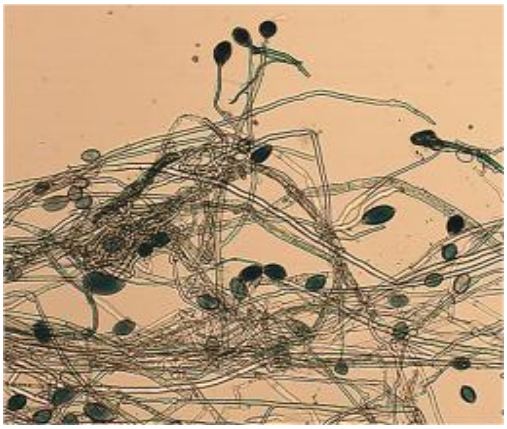
	14/20	9/20
Del 154	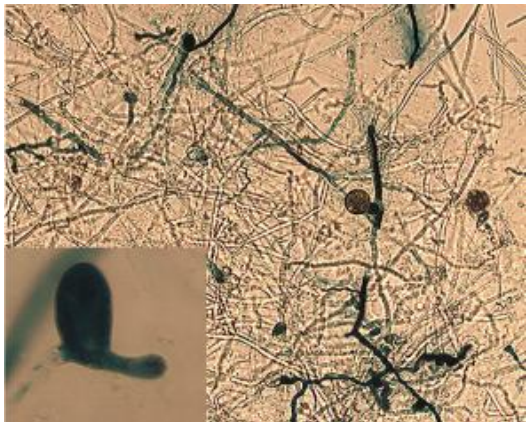	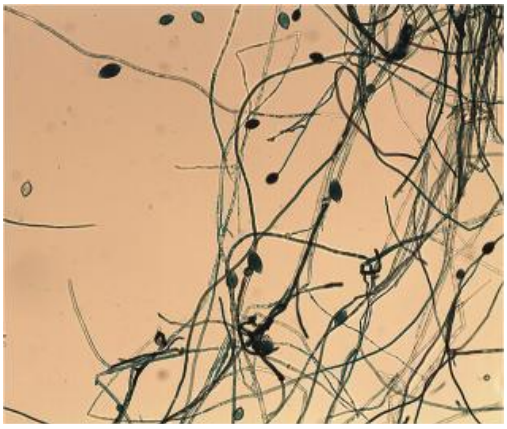
	16/20	14/20
Del 131	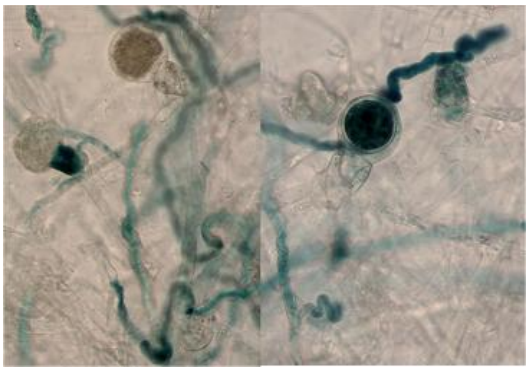	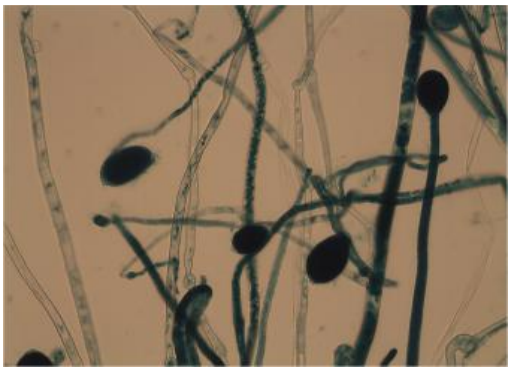
	11/20	8/20

Continue from figure 1. 5

	M	A
Del 119	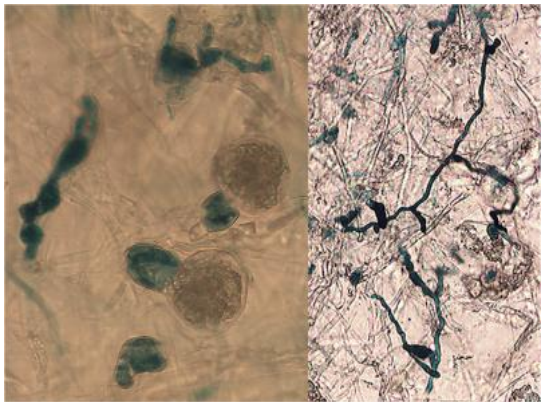	
	3/4	3/4
Del 101	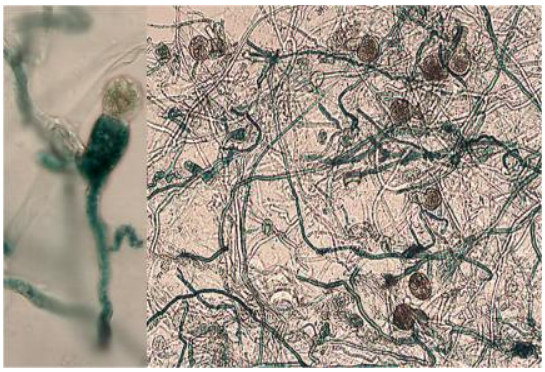	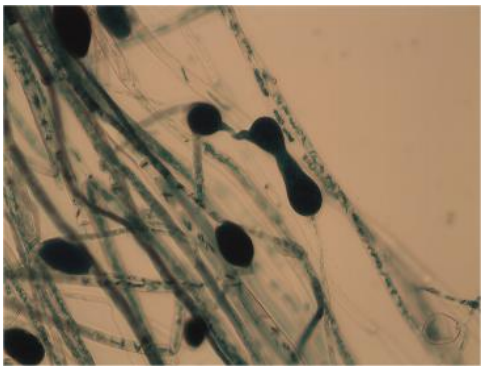
	14/20	14/20
Del 70	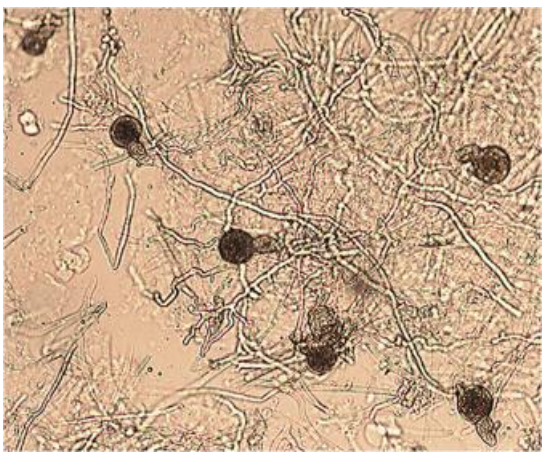	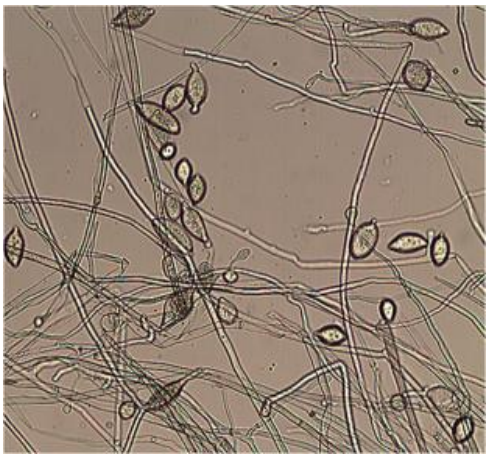
	0/29	0/29

Continue from figure 1.5

	M	A
Del 119-53	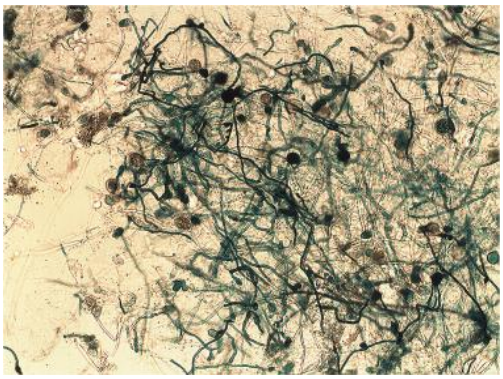	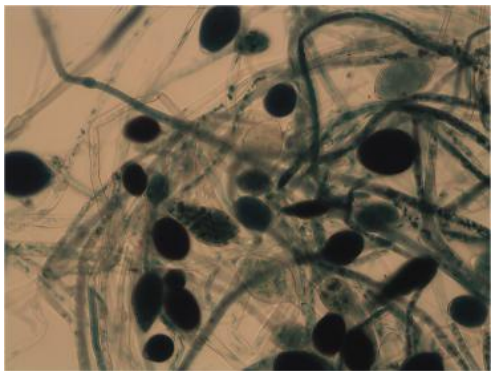
	10/20	10/20
Del 119-70		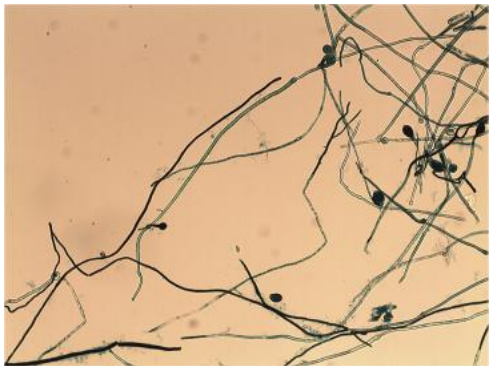
	13/19	9/19
(1-2)-SPIP-*NIFS*	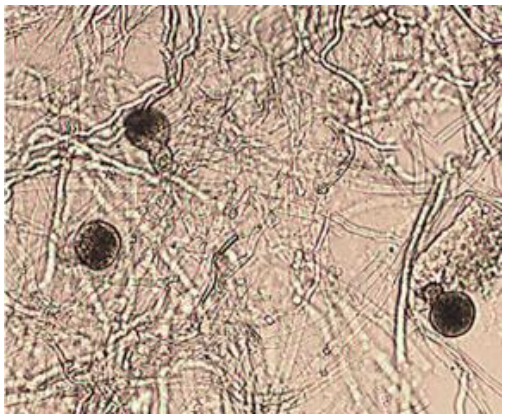	
	0/5	3/5

Figure 1.6. Northern analysis of selected PITG_02525 promoter deletion transformants. Sporulating hyphae and mating tissues of two transformants with full length promoter and four transformants each from Del162 and Del154 were cultured for 10 days and RNA was extracted from them. For each transformant number, GUS expression in asexual tissue and mating tissue was compared. 8811 (A1) and 618 (A2) were nontransformed negative controls.

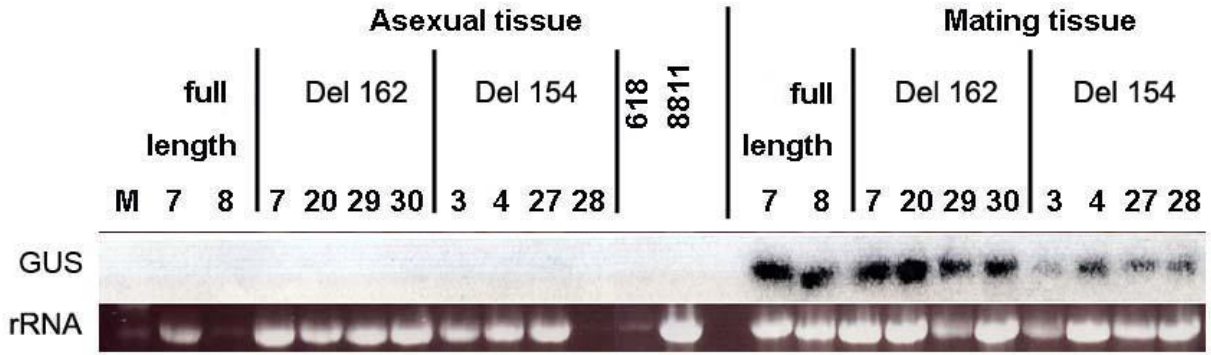
Asexual tissue
Mating tissue
full length
Del 162
Del 154
618
8811
full length
Del 162
Del 154
M 7 8 7 20 29 30 3 4 27 28 7 8 7 20 29 30 3 4 27 28
GUS
rRNA

Sequential deletions of the promoters of PITG_ 00483

After comparison with the promoters of the homologous genes in *P. sojae* and *P. ramorum*, long conserved motifs were located in *P. infestans pum* promoter. Inr and FPR like elements were observed in the promoter as well, however, they did not span the TSS (-30 bp, determined by Cvitanich & Judelson (2003)), but located at 90 to 75 bp region upstream of the ATG start codon.

Sequential deletions were performed to examine the functions of these conserved elements (Fig. 1.8). Ten 5' deletion constructs were developed for the Pum promoter (Fig. 1.7. and Fig. 1.8). The first promoter deletion to 644 bp upstream of the start codon (Pum644) resulted in exactly the same expression pattern as the full length promoter in mating tissues, specificallyin initiating and mature sexual structures. In sporulating tissues, GUS was observed only in sporangia and sporangiophores. A lower number of GUS-positive transformants (5/36) was generated with this construct. However, since more than 40% of the sporulating hyphae and sporangia in each GUS-positive transformant were GUS expressing, the expression pattern was considered to be true. In transformants containing 406 bp of the *pum* promoter (Pum406), a slightly longer area of the oospore and sporangia-bearing hyphae was stained, and the staining area in asexual mycelia was larger than in mating tissue. Deletion constructs containing 378, 328 and 256 bp of the *pum* promoter (Pum378, Pum328, and Pum256) had constitutive GUS expression in sporulating mycelia, however, the patterns in mating tissue remained mating-specific. Interestingly, when the promoter was deleted to 197 bp (Pum197), the

GUS activity was suddenly lost in both tissues, and resumed after the promoter was further deleted to 162bp (Pum162). The GUS expression remained constitutive in the asexual stage with truncated promoters Pum162 and Pum120, but was still mating tissue-specific. Starting from Pum93, the intensity of GUS expression started to decrease in both tissue types, and when the promoter was deleted to 50 bp away from the ATG start codon, the expression was completely lost.

With the assumption that the region between 93 bp and 50 bp upstream of ATG was responsible for the transcription of the gene, fragments from 142 bp to 50 bp, and 120 bp to 50 bp upstream of ATG were individually fused with the *NIFS* minimal promoter to see if these fragments alone were able to drive transcription. However, none of the constructs showed GUS activity after examining 20 constructs. Another chimeric promoter construct was then made with the Pum120 fragment, which contained the TSS and 5' UTR region. This construct was able to restore GUS expression in sporangia, but not in mating tissues (Fig. 1.9, last row).

Figure 1.7. Promoter alignments of PITG_02525 homologs using ClustalW and BOXSHADE. The alignments include the promoters upstream of ATG of PITG_00483 (Pi00483) and its homologs from *P. ramorum* (Pr00483) and *P. sojae* (Ps00483). Numbers with arrows at the top of the panels indicate 5' sequential deletion points from the ATG used in promoter studies of this gene. Arrows below the panels indicate the starting and ending points of the promoter fragments that were fused with *NIFS* minimal promoter. TSS and core promoter elements INR and FPR positions are labeled. The original alignment was performed with 800 bp sequences. Only 620 bp are shown here to save space. Black shading represents the conserved regions among the three homologues.


406 bp to ATG
328
279
256
197
162
120
93
Chimeric
50
INR
FPR
TSS
ATG

Figure 1.8. Schematic diagrams of truncated promoters used to test the transcriptional activity of the PITG_00483 promoter. Truncated promoters were fused with a GUS reporter gene in the pNPGUS vector, generating 10 deletion constructs, 644 to 50, which are the 644 bp to 50 bp regions upstream of the ATG start codon. Whether the plasmids confer GUS activity in mating and sporulating hyphae (SPH) or not are indicated by plus and minus signs. Plus, "+", stands for expression, "-" stands for no expression, "++" indicates constitutive expression, and "+/-" means more than 1 of the transformants were GUS-positive, but the expression was not convincing because less than 5% of the tissues were stained. Sequence of Del 120, as shown to be highly conserved among *Phytophthora* species, were cloned in front of a minimal promoter to test its function in the regulation of transcription.

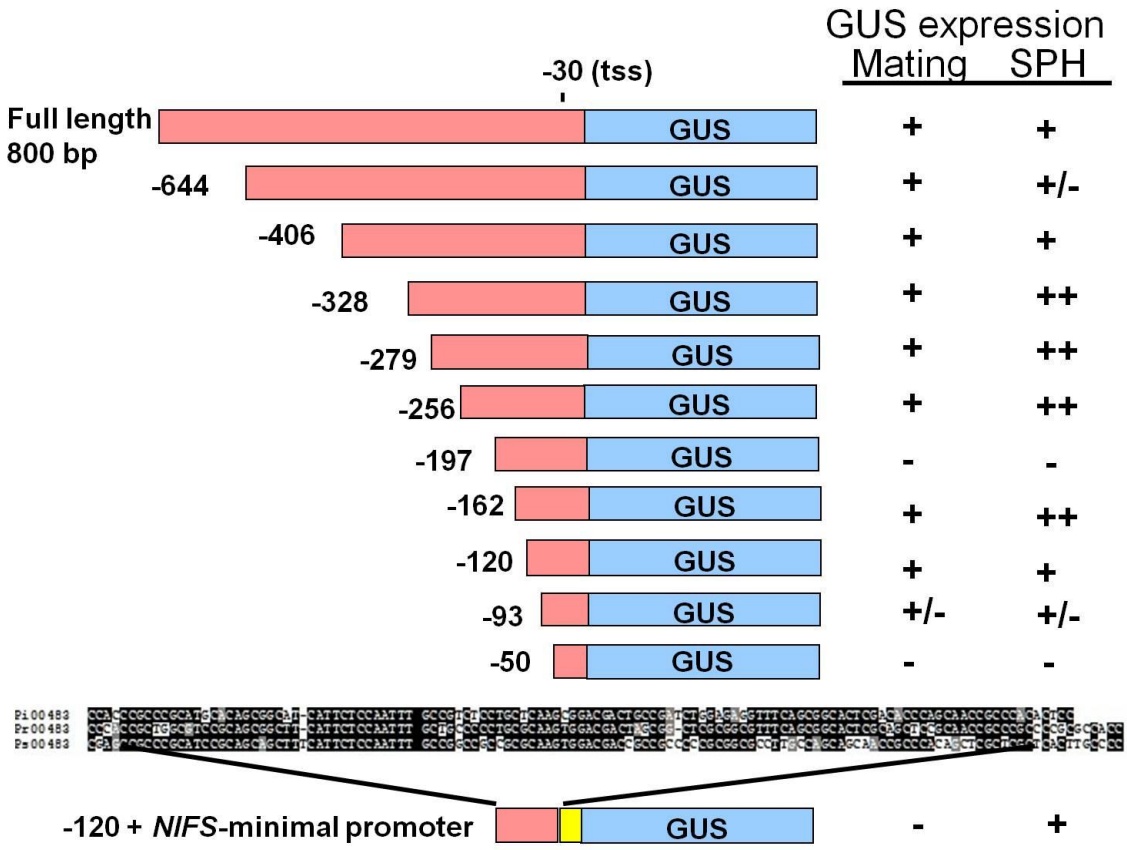
GUS expression
Mating SPH
-30 (tss)
Full length
800 bp
GUS
+ +
-644
+ +/-
-406
+ +
-328
+ ++
-279
+ ++
-256
+ ++
-197
- -
-162
+ ++
-120
+ +
-93
+/- +/-
-50
- -
-120 + NIFS-minimal promoter
- +

Figure 1.9. GUS expression in transformants containing serial deletions of the PITG_00483 promoter. Each row of panels represents the GUS expression pattern of one deletion construct, whose number is indicated at the left of the row. “M” indicates mating tissue and “A” indicates asexual tissue. The fractions indicated at the bottom of each panel show the number of GUS-positive transformants versus the total number of transformants obtained with that particular construct.

M A

Pum644

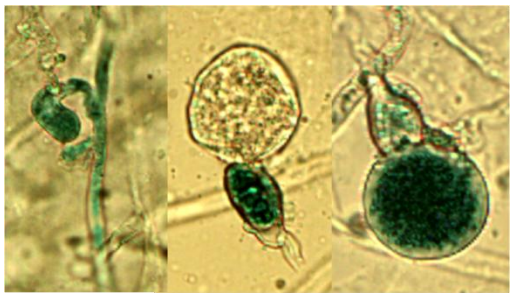

25/36

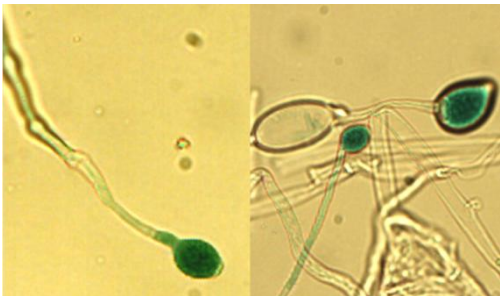

5/36

Pum406

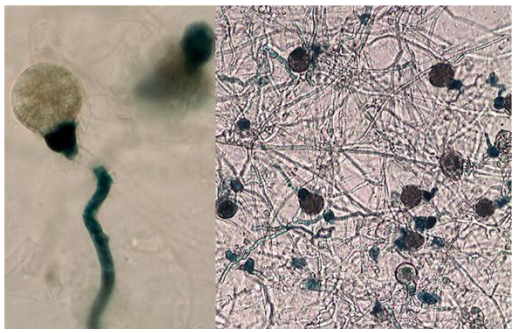

9/19

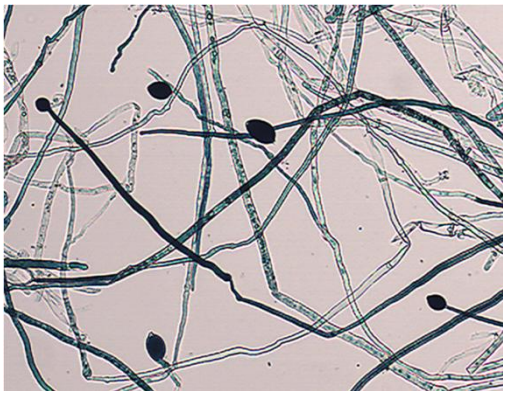

9/19

Pum328

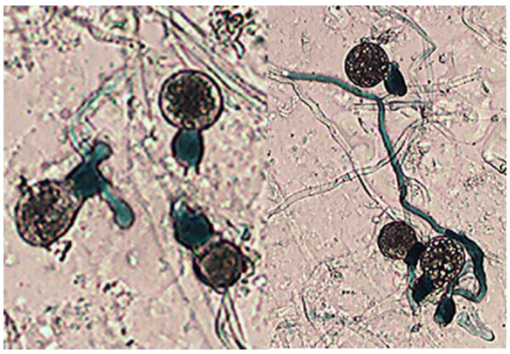

13/20

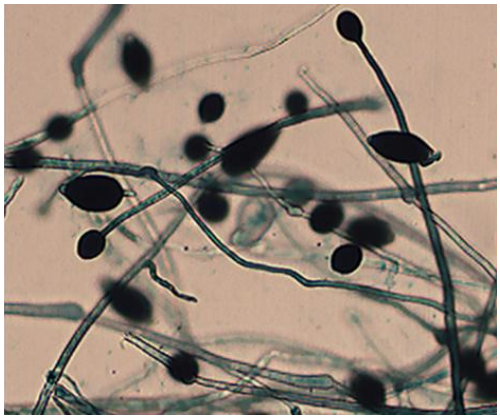

14/20

Continue of Figure 1. 9

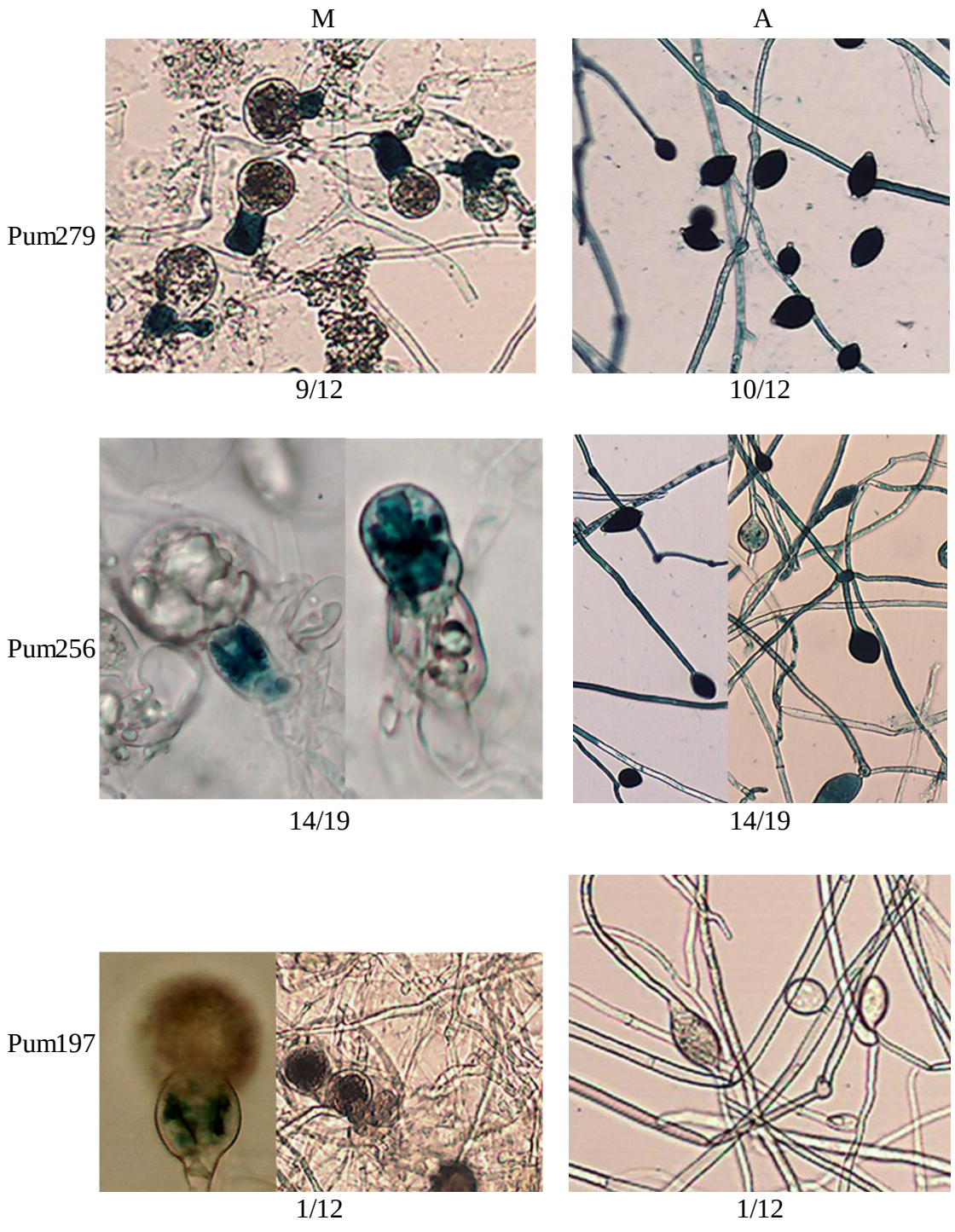

Continue of Figure 1. 9

	M	A
Pum162	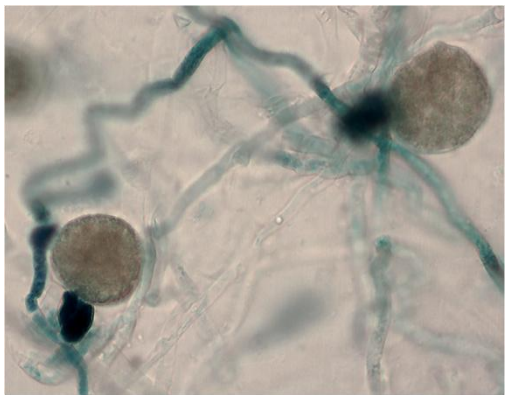	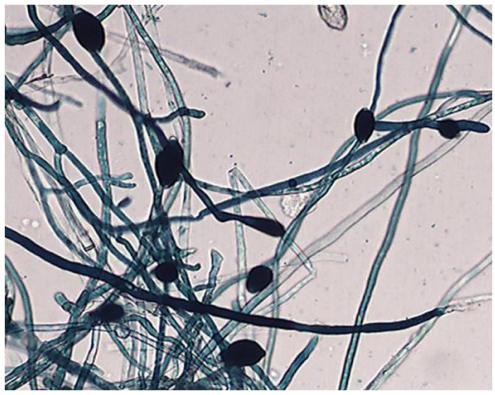
	15/20	15/20
Pum120	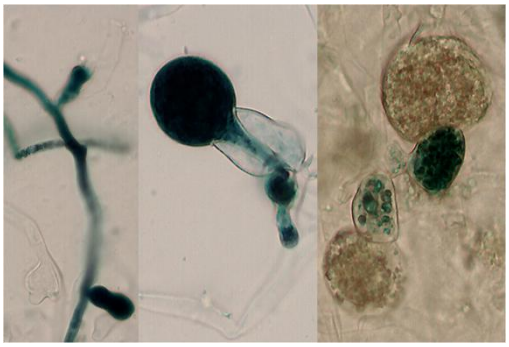	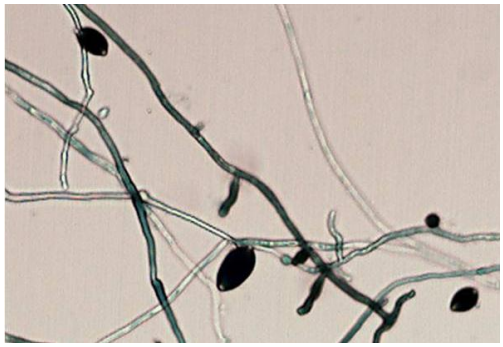
	18/20	19/20
Pum93	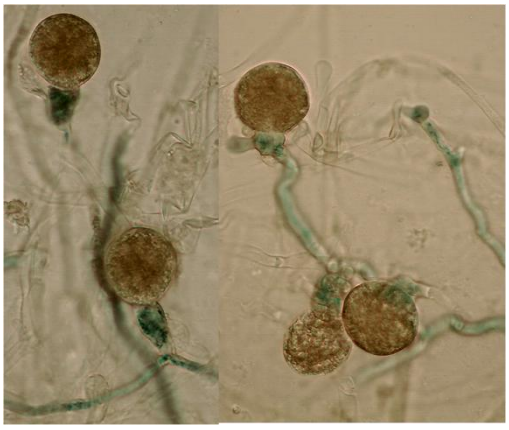	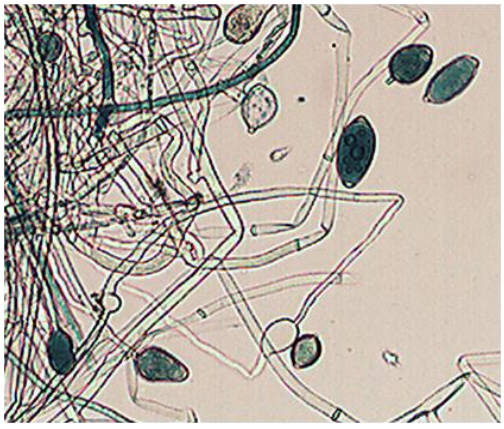
	4/12	4/12

Continue of Figure 1. 9

	M	A
Pum50	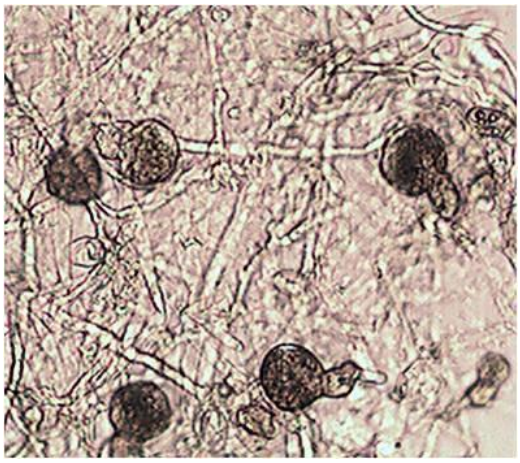	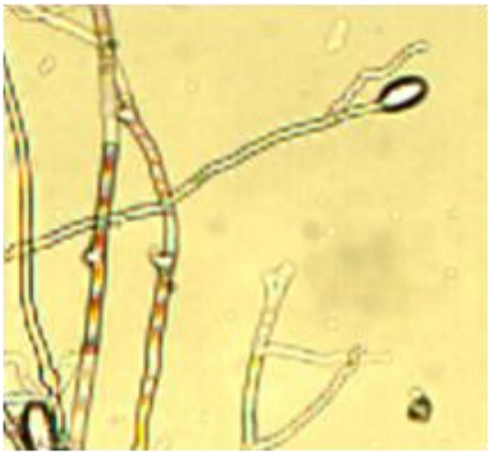
	0/20	0/20
Pum120-Nifs	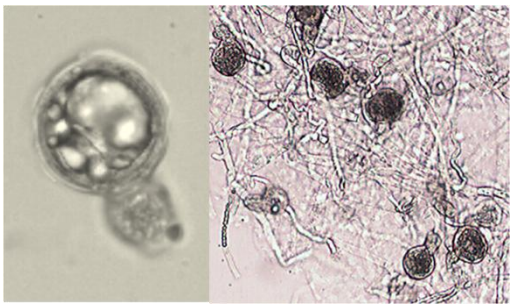	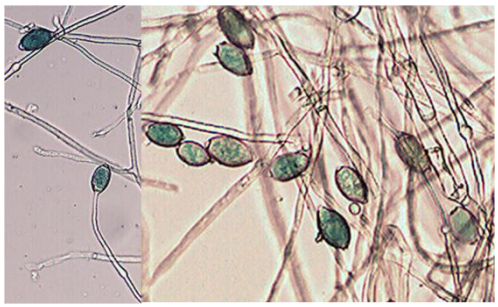
	1/14	7/14

Discussion

In this study, five *P. Infestans* mating-specific genes, PITG_02525, 01038, 01958, 11454, and 17302, were subjected to promoter analysis by examining their expression patterns in mating and in sporulating hyphae. Functional promoters of three genes of the genes, PITG_02525, PITG_01958 and PITG_17032, were cloned upstream of a GUS reporter in the pNPGUS vector and transformed into *P. infestans* to observe the resulting expression patterns.

Despite their diverse functions, these genes did share some of the general features that have been observed or predicted in prior studies (McLeod et al., 2004; Haas et al., 2009). Inr elements were found in all of the genes (data not shown). Consistent with the previous findings, Inr and FPR elements were identified residing around the TSS in four of the mating-specific genes (McLeod, Smart et al. 2004). However, in the PITG_00483 (*pum* promoter), Inr and FPR like elements were located 60 bp upstream of the TSS predicted by 5' RACE. This Inr-FPR region might indicate that another TSS can be used at a different stage, and it might be the reason that after deleting that region (between Pum93 and Pum50), the expression of GUS was abolished (Fig. 1.9).

The expression patterns of the full length promoters of PITG_02525, PITG_01958, PITG_17032 and Pum in mating tissues appeared to be identical to the histochemical staining study. We were not able to find a gene that matched a discrete development stage or a specific kind of sexual structure. This result indicated that these four genes are expressed at the same time and same location during sexual reproduction

in *P. infestans*, and it is very likely that they participate in the same set of signaling pathways and are regulated by common transcription factors. The higher probability of antheridia showing GUS expression could be explained by the sexual preference of the strain 88069 (A1), which probably tends to act as male when outcrossed with the A2 strain. This sexual preference of *P. infestans* strains was observed in a previous report (Judelson et al., 1993). It is worth noting that the preference of different A1 strains can be altered by environmental or experimental conditions such as the distance to the A2 strain during mating.

The PITG_02525 promoter was subjected to deletion analysis together with the promoter of PITG_00438 to identify key transcriptional regulatory components. In the PITG_02525 promoter, sequences were trimmed to down to only 49 bp, which contained the 24 nt core promoter elements, TSS, Inr, FPR, and SAAS. This 49-nt sequence was still able to activate the transcription. When the 31 nt core promoter region was deleted, transcription was blocked (Fig. 1.5, Del101 and Del70). In PITG_00483, Inr and FPR like elements did not appear be to immediately downstream of the TSS, but were 43 bp upstream of it. There was no SAAS-like element detected. The expression of GUS was also stopped in both mating tissue and sporulating tissue when these two elements were removed (Fig 1.9, Del93 and Del50). From the structure of these two promoters, it appeared that the core promoter elements, Inr+FPR, were essential for the transcription of both genes.

During the detailed analysis, the TCTTCTAA motif in the PITG_02525 promoter between the region of 215 bp and 169 bp upstream of ATG was examined. This is a

commonly found conserved motif in plant promoters (Barta et al., 2005) that might have a repressor function. Since GUS expression was increased in asexual tissues after removing this motif (Fig. 1.5. Del215 and Del196), it was speculated that the motif serves the role of repressing the gene's transcription during sporulation. However, fusing it with a sporulation specific chimeric promoter construct did not show that it was capable of suppressing GUS expression (Fig. 1.5, (1-2)-SPIP-*NIFS*). It is likely that there are more regulatory element(s) in addition to the TCTTCTAA motif that work together to suppress the activity of this promoter during sporulation. In fact, as long as the core promoter region remained, any deletion of the PITG_02525 promoter appeared to only increase gene's expression and eventually led to constitutive expression. It is possible that the transcription factor(s) that represses this elicitin-like gene is only absent in mating tissues where the gene is expressed. In hyphae and sporangia, the gene is usually in the repressed state.

The pumilio promoter was more complicated to study since this gene is involved in both sexual and asexual reproduction. There is the possibility that different motifs act at different stages, or that one motif plays different roles in two stages. At first, 5' deletions gradually increased the level of GUS expression. Strangely, when the promoter was trimmed down to about 200 bp, GUS expression abruptly stopped in both mating and asexual tissues (Fig. 1.9, Pum197). When another 30 bp region was removed, the expression restored (Fig. 1.9, Pum162). This suggests that that when deleting from 256 bp to 197 bp upstream of ATG, an important activator motif was removed, so that the transcription was eliminated. However, with the further deletion, the promoter might

have changed its structure and initiated from a new site to compensate for the loss of the activator. The fact that there was a set of core promoter-like elements sitting upstream of the experimentally detected TSS (30 bp away from ATG) suggested a potential alternative TSS. Further evidence was provided when the promoter was deleted to Pum93, which was immediately 5' of the region containing the Inr and FPR elements (at 93 to 77 bp upstream of ATG), as the transcription level started to decrease. The reduction of expression was probably due to inefficient transcription factor binding to the core promoter-like elements since there was not enough sequence for the factor(s) to bind. The theory was supported by the fact that if the core promoter like elements were deleted, GUS expression was abolished completely (Fig. 1.9, Pum50). However, to prove the theory, 5' RACE would be needed to confirm the altered TSS. The Inr and FPR like elements were fused with the*NIFS*-minimal promoter construct to see if it was able to drive the expression by itself. However, when only fusing this motif and some upstream sequences to the minimal promoter, no GUS expression was observed (not shown). This suggested that this motif could not work alone. The downstream region which contained the experimentally detected TSS and 5' UTR was then added back to the 3' end of this motif, and the whole fragment became the same truncated promoter sequence as in the Pum120 construct. This longer sequence was fused back with the Nifs-minimal promoter. The resulting construct was shown to be able to activate GUS expression during sporulation modestly, but not in mating tissues (Fig. 1.9, Pum120-Nifs). One possible explanation is that this fragment containing Inr, FPR, and TSS alone is enough to drive the expression of GUS during sporulation, but that other regulatory motifs located

downstream are needed to start transcription in oospores. This could be an example of a motif which could act differently during different developmental stages.

The five chosen genes were annotated to have different functions (Fig 1.1.A.), but a trend could be observed from the functional predictions. PITG_02525 has an N-terminal elicitin domain sequence (NCBI conserved domain database, *E*-value=2.33 e^{-21}), and thus it was predicted to encode an elicitin-like protein. As discussed earlier in this report, many elicitin family proteins have sterol and lipid binding functions. Since oosporogenesis happens in the late stage of the pathogen's life cycle, which occurs inside the host, and the pathogen should have entered its necrotrophic stage by then, increasing the expression of elicitins may facilitate the uptake of lipids and sterols from dead host tissues, in order to generate energy through fatty acid oxidation for oosporogenesis. PITG_01038 was predicted to have two ankyrin repeat domains (NCBI conserved domain database, *E*-value=6.49e^{-04}) that mediate protein-protein interactions and transportation, and a RING finger binding domain (NCBI conserved domain database. *E*-value=2.40e^{-06}) that is also involved in protein-protein interactions. Even though the function of the gene has not been proved by scientific experiments, one can speculate that it belongs to a protein family involved in protein-protein interaction and transporting proteins into oospores. PITG_11454 encodes dynamin, which is involved in the forming of vesicles for protein transport across membranes. The up-regulation of these three genes indicated that during oosporogenesis, protein binding and transportation are very important pathways. This is probably due to the fact that oospores are storage and

survival structures, and many proteins needed for germination are being sorted and transported.

None of the proteins encoded by these genes were found in the oospore proteomics study presented in the third chapter. However, the materials for the proteomics study were 30-day-old matured oospores, whereas this study and the previous microarray study (Prakob & Judelson, 2007) were performed on 10-day-old that contain both initiating sexual structures andyoung oospores. The genes transcribed at this early stage probably are involved in oosporogenesis instead of germination, which was what the mature oospore proteins were stored for.

By identifying TSS and 5' UTR features, this study suggested that mating-induced genes possess similar promoter structures as most identified oomycete genes (Pieterse et al., 1994). Also, by comparing the expression patterns and identifying regulatory components of selected mating-induced genes, this study revealed part of the complex signaling pathway cascades used during reproduction in *P. infestans*. The genes show the same expression patterns, so possibly participate in related pathways.

References

Agrios, G. N. (2004). Plant Pathology, Academic Press.

Ah-Fong, A. M., C. A. Bormann-Chung, and H. S. Judelson (2008). "Optimization of transgene-mediated silencing in *Phytophthora infestans* and its association with small-interfering RNAs." Fungal Genet Biol **45**: 1197-205.

Andersson, B., M. Sandstrom, and A. Strömberg (1998). "Indications of soil borne inoculum of *Phytophthora infestans*." Potato Res **41**: 305-310.

Andersson, M. G. and L. Cerenius (2002). "Pumilio homologue from *Saprolegnia parasitica* specifically expressed in undifferentiated spore cysts." Eukaryot Cell **1**: 105-111.

Barta, E., E. Sebestyen, T. B. Pálfy, G. Tóth, C. P. Ortutay, and L. Patthy (2005). "DoOP: Databases of Orthologous Promoters, collections of clusters of orthologous upstream sequences from chordates and plants." Nucl Acids Res **33**: D86-90.

Blein, J. P., P. Coutos-Thévenot, D. Marion, and M. Ponchet (2002). "From elicitins to lipid-transfer proteins: a new insight in cell signalling involved in plant defence mechanisms." Trends Plant Sci **7**: 293-296.

Cvitanich, C. and H. S. Judelson (2003). "A gene expressed during sexual and asexual sporulation in *Phytophthora infestans* is a member of the Puf family of translational regulators." Eukaryot Cell **2**: 465-473.

Cvitanich, C. and H. S. Judelson (2003). "Stable transformation of the oomycete, *Phytophthora infestans*, using microprojectile bombardment." Curr Genet **42**: 228-235.

Erwin, D. C. and O. K. Ribeiro (1996). *Phytophthora* diseases worldwide, American Phytopathological Society.

Fabritius, A. L., C. Cvitanich, and H. S. Judelson (2002). "Stage-specific gene expression during sexual development in *Phytophthora infestans*." Mol Microbiol **45**: 1057-1066.

Flier, W. G., L. P. N. M. Kroon, A. Hermansen, H. M. G. van Raaij, B. Speiser, L. Tamm, et al. (2007). "Genetic struture and pathogenicity of populations of *Phytophthora infestans* from organic potato crops in France, Norway, Switzerland, and the United Kingdom." Plant Pathol **56**: 562-572.

Goodwin, E. B. (2001). "Translational repression: Not just a Puf of smoke." Curr Biol **11**: R607-R609.

Haas, B. J., S. Kamoun, M. C. Zody, R. H. Y. Jiang, R. E. Handsaker, L. M. Cano, et al. (2009). "Genome sequence and analysis of the Irish potato famine pathogen *Phytophthora infestans*." Nature **461**: 393-398.

Jobson, R. D., M. Behr, and A. C. Cuming (1999). "Pumilio homology domain proteins: Plant relatives in an extended gene family." J Exp Bot **50**: 16.

Judelson, H. S., R. Dudler, et al. (1993). "Expression and antisense inhibition of transgenes in *Phytophthora infestans* is modulated by choice of promoter and position effects." Gene **133**: 63-69.

Judelson, H. S. and S. Roberts (2002). "Novel protein kinase induced during sporangial cleavage in the oomycete *Phytophthora infestans*." Eukaryot Cell **1**: 687-695.

Judelson, H. S., B. M. Tyler, and R. W. Michelmore (1991). "Transformation of the oomycete pathogen, *Phytophthora infestans*." Mol Plant Microbe Interact **4**: 602-607.

Kamoun, S., P. Hraber, B. Sobral, D. Nuss, and F. Govers (1999). "Initial assessment of gene diversity for the oomycete pathogen *Phytophthora infestans* based on expressed sequences." Fungal Genet Biol **28**: 94-106.

Kamoun, S., P. van West, A. J. de Jong, K. E. de Groot, V. G. Vleeshouwers, and F. Govers (1997). "A gene encoding a protein elicitor of *Phytophthora infestans* is down-regulated during infection of potato." Mol Plant Microbe Interact **10**: 13-20.

Kim, K. S. and H. S. Judelson (2003). "Sporangium-specific gene expression in the oomycete phytopathogen *Phytophthora infestans*." Eukaryot Cell **2**: 1376-1385.

McLeod, A., C. D. Smart, and W. E. Fry (2004). "Core promoter structure in the oomycete *Phytophthora infestans*." Eukaryotic Cell **3**: 91-99.

Mikes, V., M. L. Milat, M. Ponchet, P. Ricci, and J. P. Blein (1997). "The fungal elicitor cryptogein is a sterol carrier protein." FEBS Letters **416**: 190-192.

Murata, Y. and R. P. Wharton (1995). "Binding of pumilio to maternal hunchback mRNA is required for posterior patterning in *Drosophila* embryos." Cell **80**: 747-756.

Osman, H., V. Mikes, M. L. Milat, M. Ponchet, D. Marion, T. Prange, et al. (2001). "Fatty acids bind to the fungal elicitor cryptogein and compete with sterols." FEBS Letters **489**: 55-58.

Pieterse, C. M., P. van West, H. M. Verbakel, P. W. Brasse, G. C. van den Berg-Velthius, and F. Govers (1994). "Structure and genomic organization of the ipiB and ipiO gene clusters of *Phytophthora infestans*." Gene **138**: 67-77.

Prakob, W. and H. S. Judelson (2007). "Gene expression during oosporogenesis in heterothallic and homothallic *Phytophthora*." Fungal Genet Biol **44**: 726-739.

Qutob, D., E. Huitema, M. Gijzen, and S. Kamoun (2003). "Variation in structure and activity among elicitins from *Phytophthora soaje*." Mol Plant Pathol **4**: 119-124.

Škalamera, D., A. P. Wasson, and A. R. Hardham (2004). "Genes expressed in zoospores of *Phytophthora nicotianae*." Mol Genet Genomics **270**: 549-557.

Smale, S. T. and J. T. Kadonaga (2003). "The RNA polymerase II core promoter." Annu Rev Biochem **72**: 449-479.

Smart, C. D. and W. E. Fry (2001). "Invasions by the late blightpathogen: renewed sex and enhanced fitness." Biol Invasions **3**: 235-243.

Souza, G. M., A. M. da Silva, and A. Kuspa (1999). "Starvation promotes *Dictyostelium* development by relieving PufA inhibition of PKA translation through the YakA kinase pathway." Development **126**: 3263-3274.

Stargell, L. A. and K. Struhl (1996). "Mechanisms of transcriptional activation in vivo: two steps forward." Trends Genet **12**: 311-315.

Tani, S., E. Yatzkan, and H. S. Judelson (2004). "Multiple pathways regulate the induction of genes during zoosporogenesis in *Phytophthora infestans*." Mol Plant Microbe Interact **17**: 330-337.

Wharton, R. P., J. Sonoda, T. Lee, M. Patterson, and Y. Murata (1998). "The Pumilio RNA-binding domain is also a translational regulator." Mol Cell **1**: 863-872.

White, E. K., T. Moore-Jarrett, and H. E. Ruley (2001). "PUM2, a novel murine Puf protein, and its consensus RNA-binding site." RNA **7**: 1855-1866.

Wickens, M., D. S. Bernstein, J. Kimble, and R. Parker (2002). "A PUF family portrait: 3'UTR regulation as a way of life." Trends Genet **18**: 150 - 157.

Wobbe, C. R. and K. Struhl (1990). "Yeast and human TATA-binding proteins have nearly identical DNA sequence requirements for transcription in vitro." Mol Cell Biol **10**: 3859-3867.

Xiang, Q., K. S. Kim, S. Roy, and H. S. Judelson (2009). "A motif within a complex promoter from the oomycete *Phytophthora infestans* determines transcription during an intermediate stage of sporulation." Fungal Genet Biol **46**: 400-409.

Chapter II

Developing a tandem affinity purification system for protein interaction studies using a translational regulator, PUMILIO.

Abstract

Identification of the targets and partners of post-transcriptional regulatory proteins during the various reproductive stages of lower eukaryotes is crucial for deciphering the regulatory pathways involved in their life cycles. In order to study protein-RNA, or protein-protein interactions in *Phytophthora infestans*, arguably the most important plant pathogen in the human history, we used PUMILIO (Pum) as a model to develop the system. Pum is a member of the evolutionarily conserved Puf family of RNA-binding proteins that repress gene expression post-transcriptionally. In *P. infestans*, *pum* is dramatically up-regulated both during the mating stage and asexual sporulation.. An *in vitro* binding affinity system using the maltose-binding protein tagged RNA binding domain (RBD) of Pum and an *in vivo* binding system with the RBD fused with a tandem affinity purification tag (TAP-tag) were tested. The TAP-tag was designed with *P. infestans* codon bias. While the *in vitro* binding assay did not yield insightful information, the Pum RBD with a potential binding partner was successfully purified using the TAP-tag method. The system is adaptable to future studies of other protein interactions.

Introduction

Sexual sporulation and asexual sporulation are central to the life cycles of many lower eukaryotes. Both sexual and asexual spores are the main agents of survival and dispersal for many species. However, detailed molecular analyses of pathways that regulate these stages have been performed only for a few groups in animals, plants and true fungi such as *Arabidopsis* and *Saccharomyces* (Casselton, 2002; Lee et al., 2006; Keene, 2007). In higher organisms, the importance of gene expression control at the translational level in directing development has been clearly demonstrated. Some of these post-transcriptional regulation mechanisms play an important part in determining when and where specific proteins are made, and are heavily used during early embryonic and germ-line development in a large number of organisms (Goodwin, 2001). Many proteins that bind to mRNAs or proteins to activate or repress their expression have been identified in humans, animals and plants (Zamore et al., 1997; Forbes & Lehmann, 1998; Moore et al., 2003; Merritt & Seydoux, 2010). In spite of their significance, information about such regulatory components is very limited and poorly studied for most of the lower eukaryotes, including oomycetes.

Understanding the regulatory machinery involved in the early reproductive stages of *P. infestans* is of particular interest as it may help us to design strategies to interrupt the most important parts in the life cycle of this economically important pathogen, and thereby help us better control late blight.

Researchers have been spending a tremendous amount of effort to characterize proteins that regulate gene expression post-transcriptionally. Among them, a well known and relatively well studied mRNA-binding family, Puf, has drawn much attention. The family was named after the first two members identified: *Drosophila* Pumilio and *Caenorhabditis elegans* FBF mRNA binding factor (Murata & Wharton, 1995; Jobson, Behr et al., 1999). All members of this family have a conserved functional domain consisting of eight repeat motifs with binding activity for mRNA 3'untranslated region (UTRs). These proteins share the general function of repressing the translation of target mRNAs either by accelerate RNA turnover, or by recruiting targets to different locations to prevent them from being translated (Wharton et al., 1998; Souza et al., 1999; Goodwin, 2001; White et al., 2001; Wickens et al., 2002). Puf family proteins have been reported to have different targets and binding partners in different organisms. In *Xenopus*, *Drosophila*, and *C. elegans*, Pum binds to cyclin B, a cell cycle regulator, whereas in yeast it is bound up with *HO* mRNA and controls mating type switching (Parisi & Lin, 1999; Sonoda & Wharton, 1999; Nakahata et al., 2001; Subramaniam & Seydoux, 2003). In *Saprolegnia parasitica*, another oomycete, *pum* is specifically expressed in asexual spores where it is present only in cysts and decays as soon as cysts germinate (Andersson & Cerenius, 2002). In *P. infestans*, *pum* is one of the genes that are dramatically up-regulated during mating stage and sporulation. During sexual development in *P. infestans*, *pum* RNA is present in both male and female structures, and during sporulation, *pum* is expressed in sporangia and young sporangiophores (Cvitanich & Judelson, 2003).

Hypothetically, its involvement in reproductive pathways may be to promote meiosis or arrest mitosis through some cell-cycle regulators, such as cyclin B.

Pum has served as a prototypic model for researchers interested in post-transcriptional regulation of gene expression, and many methods have already been developed to identify its cognate RNA or other binding partners. Crystal structure analyses of the eight RNA-binding repeats have provided detailed biochemical knowledge of Pum, and demonstrated the binding affinity of RNA sequences to the RBD (Edwards et al., 2001; Jenkins et al., 2009). Many techiques have been used to study the function of Pum including: loss of function studies, immunoprecipitation assays, affinity purification followed by differential display or microarray or cDNA library, SELEX, Ribonucleoprotein-ImmunoPrecipitation Microarray (RIP-Chip), and tandem affinity purification (Gamberi et al., 2002; Gu et al., 2004; Fox et al., 2005; Gerber et al., 2006; Dallagiovanna et al., 2008; Galgano et al., 2008). These methods have helped to identify the binding partners of Pum in some organisms, and with the aid of bioinformatics tools, consensus RNA binding sequences have also been discovered (Guindon & Gascuel, 2003; Gerber et al., 2006; Galgano et al., 2008; Kaye et al., 2009).

In order to establish tools to characterize the functions and binding specificities of translational regulatory proteins in *P. infestans*, we used the Pum RBD as the model. Firstly, a column binding assay of recombinant Pum RBD and *P. infestans* mating mRNA followed by differential display and cDNA library construction of the bound RNAs was tested. Secondly, stable transformants of *pum*-silenced strains were generated to determine the phenotypes associated with loss of *pum*. Finally, tagging the tandem

affinity purification (TAP) tag to the RBD was performed, and RBD was successfully purified after two affinity purifications, together with some potential helper proteins.

Materials and methods

Culture conditions and strains of *Phytophthora infestans*

P. infestans isolates 1306 (A1 mating type, United States), and 88069 (A1, The Netherlands) and their transformants were cultured on rye A agar as described at 18 ℃ (Judelson et al., 1991). Sporulating hyphae were obtained from 10-day-old rye cultures.

Construction of *Pum*RBD affinity purification construct and protoplast transformation of *P. infestans*

Due to the insolubility of the complete recombinant protein, the PumRBD was used to generate all the constructs in this project. The RBD fragment was amplified by polymerase chain reaction from a previously made construct containing *pum* in pGEX-6P1 (Fabritius et al., 2002) with primers PUMRBDHIND3 5'-CAGTCAAGCTTTCAATAGTAGGTCGC and PUMRBDBAMH1 5'-CTGGGATCCTCCAACAGTCTGCTGGA. The amplicon was 1101 bp. The RBD was then inserted into pMALc2x (New England Biolabs (NEB) #N8076S) downstream of the

malE gene, which encodes maltose-binding protein (MBP), and transformed into *E. coli* strain BL21.

Transformation of the construct into *P. infestans* was performed using the protoplast method and G418 selection (Judelson, 1993).

Affinity purification and RNA extraction

Crude cell extraction of MBP-RBD expressing BL21 and the following affinity pull-down assay were executed according to the manufacturer's recommendations for the pMAL^{TM} Protein Fusion and Purification System. In general, BL21 cells containing the fusion plasmid were grown in 100ml Lysogeny broth (LB) until the A_{600} reading reached 0.5. IPTG was then added to a final concentration of 0.3 mM for a duration of 2 hr to induce protein expression. The culture was then sonicated five times for 15 seconds with 2 min between each burst and centrifuged at 5000 x *g* at 4℃ for 10 min. The concentration of the protein extract was determined by Bradford assay.

Approximately 700 µg of crude extract was treated with micrococcal nuclease at 200 U/ml at 37℃ for one hr, and incubated with 300 µl of amylose resin that was pre-equilibrated with column buffer (20 mM Tris-HCl pH 7.5, 200 mM NaCl, and 1 mM EDTA) once, and RNA binding buffer (RBB: 10 mM Tris-HCl pH 7.5, 150 mM KCl, 15 mM $MgCl_2$, 10U/µg RNase inhibitor (Invitrogen)) once, and RBB containing 0.5% Triton X-100 once, with protease inhibitor cocktail 1ml/30g tissue (Sigma P9599). Unbound protein was removed with ten 1 ml washes in RBB containing 0.5% Triton X-

100 and the washed beads were resuspended in 350 µl of RBB. 900 ng of *P. infestans* mating mRNA was passed through 40 µl of amylose resin, and then incubated with the RBD bound resin at 4°C for 1 hr, with the addition of 1 µg/µl heparin. The beads were then washed four times in RBB containing 0.2% Triton X-100 to remove unbound RNA, and boiled in 200 µl of TE (10 mM Tris-HCl pH 8, and 1 mM EDTA) containing 1% SDS for 3 min to release the RNA. The RNA was then phenol/chloroform-extracted, chloroform-extracted twice, ethanol-precipitated with 20 µg of glycogen, and washed with 70% ethanol. The RNA was dried and resuspended in 7 µl of RNase-free-water.

Differential display

The differential display method was carried as described (Liang & Pardee, 1998). Briefly, RNAs extracted from the previous step were reverse transcribed with one of three different 3' primers containing a stretch of 11 T nucleotides followed by an A, C, or G nucleotide. The first cDNA strand was amplified with the same 3' primers and 10 random 5' primers from GenHunter Corp and with the incorporation of ^{32}P-α-dCTP. The radioactively labeled PCR products were then resolved on 6% PAGE to profile the RNA population.

cDNA library construction

RNA obtained from the previous step was reversed transcribed using the Clontech SMART cDNA Library Construction Kit with Powerscript^{TM} RTase. The cDNA was packaged into λTripleX2 and then sequenced.

Silencing *pum*

Sense DNA sequence of the full length *pum* ORF (3 kb) was cloned into pTEP5 which contains a neomycin phosphotransferase gene that confers G418 resistance. The construct was transformed into *P. infestans* strain 1306 using protoplast transformation. The transformants were grown on 150-mm rye medium plates supplemented with 25 μg/ml G418 and 11 to 12-day-old sporulating hyphae were harvested. RNA was extracted from the sporulating tissue using the QIAGEN RNeasy Plant Mini Kit (#74904) and the manual from the kit was followed during extraction.

Northern blot analysis was then employed to examine the expression level of the pumilio gene. RNA blotting was performed with total RNA (5 μg) and 1.2% agarose/6.6% formaldehyde gels. The RNA was transferred to nylon membranes by capillary blotting in 10x SSPE (1.8 M NaCl, 0.1 M $NaHPO_4$, 0.01 M EDTA pH 7.7) and fixed by UV cross-linking. Hybridizations were performed with ^{32}P-labeled randomly primed probes. Probes were made from either *pum*, actin (*ActA*), elongation factor 1 α (*Ef1*), *Cdc14* (a sporulation-induced gene), or three genes that showed relatively stable expression levels

across different development stages (Pi003864 (PITG_18578), Pi004824 (PITG_00123) and Pi005393 (PITG_12277)). Signals were detected by phosphorimager analysis using the Quantity One software for Macintosh (Bio-Rad, Richmond, Calif). High-stringency washes were in 0.2 x SSPE, 0.2% (w/v) SDS, 0.1% (w/v) sodium pyrophosphate at 65 ℃. Low-stringency washes were in 1 x SSPE, 0.2% sodium dodecyl sulfate, 0.1% sodium pyrophosphate at 65 ℃.

Construction of pumilio RBD with tandem affinity purification tag expression vector

The coding sequence for the C-terminal tandem affinity purification (TAP)-tag was adapted from the previously described amino acid sequence (Rigaut et al., 1999) and the sequence was produced by GENEART Co. using the *P. infestans* codon usage preference (Randall et al., 2005). The TAP-tag consists of a calmodulin-binding peptide (CBP), followed by a TEV cleavage site, and then two copies of Protein A. The 826 bp *pum* native promoter was amplified from strain 88069 genomic DNA introducing EcoRI restriction enzyme sites on both ends with primers PumPrm5'EcoRI (5'-GAATTCCCGCCGCGTTGTGATCCC), and PumPrm3'EcoRI (5'-GAATTCGGGCGGTTGCTGGGTGTC), and then introduced into pTOR. RBD (1206bp) was amplified from strain 88069 genomic DNA as well, with primers PumHD5'EcoRI (5'-CTGAATTCTCCAACAGTCTGCTGGA) and PumHD3'HindIII (5'-AAGCTTATAGTAGGTCGCCTGCT) and cloned into pGEMT-EZ. The TAP fragment

was amplified from the GENEART Co. construct first with primers Tag5'HindIII (5'-ATAAGCTTTCGATCGAGAAGCGCC) and Tag3'HindIII (5'-ATAAGCTTTCATTACGTCGACTTGC), and then inserted into pGEMT-EZ downstream of the RBD. RBD and TAP were excised from pGEMT-EZ with EcoRI and SpeI and transformed into pTOR downstream of the *pum*native promoter. The 5' HAM promoter on the pTOR vector was then removed, but the 3'HAM terminator was retained. The TAP fragment was also introduced into pTOR by itself, between EcoRI and SpeI sites, using the 5' HAM promoter and 3' HAM terminator, to serve as the control in this experiment.

The resultant plasmids, PumTAP-tag and pXTAP, were introduced into zoospores released from 10-day-old cultures of strain 88069 of *P. infestans* by electroporation transformation (Blanco & Judelson, 2005). Expressions of RBD-TAP fusion protein and TAP in transformants were verified by Western blot.

SDS-PAGE and Western blot

Stacking and separateing gel master mix buffers were prepared according to Current Protocols in Molecular Biology (Ausubel et al., 1994), and 10% SDS-PAGE was used to resolve 1 µg of crude extracts from each transformant.

The proteins were transferred from SDS-PAGE to Hybond membranes overnight at 15 V in transfer buffer (1. 25 mM Tris pH 8.3, 192 mM glycine, and 20% methanol) at 4 ^{o}C. The membranes were then blocked with 1x PBS (10 mM sodium phosphate, pH 7.2, 0.9%

(w/v) sodium chloride) with 5% dry milk overnight at 4 ^{o}C. After blocking, without washing, the membrane was placed in 1x PBS with chicken IgY antibody in a 1:1000 dilution and incubated for 1hr at room temperature. After the primary antibody incubation, the membrane was washed three times with 1x PBS for 15 min each, and then washed 3 times for 5 min each time with 1x PBS with 0.1% Tween. The membranes were then incubated for 1 hr in 1x PBS with 0.1% Tween with the secondary antibody, anti-chicken-HRP in a 1:1000 dilution. After the secondary incubation the membrances were washed rapidly three times with 1x PBS with 0.1% Tween and then washed three to four times for 20 min every time. The membranes were developed using ECL Plus Western Blotting Detection Reagents (GE Health) according to the manufacturer's protocol. The signal was detected by AFP MiniMed-90 film processor (Cat. 9992305300-u).

Tandem affinity purification

Eleven day old sporulating hyphae were collected after growing each transformant on a 150 mm rye medium plate, and were ground with a mortar and pestle in liquid nitrogen.

7 g of sporulating hyphae from each construct were used in the first run of affinity purification and 15 g in the second run. Ground samples were suspended in 15 ml of buffer A (20 mM Tris-HCl, pH 8.0, 150 mM NaCl, 10 mM EDTA, pH 8.0, 0.2% Nonidet P-40, 0.02 mg/ml heparin, 1.5 mM DTT, 1 mM PMSF, 0.5 µg/ml leupeptin, 0.8 µg/ml pepstatin, 20 units/ml DNase I, 100 units/ml Rnasin (Promega)). The suspension was

centrifuged twice at 4 ℃ and 10,000 × *g* for 10 min. The lipid layer on top was aspirated off after each centrifugation. Cleared extract (12.5 ml) was incubated with 200 µl of a slurry (50% v/v) of IgG-agarose beads (Sigma) for 90 min at 4 ℃. The beads were washed once with buffer A for 15 min at 4 ℃, and three times for 15 min at 4 ℃ with buffer B (20 mM Tris-HCl, pH 8.0, 150 mM NaCl, 1 mM EDTA, pH 8.0, 10% glycerol, 0.01% Nonidet P-40, 1 mM DTT, 10 units/ml RNasin). RBD and the calmodulin-binding-peptide together with the cognate RNAs were released from beads by incubation with 150 units of AcTEV protease (Invitrogen) for 2 h at room temperature. The cleaved product was then passed through 100 µl of calmodulin Sepharose 4B slurry (50% v/v). The eluates from the second purification were resolved by 10% SDS-PAGE. RNA was isolated from eluates containing the RBD using TRIzol reagent (Invitrogen) followed by the RNeasy Mini kit (Qiagen) according to the manufacturer's protocols.

Results

Expression of the MBP-RBD fusion protein

Pum RBD was initially expressed using the pGEX-6P1 system in *E.coli* BL21 strain cells. However, after induction with IPTG, the expressed fusion protein was detected in the insoluble fraction, and this occurred even when the induction was repeated at a lower temperature (28 ℃), and for a longer time (4hrs, results not shown). Therefore the RBD coding sequence was transferred into the pMAL-c2x system, tagged with the

42.5 kDa maltose binding protein (MBP). In this case the 78 kDa MBP-RBD fusion protein was detected in the soluble fraction of the crude extract (Fig. 2.1). After passing through the amylose resin, the fusion protein was purified fromthe crude extract.

Figure 2.1. Expression of the *P. infestans* Pum RBD in the pMAL-c2x system induced by IPTG and purified through amylose resin. Subsamples from cells before induction, two hours after induction, total extract after sonicating, soluble extract, insoluble extract and purified MBP-RBD fusion proteinwere analyzed on 10% SDS-PAGE.

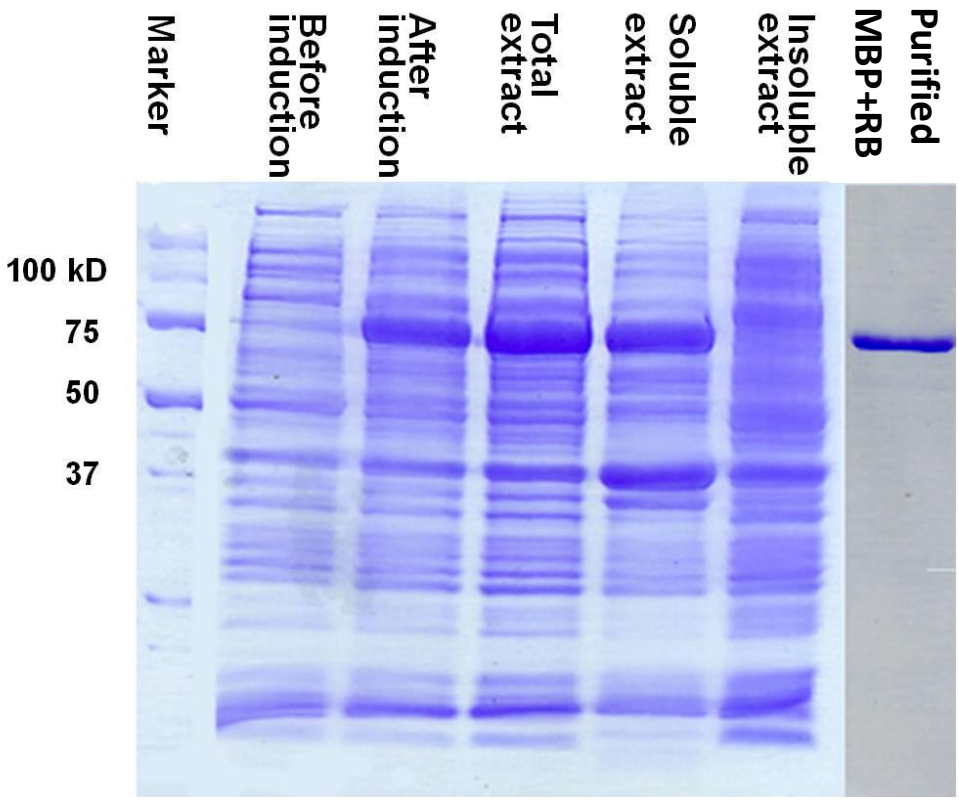
Marker
Before induction
After induction
Total extract
Soluble extract
Insoluble extract
Purified MBP+RB
100 kD
75
50
37

Differential display assay of affinity purified Pum-bound RNA

150 μg mRNA was extracted from mating tissue and sporulating tissue of *P. infestans*, and incubated with the amylose-bound fusion protein, extracted and analyzed. A total of 0.5 μg and 0.8 μg of mRNA were obtained from the mating and nonsporulating RNA pull-down.

A differential display assay was initially employed to compare the differences between the two eluates by resolving the two extracted RNA samples separated by denaturing PAGE. 20, 8, 4, and 2 ng of cDNA were reverse transcribed as described in Materials and Methods.

The amplification was first tested with asexual mRNA without the incorporation of ^{32}P-α-dCTP and the resulting products were resolved on a 1.5% agarose gel stained with SYBR Gold. No visible band was detected from the agarose gel in two attempts. To increase the sensitivity of detection, ^{32}P-α-dCTP was added to the cDNA amplification.

The radioactively labeled PCR products were resolved by 6% PAGE. However, after one hour exposure to the phosphorimager, no specific amplification was detected from any pair of the primers even after repeating the process (not shown).

cDNA library construction of affinity-purified Pum bound RNA

The strategy of constructing a cDNA library and sequencing the resulting constructs was tried next in order to identify RNAs from the affinity purification. Two

preliminary assays on *P. infestans* mating mRNA were carried to determine the sensitivity of reverse transcription for detecting low abundance RNA. Control total RNA at 900, 100, 10, 1, 0.01, and 0.0001 ng was reverse transcribed and amplified using the Clontech SMART cDNA construction kit with Powerscript^{TM} RTase. The results showed that a smear of cDNA ranged from 150 bp-4 kb can be detected from as little as 10 ng of RNA templates (Fig. 2.2.A). Another 100 ng of mRNA from the control RNA was reverse transcribed after incubating and boiling with amylase resin to confirm the presence of intact mRNA after boiling and eluting the RNA from the column (Fig. 2.2.A).

900 ng of *P. infestans* mating mRNA was used to perform the binding assay. The RNA was dried and resuspended in 3 µl of RNase-free-water and cDNA was then packaged into phage. Screening of 138 phage plaques identified inserts of ranging from 50-3500 bp in size. Three bands with the sizes of 600 bp, 760 bp, and 3500 bp (Fig. 2.2.B) were selected and cloned into pGEMT-EZ and subjected to sequencing. However, sequencing of these plaques only yielded AT-rich sequences that could not be matched to the *P. infestans* database, which suggested that the cloned products might be PCR artifacts instead of real RNA targets.

Since *in vitro* binding assays did not yield insights about the target RNAs of Pum, we then constructed silencing constructs in order to directly observe the loss of function phenotypes.

Figure 2.2. cDNA library construction of mRNA obtained from the MBP-RBD affinity binding assay. (A) Sensitivity assays of reverse transcription on low quantity of RNA. 900, 100, 10, 1, 0.1, 0.01, 0.001 and 0.0001 ng of mRNA were reversed transcribed into cDNA and amplified with Clontech SMART cDNA Library Construction. In another assay (last lane), 100 ng of mRNA was mixed with amylose resin and boiled, then extracted and reserve transcribed. (B) PCR of phage plaques packaged with cDNA made from Pum-bound mRNA. Circled bands were cloned into pGEMT and sequenced.

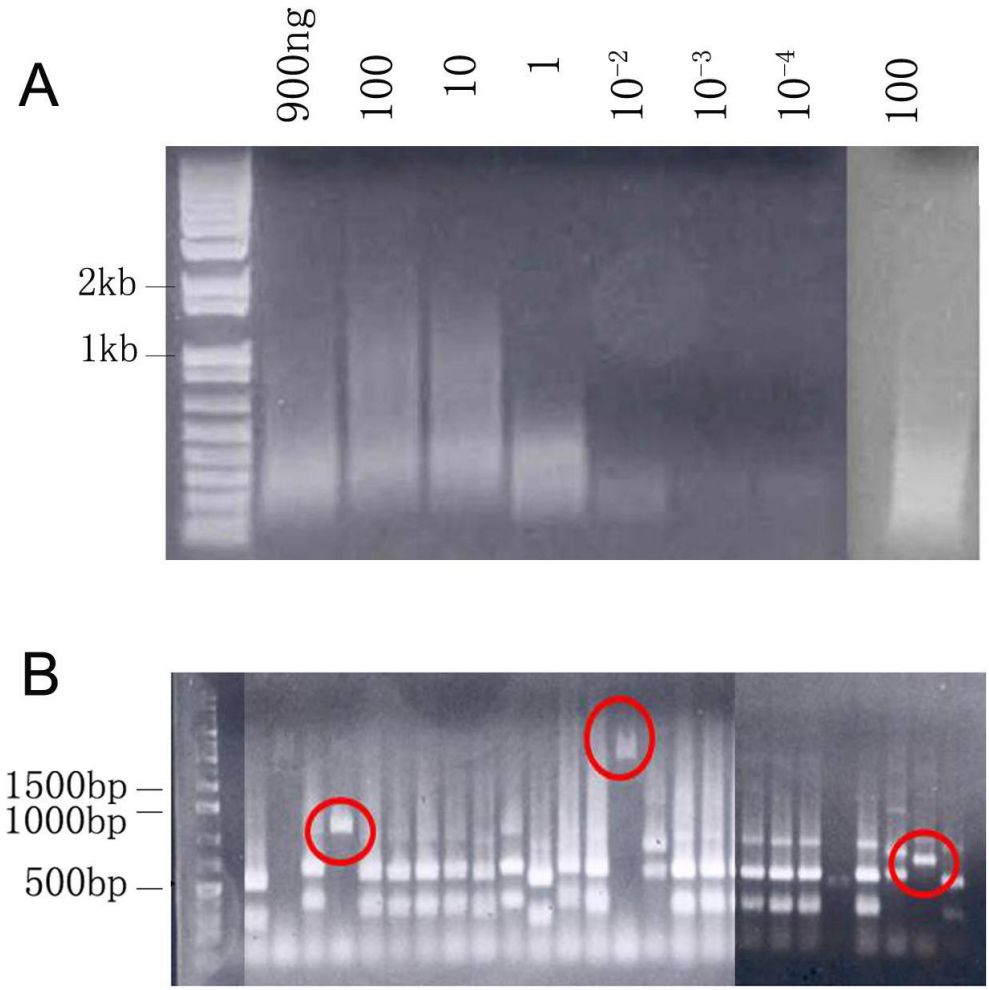
A
900ng
100
10
1
10⁻²
10⁻³
10⁻⁴
100
2kb
1kb
B
1500bp
1000bp
500bp

Silencing of *pum*

In order to directly observe the phenotype of *pum*-silenced strains, a silencing construct was developed. In *P. infestans*, the use of a sense open reading frame (ORF) was reported to function better than antisense ORF in inducing silencing, and protoplast transformation shown to be better than electroporation transformation (Ah-Fong et al., 2008). Therefore, the full length pumilio ORF was cloned into vector pTEP5 and transformed into strain 1306 by protoplast transformation in an attempt to generate stable *pum* silenced transformants. A total of 540 transformants were generated and their *pum* expression was screened by Northern blot using *pum-RBD* as probe. Only one silenced strain, number 29, was obtained (Fig. 2.3.A). Silencing of this strain was confirmed by extracting RNA from another fresh culture and blotting with *pum-RBD* and *Ef1* (data not shown). Preliminary observations showed the silenced strain has normal asexual growth, but no sexual spores were produced. However, this strain ceased to grow after being subcultured for several passages.

Besides strain 29, transformant 235 also showed a weak signal when hybridizing with the *pum-RBD* probe in RNA blots in multiple independent assays (Fig. 2.3.B and C). It grows much slower than the wild type 1306 strain (about 25% of the normal growth rate), and the culture was cotton like, with denser aerial hyphae, but producing fewer sporangia. However, since the signals of the control genes were also low in the RNA blot (Fig. 2.3.C), it was not considered as a true silenced strain.

The transcription levels of three additional genes were measured in cultures of different ages (11 days, and 14-15 days) to examine if they can be served as internal

control genes for *pum*, since these genes showed relatively stable expression throughout the different developmental stages of *P. infestans* and *P. phaseoli* in the microarray study (Prakob & Judelson, 2007). Unfortunately, none of these three genes showed concordance with the expression pattern of the pumilio transformants (Fig. 2.3.C). When *pum* showed relatively stable expression across the samples, the other genes fluctuated dramatically.

Figure 2.3. Identification of *pum* silenced strains. (A) Screening *pum* silencing transformants by Northern blots with *Ef1* as the expression control. (B) Screening *pum* silencing transformants by Northern blots using *Cdc14* as the expression control and ribosomal RNA (rRNA) as loading control. (C) Comparison of the expression level of *pum* to that of Pi003864, Pi004824 and Pi005393 in 10 *P. infestans* transformants generated by protoplast transformation of sense ORF of *pum*. Expression patterns were compared with transformants cultured for 11 days (11-d-o) and/or 14 or 15 days old (14-d-o, 15-d-o).

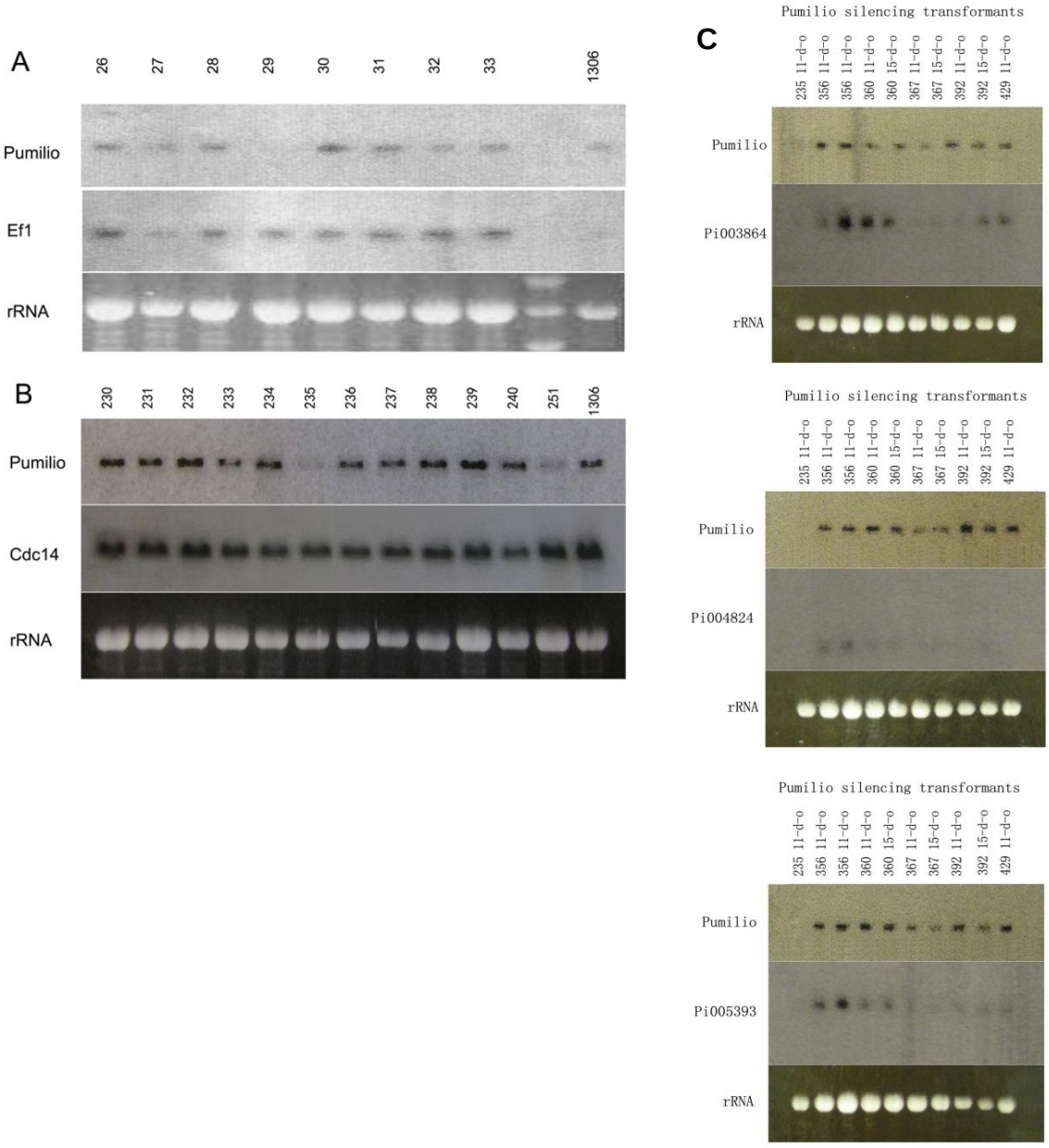
A
26
27
28
29
30
31
32
33
1306
Pumilio
Ef1
rRNA
B
230
231
232
233
234
235
236
237
238
239
240
251
1306
Pumilio
Cdc14
rRNA
C
Pumilio silencing transformants
235 11-d-o
356 11-d-o
356 11-d-o
360 11-d-o
360 15-d-o
367 11-d-o
367 15-d-o
392 11-d-o
392 15-d-o
429 11-d-o
Pumilio
Pi003864
rRNA
Pumilio silencing transformants
Pumilio
Pi004824
rRNA
Pumilio silencing transformants
Pumilio
Pi005393
rRNA

TAP-tag purification of Pum bound RNA

The TAP-tag was constructed according to previous studies (Gerber et al., 2006). The TAP-tag fragment was generated by GENART Inc. using *Phytophthora* codon bias (Fig. 2.4.A). The TAP-tag was fused at the C-terminus of the Pum RBD and terminated with the 3' HAM terminator. The native *pum* promoter was fused in front of the tag to minimize the impact on the microorganism. The whole cassette was cloned into pTOR vector with the 5' HAM promoter removed. The resulting construct was called PumTAP-tag (Fig. 2.4.C, upper panel). Meanwhile, a TAP-tag fragment without the Pum RBD was cloned into pTOR under the control of 5' HAM and the 3' HAM terminator. This construct served as a control for any nonspecific binding. This control construct can also be used as the backbone for constructing vectors for use in future protein interaction assays. Protein functional domains can be tagged at either the N-terminus or C-terminus with the provided enzyme sites (Fig. 2.4.C, lower panel). This construct was later named pXTAP.

The two constructs were transformed into strain 88069 (A1) by electroporation. A total of 45 transformants were obtained for the PumTAP-tag construct and 21 transformants for the pXTAP construct. Crude protein extracts were made from eight arbitrarily selected transformants using Buffer A (Materials and methods). 10 g of each extract was examined for tag expression by Western analysis using chicken IgY as the primary antibody and anti-chicken HRP as the secondary antibody (Fig. 2.4.D). PumTAP-tag-expressing transformant number 5 and pXTAP expressing transformant number 1 were cultured for column pull-down assays.

The TAP-tag purification procedure was designed and carried out as described in Fig. 2.4.B. A total protein extract was made from each strain and was passed through an IgG column, and then cleaved by TEV protease. The eluates were then each passed through a calmodulin column. To exclude the nonspecific binding proteins that bound to IgG and calmodulin columns, eluates after passing through only one of the two columns were saved (Fig 2.5.A, calmodulin only, and IgG only lanes). They were compared with eluates after two column purifications on SDS-PAGE and the bands that were present in all the eluates were considered as nonspecific binding proteins. Five fractions of eluates were obtained for each construct after two column purifications.

A protein band of 52 kDa unique to PumTAP-tag was detected, including the 43kDa Pum-RBD, and the 9kDa calmodulin-binding peptide. The PumTAP-tag protein started to be eluted from the second fraction was most abundant in the third fraction, and was completely eluted from the column after the fourth fraction (Fig. 2.5.A, PumTAP 2, 3, and 4). An unknown band with a size of 100k Da was unique to PumTAP-tag eluates (Fig. 2.5.A, PumTAP 2 and 3) as well, which may be a potential binding partner. TEV protease (about 28k Da) can also be seen being eluted from the columns (Fig. 2.5.B).

Fractions two to four of PumTAP-tag eluates were then combined and RNA was extracted from it. This RNA can be used for further analysis in constructing a cDNA library to identify potential Pum RNA targets.

A repetition of the whole assay was done in order to obtain a larger amount of Pum-binding RNA for the subsequent analysis. However, PumTAP-tag was not purified

from this second experiment, even though Western analysis proved that the PumTAP-tag fusion protein was still expressed in the transformants (data not shown).

Figure 2.4. The TAP strategy: rationale and expression. (A) Sequence and structure of the TAP tag. The various domains constituting the TAP tag are indicated. (B) Overview of the TAP procedure. (C) Constructs of the PumTAP-tag and pXTAP that were used for expression. Enzyme sites that were used to insert each fragment were indicated. (D) Western blots detecting the expression of PumTAP-tag and the pXTAP in *P. infestans*. 88069 was the untransformed wild type strain. Eight transformants from each construct were arbitrarily selected and subjected to the assay to detect the expression of the fusion proteins (upper half of each panel). SDS-PAGE from each assay (lower half of each panel) was stained by Coomassie brilliant blue R-250.

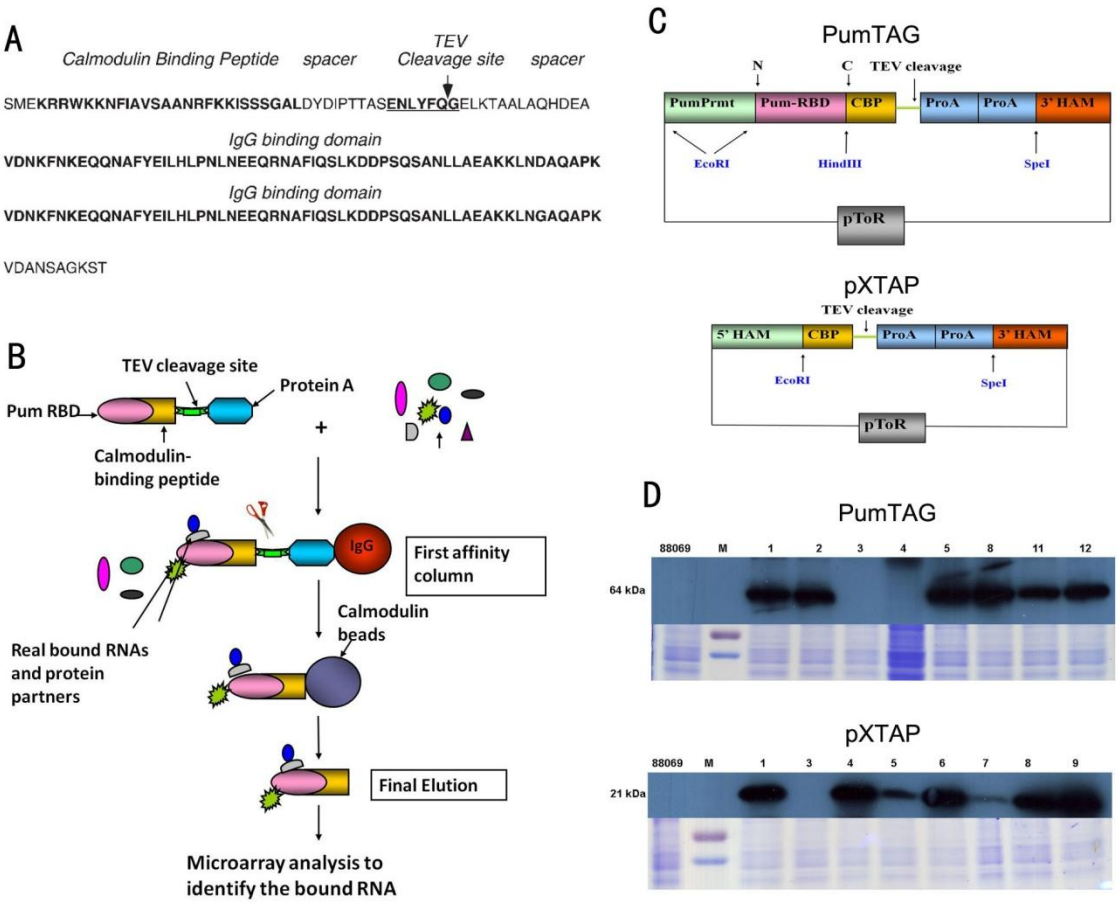
A
Calmodulin Binding Peptide
spacer
TEV
Cleavage site
spacer
SMEKRRWKKNFIAVSAANRFKKISSSGALDYDIPTTASENLYFQGELKTAALAQHDEA
IgG binding domain
VDNKFNKEQQNAFYEILHLPNLNEEQRNAFIQSLKDDPSQSANLLAEAKKLNDAQAPK
IgG binding domain
VDNKFNKEQQNAFYEILHLPNLNEEQRNAFIQSLKDDPSQSANLLAEAKKLNGAQAPK
VDANSAGKST
B
TEV cleavage site
Protein A
Pum RBD
Calmodulin-binding peptide
+
IgG
First affinity column
Calmodulin beads
Real bound RNAs and protein partners
Final Elution
Microarray analysis to identify the bound RNA
C
PumTAG
N
C
TEV cleavage
PumPrmt
Pum-RBD
CBP
ProA
ProA
3' HAM
EcoRI
HindIII
SpeI
pToR
pXTAP
TEV cleavage
5' HAM
CBP
ProA
ProA
3' HAM
EcoRI
SpeI
pToR
D
PumTAG
88069
M
1
2
3
4
5
8
11
12
64 kDa
pXTAP
88069
M
1
3
4
5
6
7
8
9
21 kDa

Figure 2.5. Results from the TAP assay. (A) Crude extracts from PumTAP-tag expressing and TAP-tag expressing transformants were passed through a calmodulin column only, or passed through IgG column only. Protein eluates of TAP-tag expressing transformant extracts passed through both columns are shown in lanes pXTAP 1-5. Protein eluates of PumTAP-tag containing extracts passed through both coulumns are shown in lanes PumTAP 1-5. (B) Pum-TAP-tag eluate after a second purification that contained the TEV, RBD+CBP (RNA binding domain + calmodulin binding protein) fusion, and an unknown protein (shown by the arrows) was compared to the eluate from expression of TAP-tag alone (pXTAP3).

A

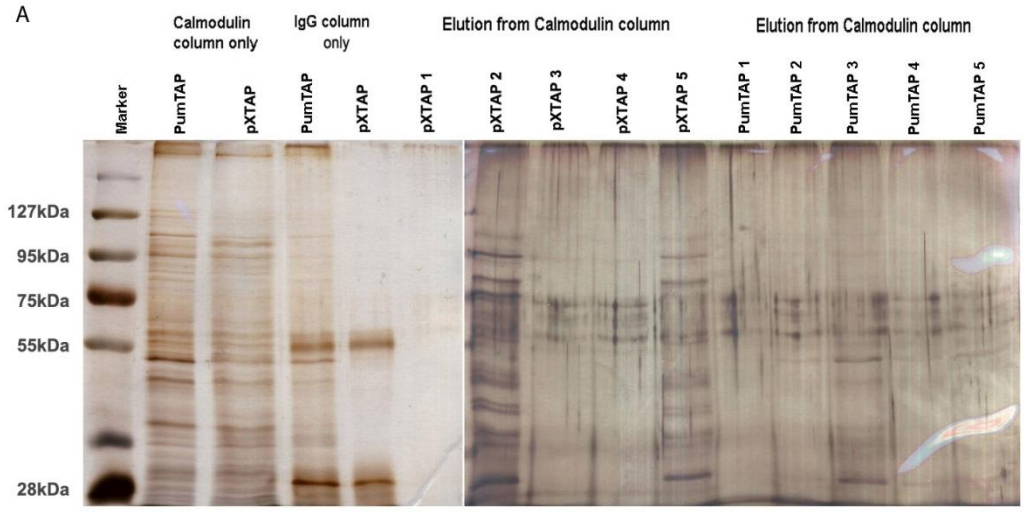
Calmodulin column only
IgG column only
Elution from Calmodulin column
Elution from Calmodulin column
Marker
PumTAP
pXTAP
PumTAP
pXTAP
pXTAP 1
pXTAP 2
pXTAP 3
pXTAP 4
pXTAP 5
PumTAP 1
PumTAP 2
PumTAP 3
PumTAP 4
PumTAP 5
127kDa
95kDa
75kDa
55kDa
28kDa

B

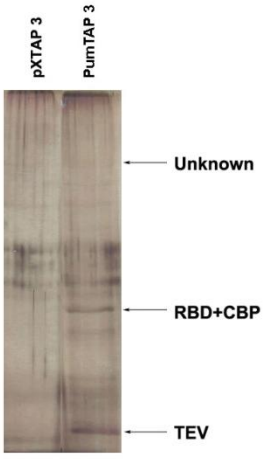
pXTAP 3
PumTAP 3
Unknown
RBD+CBP
TEV

Discussion

Three methods were tested in this study to establish a system for studying post-transcriptional regulatory proteins in *P. infestans* using a RNA-binding protein, Pum, as the model.

Firstly, an *in vitro* binding assay followed by two forms of RNA profiling was performed. RNAs were incubated with maltose binding protein tagged RBD and extracted from the amylose resin that the fusion protein was attached to. Similar strategies have been proven to be successful with RNA from other organisms (Fox et al., 2005; Chen et al., 2008), and artificially generated random RNA pools (Cheong & Hall, 2006; Lu et al., 2009). However, even when sensitivity reconstruction assays indicated that the amount of RNA and fusion protein we used in the experiments should have been sufficient (~50 times of minimum detection threshold) to detect specific bound RNAs, we failed to obtain any meaningful information from the cDNA pool. Since the activity of Pum in *P. infestans* was completely unknown, it is possible that it needs other chemical conditions or binding partners to bind to RNAs, and our *in vitro* assays did not provide the appropriate environment for the binding to be successful. Also, RNA is prone to degradation, so many technical problems may potentially underlying the problems in the *in vitro* assays.

We then tried to silence the only copy of this gene in *P. infestans* to directly obtain the phenotypes of a *pum* silenced strain. *Pum* has been silenced or mutated to lose its function in many other organisms, including human, *Drosophila*, *Caenorhabditis elegans*, and budding yeast (Forbes & Lehmann, 1998; Gamberi et al., 2002; Moore et al.,

2003; Gu et al., 2004). Some of these organisms have only one copy of *pum*-like *P. infestans*, such as *Drosophila*, and some have several copies, such as budding yeast. Silencing *pum* in *Drosophila* caused the symmetric development of the embryos, without cell differentiation (Macdonald, 1992) and in humans, which have two copies of *pum*, mutation leads to male sterility.

In *P. infestans*, we hypothesized that Pum binds to cell cycle regulators such as cyclin B to control the development of the reproduction structures. The one *pum*-silenced transformant did not initiate normal sexual structures after being mated with the compatible mating type, but could reproduce asexually similar to the wild type. However, this transformant did not survive for long. The low viability of this strain and our failure to generate other true silenced strains after screening 540 transformants suggested that *pum* may be essential to *P. infestans*. Other systems such as fusing an inducible promoter to the ORF may serve better for this purpose in order to maintain the viability of the microorganism. There has been research done on constructing tetracycline inducing system in *P. infestans* (Judelson et al., 2007), however, optimization of the system might be needed before applying it to *pum*.

Bioinformatic tools are increasingly important in the study of signaling pathways or proteomics data. In the previous work on yeast Puf proteins (Gerber et al., 2004), a consensus RNA-binding element was defined. The 8-nt core motif (UGUA(A/C/U)AUA) was conserved in the 3'UTRs of Pum target mRNAs in a number of systems (Wharton et al., 1998; Zamore et al., 1999; White et al., 2001; Gerber et al., 2006). We performed a

search for this motif in the region of 0 bp to 120 bp downstream of the stop codon of *P. infestans* expressed genes, and 297 genes were identified that possessed the motif.

Included among these 297 genes were a group of 10 major facilitator superfamily proteins (MFS) and three proteins belonging to the ATP-binding cassette (ABC) superfamily. While ABC family proteins are capable of transporting both small molecules and macromolecules in response to ATP hydrolysis, MFS proteins are single-polypeptide secondary carriers capable only of transporting small solutes in response to chemiosmotic ion gradients (Pao et al., 1998). Suppressing these transporters suggests a lower rate of metabolism, which is a major feature of the dormant oospores. Another interesting potential target, M96 (mating-specific protein 96), which encodes a low complexity extracellular protein that might be a component of *P. infestans* oospore walls, was found as well (Cvitanich et al., 2006). Both *M96* and *pum* are highly up-regulated during oosporogenesis, so Pum might be one of the regulators of *M96*. As mentioned previously, cyclin B was known to be one of the Pum targets, however, cyclin B in *P. infestans* did not contain the binding motif in its 3' UTR.

It was found that Pum in *Drosophila* needs binding partners to recruit the target RNA (Asaoka-Taguchi et al., 1999). In yeast, one of the Pum proteins is linked to the mitochore, a structure involved mitochondrial replication, and binds to the Arp2/3 complex, the force generator for actin-dependent mitochondrial movement. However, none of these partners had homologues in *P. infestans*.

Because of the difficulty in identifying pumilio binding partners *in vitro*, the tandem affinity purification (TAP) method was then employed in an attempt to detect *in*

vivo binding partners. This would allow Pum to be expressed in its natural cellular environment where it could function normally. The TAP-tag strategy has been suggested to allow rapid purification of complexes from a relatively small amount of cells without the necessity of intensive knowledge of the composition of target protein complex, activity or function. It involves creating a fusion protein with a designed sequence, the TAP tag, on either the N-terminus or the C-terminus of the expressed protein. Reports showed that the optimal ends for adding the TAP-tag differs in each organism (Rohila et al., 2004; Drakas et al., 2005; Gerber et al., 2006). The pXTAP system that we designed in this report was suitable for tagging either terminus and in the Pum study we employed a C-terminal tag.

One of the main obstacles to studying protein interactions is contamination of samples by nonspecifically bound substrates to either the tag or beads used in the experiment. We used *P. infestans* transformants expressing the TAP-tag alone to serve as the background control in order to be able to identify specific Pum interacting proteins and the specific Pum-binding RNA. These TAP-tag expressing strains are better controls than wild type *P. infestans* strains since nonspecific binding to the tag could also be detected.

We have shown that the TAP-tag system was able to purify fusion proteins with their potential partners, however, there is also the possibility that fusing a tag may change the folding of the protein and reduces its function. Further analysis of the eluted RNA is needed to confirm whether this TAP-tag affected the folding of the RBD.

References

Ah-Fong, A. M., C. A. Bormann-Chung, and H. S. Judelson (2008). "Optimization of transgene-mediated silencing in *Phytophthora infestans* and its association with small-interfering RNAs." Fungal Genet Biol **45**: 1197-205.

Andersson, M. G. and L. Cerenius (2002). "Pumilio homologue from *Saprolegnia parasitica* specifically expressed in undifferentiated spore cysts." Eukaryot Cell **1**: 105-111.

Ausubel F. M., R. Brent, R. E. Kingston, . D. Moore, J. G. Seidman, J. A. Smith, et al. (1994). Current Protocols in Molecular Biology. Wiley, New York

Blanco, F. A. and H. S. Judelson (2005). "A bZIP transcription factor from *Phytophthora* interacts with a protein kinase and is required for zoospore motility and plant infection." Mol Microbio **56**: 638-648.

Chen, G., W. Li, Q. S. Zhang, M. Regulski, N. Sinha, J. Barditch, et al. (2008). "Identification of synaptic targets of *Drosophila* pumilio." PLoS Comput Biol **4**: e1000026.

Cheong, C. and T. Hall (2006). "Engineering RNA sequence specificity of Pumilio repeats." Proc Natl Acad Sci USA **103**: 13635-13639.

Cvitanich, C. and H. S. Judelson (2003). "A gene expressed during sexual and asexual sporulation in *Phytophthora infestans* is a member of the Puf family of translational regulators." Eukaryot Cell **2**: 465-473.

Cvitanich, C. and H. S. Judelson (2003). "Stable transformation of the oomycete, *Phytophthora infestans*, using microprojectile bombardment." Curr Genet **42**: 228-235.

Dallagiovanna, B., A. Correa, C. M. Probst, F. Holetz, P. Smircich, A. M. de Aguiar, et al. (2008). "Functional genomic characterization of mRNAs associated with TcPUF6, a pumilio-like protein from *Trypanosoma cruzi*." J Biol Chem **283**: 8266-8273.

Drakas, R., M. Prisco, and R. Baserga (2005). "A modified tandem affinity purification tag technique for the purification of protein complexes in mammalian cells." Proteomics **5**: 132-137.

Edwards, T., S. Pyle, R. P. Wharton, and A. K. Aggarwai (2001). "Structure of Pumilio reveals similarity between RNA and peptide binding motifs." Cell **105**: 281-289.

Fabritius, A. L., C. Cvitanich, and H. S. Judelson (2002). "Stage-specific gene expression during sexual development in *Phytophthora infestans*." Mol Microbiol **45**: 1057-1066.

Forbes, A. and R. Lehmann (1998). "Nanos and Pumilio have critical roles in the development and function of *Drosophila* germline stem cells." Development **125**: 679-690.

Fox, M., J. Urano, and R. A. Reijo Pera (2005). "Identification and characterization of RNA sequences to which human PUMILIO-2 (PUM2) and deleted in Azoospermia-like (DAZL) bind." Genomics **85**: 92-105.

Galgano, A., M. Forrer, L. Jaskiewicz, A. Kanitz, M. Zavolan, and A. P. Gerber (2008). "Comparative analysis of mRNA targets for human PUF-family proteins suggests extensive interaction with the miRNA regulatory system." PLoS ONE **3**: e3164.

Gamberi, C., D. S. Peterson, L. He, and E. Gottlieb (2002). "An anterior function for the *Drosophila* posterior determinant Pumilio." Development **129**: 2699-2710.

Gerber, A., D. Herschlag, and P. O. Brown (2004). "Extensive association of functionally and cytotopically related mRNAs with Puf family RNA-binding proteins in yeast." PLoS Biol **2**: e79.

Gerber, A., S. Luschnig, M. A. Krasnow, P. O. Brown, and D. Herschlag (2006). "Genome-wide identification of mRNAs associated with the translational regulator PUMILIO in *Drosophila melanogaster*." Proc Natl Acad Sci USA **103**: 4487-4492.

Goodwin, E. B. (2001). "Translational repression: Not just a Puf of smoke." Curr Biol **11**: R607-R609.

Gu, W., Y. Deng, D. Zenklusen, and R. H. Singer (2004). "A new yeast PUF family protein, Puf6p, represses ASH1 mRNA translation and is required for its localization." Genes Dev **18**: 1452-1465.

Guindon, S. and O. Gascuel (2003). "A simple, fast, and accurate algorithm to estimate large phylogenies by maximum likelihood." Syst Biol **52**: 696-704.

Jaruzelska, J., M. Kotecki, K. Kusz, A. Spik, M. Firpo, and R. A. Reijo Pera (2003). "Conservation of a Pumilio-Nanos complex from *Drosophila* germ plasm to human germ cells." Dev Genes Evol **213**: 120-126.

Jenkins, H. T., R. Baker-Wilding, and T. A. Edwards (2009). "Structure and RNA binding of the mouse Pumilio-2 Puf domain." J Struct Biol **167**: 271-276.

Jobson, R. D., M. Behr, and A. C. Cuming (1999). "Pumilio homology domain proteins: Plant relatives in an extended gene family." J Exp Bot **50**: 16.

Judelson, H. S. (1993). "Intermolecular ligation mediates efficient cotransformation in *Phytophthora infestans*." Mol Gen Genet **239**: 241-50.

Judelson, H. S., R. Narayan, A. M. Ah-Fong, S. Tani, and K. S. Kim (2007). "Performance of a tetracycline-responsive transactivator system for regulating transgenes in the oomycete *Phytophthora infestans*." Curr Genet **51**: 297-307.

Judelson, H. S., B. M. Tyler, and R. W. Michelmore (1991). "Transformation of the oomycete pathogen, *Phytophthora infestans*." Mol Plant Microbe Interact **4**: 602-607.

Kaye, J. A., N. C. Rose, B. Goldsworthy, A. Goga, and N. D. L'Etoile (2009). "A 3'UTR pumilio-binding element directs translational activation in olfactory sensory neurons." Neuron **61**: 57-70.

Liang, P. and A. Pardee (1998). "Differential display. A general protocol." Mol Biotechnol. **10**: 261-267.

Lu, G., S. Dolgner, and T. M. Hall (2009). "Understanding and engineering RNA sequence specificity of PUF proteins." Curr Opin Struct Biol **19**: 110-115.

Macdonald, P. M. (1992). "The *Drosophila* pumilio gene: an unusually long transcription unit and an unusual protein." Development **114**: 221-232.

Merritt, C. and G. Seydoux (2010). "The Puf RNA-binding proteins FBF-1 and FBF-2 inhibit the expression of synaptonemal complex proteins in germline stem cells." Development **137**: 1787-1798.

Moore, F. L., J. Jaruzelska, M. S. Fox, J. Urano, M. T. Firpo, P. J. Turek, et al. (2003). "Human Pumilio-2 is expressed in embryonic stem cells and germ cells and interacts with DAZ (Deleted in AZoospermia) and DAZ-like proteins." Proc Natl Acad Sci U S A **100**: 538-543.

Murata, Y. and R. P. Wharton (1995). "Binding of pumilio to maternal hunchback mRNA is required for posterior patterning in *Drosophila* embryos." Cell **80**: 747-756.

Nakahata, S., Y. Katsu, K. Mita, K. Inoue, Y. Nagahama, and M. Yamashita (2001). "Biochemical identification of *Xenopus* Pumilio as a sequence-specific cyclin B1 mRNA-binding protein that physically interacts with a Nanos homolog, Xcat-2, and a cytoplasmic polyadenylation element-binding protein." J Biol Chem **276**: 20945-20953.

Parisi, M. and H. Lin (1999). "The *Drosophila* pumilio gene encodes two functional protein isoforms that play multiple roles in germline development, gonadogenesis, oogenesis and embryogenesis." Genetics **153**: 235-250.

Prakob, W. and H. S. Judelson (2007). "Gene expression during oosporogenesis in heterothallic and homothallic *Phytophthora*." Fungal Genet Biol **44**: 726-739.

Randall, T. A., R. A. Dwyer, E. Huitema, K. Beyer, C. Cvitanich, H. Kelkar, et al. (2005). "Large-scale gene discovery in the oomycete *Phytophthora infestans* reveals likely components of phytopathogenicity shared with true fungi." Mol Plant Microbe Interact **18**: 229-243.

Rigaut, G., A. Shevchenko, B. Rutz, M Wilm, M. Mann, and B. Seraphin (1999). "A generic protein purification method for protein complex characterization and proteome exploration." Nat Biotech **17**: 1030-1032.

Rohila, J. S., M. Chen, R. Cerny, and M. E. Fromm (2004). "Improved tandem affinity purification tag and methods for isolation of protein heterocomplexes from plants." Plant J **38**: 172-181.

Sano, H., M. Mukai, and S. Kobayashi (2001). "Maternal Nanos and Pumilio regulate zygotic vasa expression autonomously in the germ-line progenitors of *Drosophila melanogaster* embryos." Dev Growth Differ **43**: 545-552.

Sonoda, J. and R. P. Wharton (1999). "Recruitment of Nanos to hunchback mRNA by Pumilio." Gene Dev **13**: 2704-2712.

Souza, G. M., A. M. da Silva, and A. Kuspa (1999). "Starvation promotes *Dictyostelium* development by relieving PufA inhibition of PKA translation through the YakA kinase pathway." Development **126**: 3263-3274.

Subramaniam, K. and G. Seydoux (2003). "Dedifferentiation of primary spermatocytes into germ cell tumors in *C. elegans* lacking the pumilio-like protein PUF-8." Curr Biol **13**: 134-139.

Wharton, R. P., J. Sonoda, T. Lee, M. Patterson, and Y. Murata (1998). "The Pumilio RNA-binding domain is also a translational regulator." Mol Cell **1**: 863-872.

White, E. K., T. Moore-Jarrett, and H. E. Ruley (2001). "PUM2, a novel murine Puf protein, and its consensus RNA-binding site." RNA **7**: 1855-1866.

Wickens, M., D. Bernstein, J. Kimble, and R. Parker (2002). "A PUF family portrait: 3'UTR regulation as a way of life." Trends Genet **18**: 150-157.

Ye, B., C. Petritsch, I E. Clark, E. R. Gavis, L. Y. Jan, and Y. N. Jan (2004). "Nanos and Pumilio are essential for dendrite morphogenesis in *Drosophila* peripheral neurons." Curr Biol **14**: 314-321.

Zamore, P., J. Williamson, and R. Lehmann (1997). "The Pumilio protein binds RNA through a conserved domain that defines a new class of RNA-binding proteins." RNA **3**: 1421-1433.

Zamore, P. D., D. P. Bartel, R. Lehmann, and J. R. Williamson (1999). "The PUMILIO-RNA interaction: a single RNA-binding domain monomer recognizes a bipartite target sequence." Biochemistry **38**: 596-604.

Chapter III

Comparative proteomics study of oospores and nonsporulating hyphae of *Phytophthora infestans*

Abstract

Phytophthora infestans is a notorious plant pathogen that causes potato and tomato late blight. The sexual spores (oospores) of *P. infestans* are very important to the survival of this pathogen since the thick wall of this dormant structure can shield it from extreme environmental factors and chemicals, and the mating process diversifies the population by allowing recombination between the two mating types. Oospores were also proved to be able to initiate a disease cycle in a new growing season. In order to understand the biological and biochemical components and features of the mature oospores and provide knowledge on proteins that are important for oospore germination, a global proteomics comparison of the vegetative (nonsporulating hyphae (NSH)) and sexual (oospore) life stages of *P. infestans* was conducted to identify candidate proteins needed for oospore germination.

A total of 1115 proteins were identified from nonsporulating mycelium and 957 candidates from oospores were identified. Among them, 202 proteins were unique to NSH and 44 proteins were unique to oospores. A total of 17 functional classes of proteins were identified and all were present in both of the stages. Our study revealed that many

proteins or protein functional groups that are important to germination are more abundant in oospores. Enzymes participating in carbohydrate and fatty acid oxidation pathways are abundant in order to satisfy the intense need of energy during germination, and concentrated antioxidant and anti-stress proteins could be ready to function in protecting the germ tubes. The abundant secreted proteins identified could be involved in host infection or nutrient uptake. From these results, we propose that the proteins detected in oospores were synthesized during an earlier stage of oosporogenesis and stored in the mature oospore to facilitate germination.

Introduction

Phytophthora infestans, arguably the most notorious plant pathogen in the world, can reproduce both sexually and asexually. During a disease cycle, it is mainly the asexual life cycle that is responsible for rapid propagation and dispersal, however, sexual reproduction is essential for the pathogen's long-term survival.

P. infestans is heterothallic, which indicates that it needs two compatible mating types to sexually reproduce, A1 and A2 (Brasier, 1992). Sexual reproduction can be broken into two stages. The first stage is called gametogenesis or oosporogenesis. Under natural conditions, this stage starts about 5 to 6 days after inoculation of both of the mating types. In this period of time, two mating types sense the mating hormone from one other, and sexual structure differentiation begins. Male or female gametangia (antheridia and oogonia) develop while meiosis occurs, followed by oogonia penetrating

the antheridia, whereupon their nuclei fuse together. During nuclei fusion, the outer wall of the oospore develops first and the inner wall forms later. When the inner wall is accreted and a central ooplast vacuole develops, the oospore is in the process of reaching maturity (Beakes & Gay, 1978; Elliott, 1983; Drenth et al., 1995). Many metabolic processes are active during this stage since the cytoplasm can be seen packed with ribosomes and contains abundant endoplasmic reticulum, mitochondria and Golgi dictyosomes. A high level of protein production and transportation as well as energy production occurs at this stage. Most of the energy is stored as lipid, since large drops of lipids could be observed in the cytoplasm (Fukutomi et al., 1971; Beakes & Gay, 1978; Fox et al., 1983; Smirnov et al., 2008). When the inner wall forms, there is a reduction in number of mitochondria, and the Golgi apparatus disappears (Beakes & Gay, 1978; Drenth et al., 1995). This stage of oosporogenesis is completed in 24 hours to 48 hours. Oospores that were less than 19-day-old were considered young spores (Jiang et al., 1989).

The second stage of sexual reproduction in *P. infestans* is oospore maturation. Thick-walled mature oospores are detectable about 10 days after inoculation (Drenth et al., 1995). During this time, the cytoplasm of the mature oospore contains abundant, often whorled, fragments of membrane. These observations indicate considerable disruption of organelles during oospore maturation and that minimal cellular activities are taking place. A centrally located globule and numerous storage bodies surrounding the globule can be seen. 37% of the mature oospore dry weight was found to be composed of lipid, of which fatty acids represented about 78% (Fox et al., 1983).

After a period of dormancy, up a year under natural conditions (Chang & Ko, 1991), oospores will germinate and form a germ tube. A germ-sporangium will form at the end of the germ tube, and then enter the asexual life cycle. During germination, the central globule develops inward and becomes surrounded by vacuoles. The thick oospore wall becomes thin. A great reduction in total fatty acid content was observed during germination while protein content was increased (Ruben & Stanghellini, 1978; Ruben et al., 1981; Beakes et al., 1986).

The multi-layered thick walls of oospores can effectively protect lipids, proteins, and carbohydrates inside the cell from extreme temperatures, water stress, and chemicals. Oospores can also facilitate disease dispersal. Both in northern Europe and North America, it was reported that oospores have the ability to survive the winter conditions and initiate disease epidemics earlier than asexual spores and vegetative hyphae in the season (Andersson et al., 1998; Medina & Platt, 1999; Flier et al., 2007). By allowing the exchange of genetic traits, sexual reproduction diversifies the population and produces more competitive, aggressive and chemical resistant strains, as the pathogen's fitness is enhanced.

Granting the importance of sexual reproduction in the *P. infestans* life cycle, the biological features of this process at the molecular and biochemical level have been little studied. Only a few studies have been done on the identification of candidate genes that are important for oosporogenesis. A microarray study found that of the 15,644 unique genes on an Affymetrix chip, 87 were induced at least 10-fold 10 days after mating, with 28 genes induced by more than 100-fold. These genes encoded regulatory molecules such

as protein kinases, protein phosphatases, and transcription factors, plus enzymes with metabolic, transport, or cell-cycle activities (Prakob & Judelson, 2007). Genes up-regulated at this stage may be responsible for oospore formation and maturation. In mature oospores, since there is a very low cellular metabolic rate, proteins needed for survival and germination need to have been pre-synthesized and stored. When the conditions are right for germination, the oospores can utilize these ready-made proteins to initiate cell activities right away. However, there has been no detailed research on identification and characterization of these proteins in detail with respect to their roles during oospore germination.

With the completion of the genome sequencing of *P. infestans*, *P. sojae* and *P. ramorum*, and the partially available databases of several other oomycetes species, such as *P. capsici*, and *Hyaloperonospora arabidopsidis*, the monitoring of global changes in the proteome has been an increasingly attractive approach to researchers for understanding the molecular and biochemical basis of development, pathogenesis, and host-pathogen interactions. Traditional proteomics studies heavily rely on 2-dimensional gel electrophoresis followed by LC-MS/MS (Ebstrup et al., 2005; Medina et al., 2005; Zahedi et al., 2005). Two- dimensional gels are generally biased towards the detection of highly abundant proteins and only detect a limited number of proteins, ranging from a few to maximum a hundred of proteins. More recently, an approach called multidimensional protein identification technology (MudPIT) was developed (Link et al., 1999), and thousands of proteins can be identified using this approach.

In MudPIT analysis, by exploiting a peptide's unique physical properties of charge and hydrophobicity, complex mixtures can be separated prior to sequencing by tandem MS so that peptides generated from thousands of proteins can be identified, whereas the 2-dimensional gel method sensitivity is about 10-fold lower (Link et al., 1999; Ebstrup et al., 2005; Bohmer et al., 2007; Islam et al., 2008; Savidor et al., 2008; Miike et al., 2010; O'Brien et al., 2010). In addition, accurate quantification of the target proteins had been restricted with 2-dimensional gels until approaches using isotope-coded affinity tags (ICAT) were developed (Baudouin-Cornu et al., 2009). An improved approach analogous to ICAT called *iTRAQ* (isobaric tag for relative and absolute quantification) has been developed recently and is marketed by Applied Biosystems Inc. This method is based on the covalent labeling of the N-terminus and side-chain amines of peptides from enzymatic protein digests with tags of varying mass. There are currently two widely used isobaric tag systems: 4-plex and 8-plex, which can be used to label all peptides from 4 or 8 different samples/treatments (Applied Biosystems, Warrington, UK). A database search is then performed using the LC-MS/MS data to identify the labeled peptides and hence the corresponding proteins. The fragmentation of the attached tag generates a low molecular mass reporter ion that can be used to relatively quantify the peptides and the proteins from which they originated, using software such as MASCOT, SEQUEST, ProteinIQ, and SCAFFOLD.

In spite of the rapid advancement of knowledge with the aid of these new technologies in animals and plants, only very few proteomics studies have been performed on *Phytophthora spp.*, and these were all focused on asexual stages of the

pathogens (Shepherd et al., 2003; Ebstrup et al., 2005; Bruce et al., 2006; Savidor et al., 2008; Bhadauria et al., 2010). By using 2-dimensional gel electrophoresis, it was estimated that roughly 1% of the proteins are specific to each of the five asexual stages, which are mycelia, sporangia, zoospores, cysts, and germinating cysts (Shepherd et al., 2003), whereas by using MudPIT, about 10% of the proteins identified were unique to each of the mycelium and germinating cyst stages (Savidor et al., 2008). In mycelia, proteins involved in transport and metabolism of amino acids, carbohydrates, and other small molecules have higher concentrations compared to germinating cysts. In the germinating cysts, more concentrated proteins were associated with cellular repair, secreted proteins, lipid transport and metabolism, cytoskeleton, reactive oxygen species scavenging, amino acid metabolism, and protein synthesis that presumably function during early infection (Ebstrup et al., 2005; Savidor et al., 2008).

The global proteome of mature oospores has never been unveiled. The aim of this part of the study was to uncover the proteome of oospores and identify candidate proteins involved in spore germination and initiation of infection. This was achieved by comparing the proteomes of mature oospores and the nonsporulating hyphae using MudPIT with iTRAQ quantification. This information may be useful in the development of new approaches to limit the damage caused by *P. Infestans*.

Materials and methods

Culture conditions and strains of *Phytophthora infestans*

P. infestans isolates 618 (A2), and 88069 (A1) were cultured on polycarbonate membranes on rye A agar as described at 18 ℃ (Judelson et al., 1991) for 30 days. Strips of oospore-containing mating tissues were harvested to extract oospores. Average size of each strip was 10 mm x 90 mm. Nonsporulating hyphae were obtained from 3-day-old germinating sporangia submerged in rye A broth (rye A clarified by centrifugation at 5,000 x *g*).

In order to obtain the highest amount of viable oospores, the numbers and percentages of viable oospores produced by four combinations of mating types, using two A1 and two A2 strains, were compared. Oospores aged 10 days, 15 days, 30 days, and 45 days from 8811 (A1) x 618 (A2), 88069 (A1) x 618 (A2), 8811 (A1) x E13a (A2), and 88069 (A1) x E13a (A2) mating tissues were stained using tetrazolium bromide (MTT) (Sutherland & Cohen, 1983). A piece of 4 mm^2 mating tissue was added into 30 µl of 0.1 % tetrazolium bromide (MTT) in 0.1 M potassium phosphate buffer (pH 5.8), and then incubated at 37 ℃ for 2 days (Pittis & Shattock, 1994). The total number of oospores borne on the tissue was counted, and the number of viable oospores (rosy pink color after MTT staining) was also recorded.

Oospore purification and protein extraction

The effectiveness of both mechanical and enzymatic for generating pure oospores was tested. Mechanical separation of oospores and mycelia was first carried as described by Cvitanich and Judelson (2003). Briefly, the mating tissues were homogenized five times for 2 min each in 50 ml of sterile deionized water at 4 ℃ in a Brinkman Polytron (speed 7) and passed through a 100 µm nylon mesh. The oospores that remained intact after this treatment were concentrated by centrifugation for 10 min at 4,000 x g. The oospores were then resuspended in 20 ml of deionized water, spun at 650 x g for 5 min and the supernatant was removed. This washing step was repeated 3 to 5 times to remove the small hyphal fragments. Finally the oospore suspension was centrifuged at 4,000 x g for 10 min to concentrate the oospores. The enzymatic method was performed by digesting the hyphae for 12 hr in 20 mg/ml Novozyme 234 (Calbiochem) and washing with deionized water and 0.1% SDS for five to eight times as described above.

Finally, 100 µl of 50 µm beads were added to 1.5 ml deionized water with two strips of mating tissue, and homogenized using Fastprep FP120 homogenizer at speed 6 for 1.5 min. The mixture was filtered through 100 µm and then 35 µm filters. The flow-through was centrifuged at 5700 x g for 5 min. The pallet was resuspended with 40 ml of dionized water, centrifuged at 4,000 x g and the supernatant was removed. This washing step was repeated 3 times, and another two washes were done with centrifuging at 650 x g for 5 min. Usually 1 to 3 x 10^7 oospores were obtained from 200 strips of mating

tissues (Fig. 3.1). Nonsporulating hyphae that were 3 days old were harvested and used as controls.

Proteins were extracted by breaking the oospores or the nonsporulating hyphae in extraction buffer (20 mM Tris-HCl, pH 8.0, 150 mM NaCl, 10 mM EDTA, pH 8.0, 0.2% Nonidet P-40, 0.02 mg/ml heparin, 1.5 mM DTT, 1 mM PMSF, 20 units/ml DNase I) using Qbiogene FastPrep® beadbeater with 1/4 inch ceramic spheres and 200 µm glass beads. After the tissues were homogenized twice for 1 min at speed 6, the tissues were centrifuged at 20,000 x *g* for 10 min. The supernatant was saved and the concentration of each protein sample was determined using the non-interfering protein assay™ Kit (EMD).

Two separately prepared 100 µg unlabeled oospore protein samples were sent to the University of California, Davis Proteomics center for MudPIT analysis and the results were searched against the *P. infestans* database using SCAFFOLD. Later, a 100 µg oospore sample and a 100 µg nonsporulating hyphae protein sample (containing 50 µg A1 and 50 µg A2), both unlabeled, were sent to the UC Riverside CEPCEB W.M. Keck Proteomics Core Facility.

Trypsin digestion and iTRAQ labeling

The entire experimental design of iTRAQ labeling and MS process is described in Fig. 3.1. 100 g of each protein sample were loaded onto 10% acrylamide SDS-PAGE and after the samples entered the separating phase by 1.5 to 2 cm, the electrophoresis was terminated. The gel was then stained using a colloidal blue staining kit (Invitrogen) and

gel pieces containing the proteins were excised. Gel pieces were then cut into 1 mm^2 fragments and submerged in 100 µl of 25 mM ammonium bicarbonate in 50% acetonitrile in 1.5 ml centrifuge tubes. Samples were vortexed for 1 hr and the buffer was decanted and replaced by fresh one. This destaining process was repeated until the dye was completely removed. The gel pieces were then covered with 200 µl acetonitrile for 15 minutes at room temperature, and dried by SpeedVac for 1 hr at room temperature. To each sample tube, 30 µl of dissolution buffer (0.5 M triethylammonium bicarbonate, pH 8.5) was added, followed by the addition of 1 µl of the denaturant (2% SDS), and vortexed to mix. Reducing reagent, tris-(2-carboxyethyl)-phosphine (TCEP), was then added to reach a concentration of 5 mM. The samples were mixed and incubated at 60 ℃ for 1 hour. After removing the reducing buffer, a volume of Trypsin solution (12.5 ng/µl trypsin, 50 mM ammonium bicarbonate buffer, pH 7.8) was added to just cover the gel pieces, and then incubated overnight in a water bath at 37 ℃. After removing the digestion buffer, 50 µl of 5% acetonitrile and 0.1% trifluoroacetic acid (TFA) was added to the gel slices and vortexed for 15 min at room temperature. This step was repeated twice, then 50 µl of 50% acetonitrile and 0.1% TFA were added to the gel slice and incubated for 15 min. All the washes were pooled together with the solution from the overnight digest. The eluates were reduced in volume using a SpeedVac to approximately 10 µl.

To label the peptides with iTRAQ reagent (Applied Biosystems, Warrington, UK), one unit of label (defined as the amount required to label 100 µg of protein) was thawed and reconstituted in 70 µl of 100% ethanol, with vortexing for 1 min. The reagent

solution was added to digest peptides and incubated at room temperature for 1 hr. Labeling reactions were then pooled before analysis. Proteins from nonsporulating A1 hyphae were labeled with the iTRAQ 114 reporter ion, and nonsporulating A2 hyphae were labeled with the reporter iron 116, and the two oospore samples were labeled with the 115 and 117 reporter ions, respectively. A ten-fold excess of the Cation Exchange Buffer-Load was used to dilute the sample mixture, and the diluted mixture was passed through the cation-exchange cartridge by slow injection (1 drop/second). 500 l of the Cation Exchange Buffer–Elute was then added to the cartridge and eluates were slowly injected (~1 drop/second) into a fresh 1.5-mL tube.

Figure 3.1. iTRAQ labeling and MudPIT analysis work flow. Two nonsporulating hyphae (NSH) samples (A1 and A2 as controls) and two oospore samples were each labeled with one of the four iTRAQ tags as shown. The peptide samples were pooled, fractionated by two dimensions of liquid chromatography (cation-exchange and reverse-phase), and analyzed by MS. The iTRAQ sample was analyzed three times on an ESI-QTOF mass spectrometer. In the bottom panel, at the upper right corner it shows a sample MS/MS spectrum of a single peptide from which the amino acid sequence is deduced. In addition, it reveals the four reporter ions from the iTRAQ tags, whose intensity indicates the relative abundance of that peptide in the four samples. The two controls are labeled with tags 114 and 116, and showing reporter ions at those m/z ratios, while the two oospore samples are labeled with tags 115 and 117, showing reporters at those m/z ratios. On the upper left corner of the bottom panel, peptides that were identified belonging to this protein are shown in red font and listed at the lower half of the bottom panel. The protein function was predicted according to a search of the Broad Institute of MIT and Harvard *P. infestans* database.

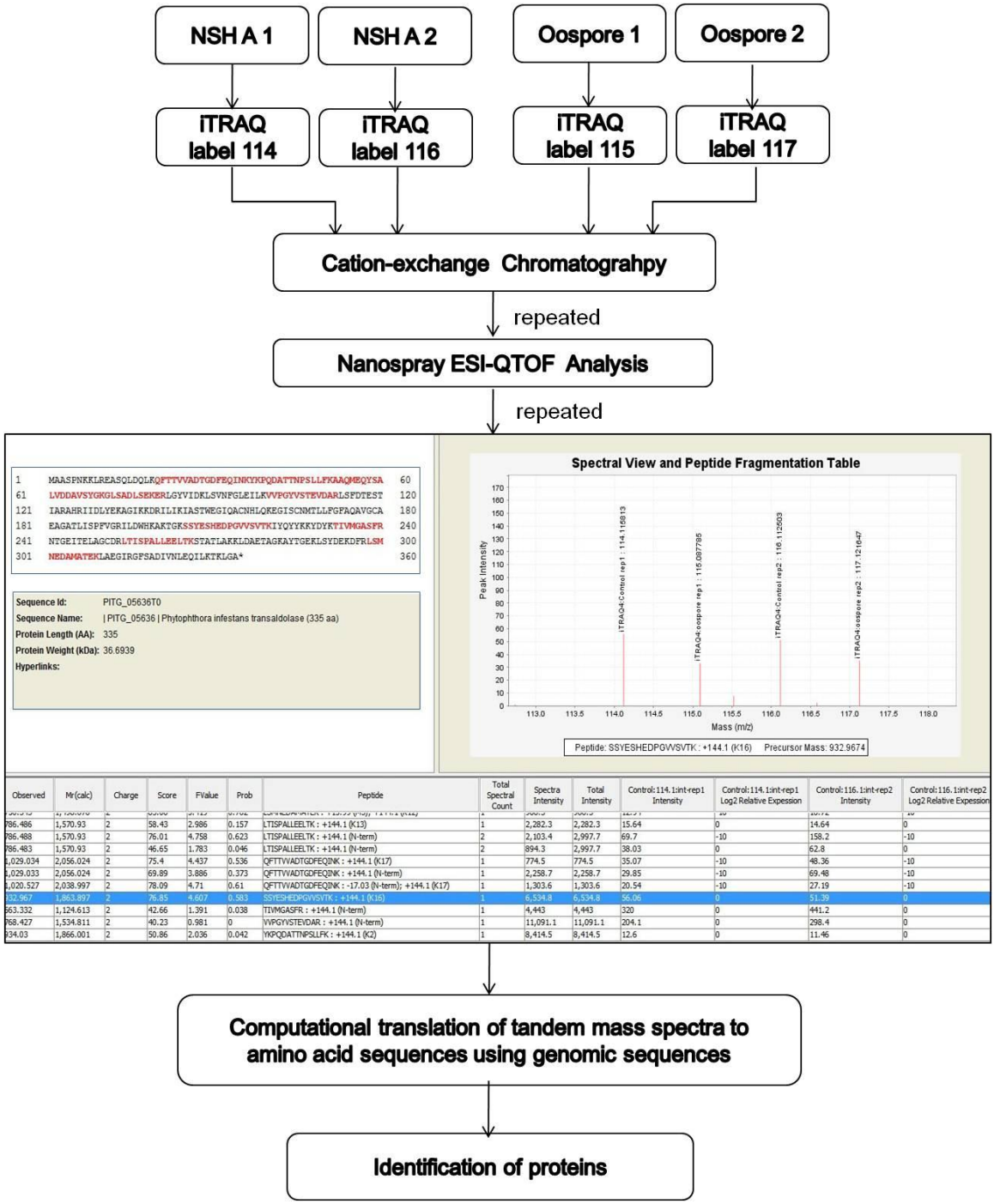
NSH A 1
NSH A 2
Oospore 1
Oospore 2
iTRAQ label 114
iTRAQ label 116
iTRAQ label 115
iTRAQ label 117
Cation-exchange Chromatograhpy
repeated
Nanospray ESI-QTOF Analysis
repeated
1 MAASPNKKLREASQLDQLKQFTTVVADTGDFEQINKYKPQDATTNPSLLFKAAQMEQYSA 60
61 LVDDAVSYGKGLSADLSEKERLGYVIDKLSVNFGLEILKVVPGYVSTEVDARLSFDTEST 120
121 IARAHRIIDLYEKAGIKKDRILIKIASTWEGIQACNHLQKEGISCNMTLLFGFAQAVGCA 180
181 EAGATLISPFVGRILDWHKAKTGKSSYESHEDPGVVSVTKIYQYYKKYDYKTIVMGASFR 240
241 NTGEITELAGCDRLTISPALLEELTKSTATLAKKLDAETAGKAYTGEKLSYDEKDFRLSM 300
301 NEDAMATEKLAEGIRGFSADIVNLEQILKTKLGA* 360
Sequence Id: PITG_05636T0
Sequence Name: | PITG_05636 | Phytophthora infestans transaldolase (335 aa)
Protein Length (AA): 335
Protein Weight (kDa): 36.6939
Hyperlinks:
Spectral View and Peptide Fragmentation Table
Peak Intensity
Mass (m/z)
iTRAQ4:Control rep1 : 114.115813
iTRAQ4:oospore rep1 : 115.087785
iTRAQ4:Control rep2 : 116.112603
iTRAQ4:oospore rep2 : 117.121647
Peptide: SSYESHEDPGVVSVTK : +144.1 (K16) Precursor Mass: 932.9674
Observed Mr(calc) Charge Score FValue Prob Peptide Total Spectral Count Spectra Intensity Total Intensity Control:114.1:int-rep1 Intensity Control:114.1:int-rep1 Log2 Relative Expression Control:116.1:int-rep2 Intensity Control:116.1:int-rep2 Log2 Relative Expression
786.486 1,570.93 2 58.43 2.986 0.157 LTISPALLEELTK : +144.1 (K13) 1 2,282.3 2,282.3 15.64 0 14.64 0
786.488 1,570.93 2 76.01 4.758 0.623 LTISPALLEELTK : +144.1 (N-term) 2 2,103.4 2,997.7 69.7 -10 158.2 -10
786.483 1,570.93 2 46.65 1.783 0.046 LTISPALLEELTK : +144.1 (N-term) 2 894.3 2,997.7 38.03 0 62.8 0
,029.034 2,056.024 2 75.4 4.437 0.536 QFTTVVADTGDFEQINK : +144.1 (K17) 1 774.5 774.5 35.07 -10 48.36 -10
,029.033 2,056.024 2 69.89 3.886 0.373 QFTTVVADTGDFEQINK : +144.1 (N-term) 1 2,258.7 2,258.7 29.85 -10 69.48 -10
,020.527 2,038.997 2 78.09 4.71 0.61 QFTTVVADTGDFEQINK : -17.03 (N-term); +144.1 (K17) 1 1,303.6 1,303.6 20.54 -10 27.19 -10
932.967 1,863.897 2 76.85 4.607 0.583 SSYESHEDPGVVSVTK : +144.1 (K16) 1 6,534.8 6,534.8 56.06 0 51.39 0
563.332 1,124.613 2 42.66 1.391 0.038 TIVMGASFR : +144.1 (N-term) 1 4,443 4,443 320 0 441.2 0
768.427 1,534.811 2 40.23 0.981 0 VVPGYVSTEVDAR : +144.1 (N-term) 1 11,091.1 11,091.1 204.1 0 298.4 0
934.03 1,866.001 2 50.86 2.036 0.042 YKPQDATTNPSLLFK : +144.1 (K2) 1 8,414.5 8,414.5 12.6 0 11.46 0
Computational translation of tandem mass spectra to amino acid sequences using genomic sequences
Identification of proteins

Mass Spectrometry and peptide identification

A Waters® nanoACQUITY UPLC® System combined with a cation exchange chromatography (SCX) and Waters® exact mass Q-Tof™ Mass Spectrometer was employed to analyze the samples. Samples were divided into 10 fractions, and four MudPIT runs were performed, each time excluding the peptides identified previously. The MS/MS spectra were evaluated with MASCOT (version 2.1, Matrix Science) and searched against sequences in the Broad Institute *P. infestans* protein database. The search was configured to assume a tryptic digest, one peptide with 95% confidence, up to one missed cleavage per peptide, Carboxyamidomethylation, iTRAQ 4-plex on N-termini and lysines as fixed mass modifications, and oxidation (*M*) as a variable mass modification. Monoisotopic mass values were used, and peptide mass tolerance and fragment mass tolerance were set at 60 ppm and 0.2 Da, respectively. The cut-off value MASCOT MudPIT score was 50. The MudPIT experiments for iTRAQ labeled proteins and MASCOT searches were carried in the CEPCEB W.M. Keck Proteomics Core Facility of the University of California, Riverside.

Data analysis

Microsoft Access and Perl scripts were used to make comparisons between life stages. Only iTRAQ labeled proteins were subjected to quantitative analysis. Signature peak values of four reporter ions of each peptide were extracted from the Pkl file generated by MASCOT. Mass-to-charge values (m/z) of the reporter ions fell between

114.1 ± 0.01, 115.1 ± 0.01, 116.1 ± 0.01, or 117.1 ± 0.01. Peptides were assigned to proteins using MASCOT.

The relative expression value of a single protein in one sample was calculated by averaging the signature peak values of the particular reporter ions of all the unique peptides identified belonging to a specific protein. For instance, if protein A has three unique peptides whose signature peak values of 114 reporter ions are 20, 30 and 40, then the relative expression value of protein A in sample A1 was (20+30+40)/3 = 30. In order to properly perform statistical analysis, the value of the relative expression level of each protein was subjected to various data transformations (O'Brien et al., 2010). Log-ratios were obtained for the averaged signature peak values of iTRAQ reporter ions (labeled as 114, 115, 116, and 117) of each protein based on the following equations: 1) *ln*(115/114), 2) *ln*(117/114), 3) *ln*(115/116), 4) *ln*(117/116), and 5) *ln*[(115+117)/(114+116)], in which *ln* is the natural logarithm. It should be noted that the log-ratio transform for these protein expression data would result in datasets with a normal distribution.

For the four datasets derived from equations 1-4, Student's *t* test was applied to determine log-ratios of proteins that were significantly different from the mean ratio of the whole sample. As the log-ratios were for the oospore samples (115 and 117) to the hyphal controls (114 and 116), a significantly higher ratio to the mean ratio implies the enrichment of a particular protein in oospores than in hyphae. In contrast, significantly lower ratios indicate a lower abundance of this protein in oospores than in hyphae.

All the proteins were classified into functional groups according to the biological processes that they are involved. The fifth derived dataset was subjected to Student's *t*-

test by the functional group to assess the abundance at a group level. As the log-ratios of the sum of 115 and 117 to the sum of 114 and 116 were standardized to a mean value of 1, if the mean log-ratio of a group is significantly higher than 1 according to the *t* test, it is considered significantly more abundant. Similarly, if the mean log-ratio of a group is significantly lower than 1, then that group has a decreased concentration. Furthermore, one-way ANOVA was carried out to detect possible significant differences of protein expression level among the functional groups. Tukey's HSD was used in ANOVA to separate the means of groups. All statistical analyses were conducted in SAS (SAS Institute, Cary, NC).

Results and discussion

Oospore culture and validation test

In order to obtain as many as possible viable oospores, different combinations of A1 and A2 strains were mated and the number of viable oospores produced by 8811 (A1) x 618 (A2), 88069 (A1) x 618 (A2), 8811 (A1) x E13a (A2), and 88069 (A1) x E13a (A2) were determined using MTT staining (Fig. 3.2). Strains 8811 and 618 appeared to yield the highest number of viable oospores, about 60% of oospores counted (Table 3.1). According to previous studies, oospores that were older than 30 days are mature, and the germination rate is usually increased while aging (Ann & Ko, 1987). Therefore, 30-day-

old oospores of 8811 x 618 and nonsporulating 8811 and 618 mycelia were used for the following analyses.

Figure 3.2. Purified oospores and oospores stained with MTT. The upper panel shows purified oospores under the optical microscope at 200 x magnification. The lower panel shows two oospores stained rosy pink (left, viable), and black (right, dead) at 400 x magnification.

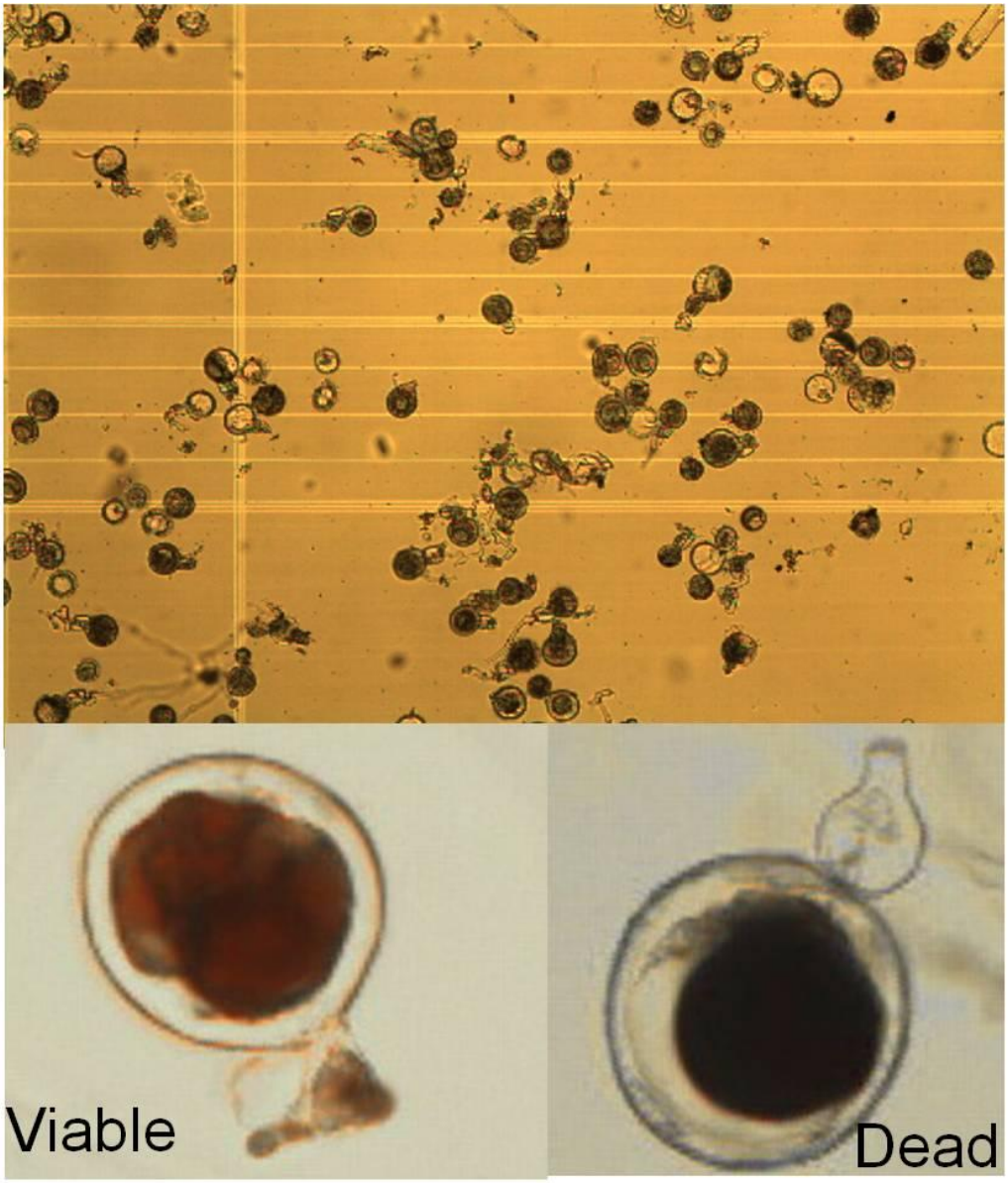
Viable
Dead

Table 3. 1. Oospore production and viability test. Oospore production numbers and viable oospore numbers for every combination of A1 and A2 (8811 (A1), 88069 (A1), 618 (A2) and E13A (A2)) were recorded. The ratios represent the average number of viable oospores versus the average total number of oospores for each mating combination grown on a 4 mm^2 piece of mating tissue on a polycarbonate membrane.

A1 / A2	8811	88069
618	135/225	92/190
E13A	35/170	59/235

Comparison of global proteomics of oospore and nonsporulating hyphae

A total of four MudPIT experiments were conducted. The first two experiments were trial runs using unlabeled oospore proteins (oospore label-free sample 1 and 2) and were sent to UC Davis Proteomics Center since MudPIT instruments were not available in UC Riverside at the time. The third MudPIT experiment, in which unlabeled nonsporulating hyphae proteins and unlabeled oospore proteins were analyzed, was carried out in the UC Riverside Proteomics Core facility (label-free NSH1 and oospore label-free sample 3). The fourth experiment was also done in UC Riverside with two iTRAQ labeled nonsporulating hyphae protein batches from mating type A1 (8811) and A2 (618) (iTRAQ NSH A1 and iTRAQ NSH A2) and two iTRAQ labeled oospore protein samples (iTRAQ oospore 1 and iTRAQ oospore 2). Only the proteins identified in the last MudPIT experiment were quantified. The first three runs only aided in protein identification. The oospore label-free sample 1 yielded 31 proteins and 170 proteins were identified from oospore label-free sample 2. The unlabeled oospore sample analyzed by UC Riverside Proteomics Core facility yielded 124 proteins (oospore label-free sample 3). The two iTRAQ-labeled oospore samples produced 835 proteins (iTRAQ oospore 1 and 2). A total of 959 non-redundant proteins were identified from oospores from all the five samples. The unlabeled nonsporulating hyphae (NSH) sample (label-free NSH 1) analyzed by UC Riverside yielded 690 proteins, whereas 837 proteins were identified from iTRAQ NSH A1 and iTRAQ NSH A2. A total of 1115 non-redundant proteins were yielded from these three nonsporulating hyphae samples. There were 913 proteins shared

between the stages, and 202 proteins unique to NSH and 44 unique to oospore samples (Fig. 3.3, Table 3.4 and Table 3 5).

As mentioned, protein quantification was solely based on iTRAQ labeled proteins, 836 from iTRAQ oospore 1 and 2, and 838 from iTRAQ NSH A1 and A2. A protein was considered to be significantly more abundant in a specific life stage if its concentration based on relative expression level, was 0.82-fold higher than in the other life stage, and its concentration was considered to be significantly decreased if the relative expression level was less than 0.24-fold of the other stage (see "Data analysis" under "Materials and Methods"). The unlabeled proteins will be quantified after a software module becomes available at UC Riverside CEPCEB W.M. Keck Proteomics Core Facility in August, 2010.

Figure 3.3. Identification of proteins in vegetative hyphae and oospores. The total identified proteome (union of two MudPIT experiments) of nonsporulating hyphae life stage of *P. infestans* was compared with the proteome of the oospores. Overlapping regions represent proteins found in both stages, whereas non-overlapping regions represent proteins that were not identified in the other life stage.

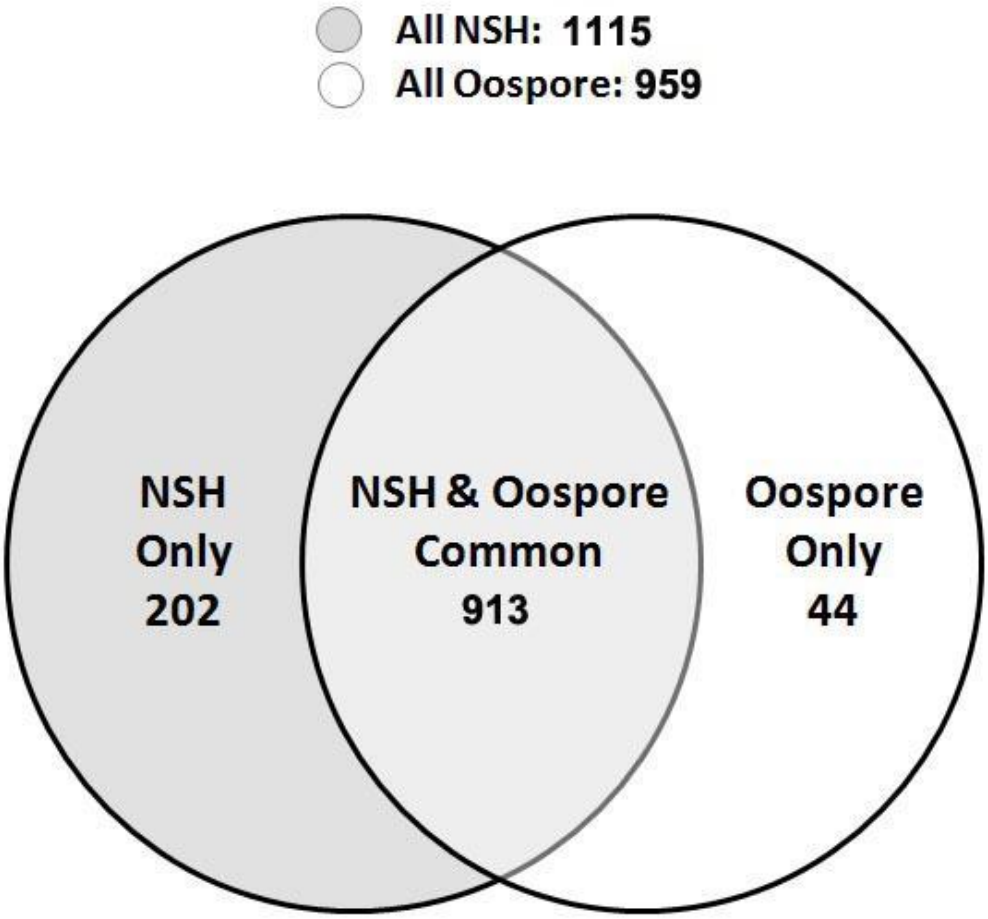
All NSH: 1115
All Oospore: 959
NSH Only 202
NSH & Oospore Common 913
Oospore Only 44

The proteins identified were grouped into 18 functional categories based on their known molecular and cellular functions based on the Broad Institute of *P. infestans* and NCBI non-redundant protein sequence databases. Members of each functional group are present in both stages. The percentage of proteins that each functional group contained was compared between the two stages (Fig. 3.4.A and B). By summing up the relative expression ratio of the proteins involved in the same functional group during a specific stage, it appeared that the proportion of each group in the whole proteome remains relatively similar across the two life stages (Fig. 3.4.C and D). Statistically, there are moderate differences between protein expression levels in each group (Fig. 3.5).

Compared to the nonsporulating hyphae, the proteomics profile in oospores revealed that proteins involved in five out of the 17 groups were more abundant in oospores than in nonsporulating hyphae. These groups include proteins involved in secreted and infection-related proteins, cell cycle and cell proliferation, fatty acid transport and metabolism, amino acid transport and metabolism, and antioxidant, anti-stress and detoxification process. Among these, secreted and infection-related proteins, and the antioxidant, anti-stress and detoxification group, were significantly more abundant in oospores (*t*-test, $p<0.05$). Seven protein functional groups were less abundant in oospores compared to hyphae. Only one of them was significantly under-represented, which was the protein transportation and metabolism group. Six other groups were moderately less abundant: DNA/nucleotide metabolism, cytoskeleton, ribosomal RNA process, mRNA processing, lipid transport and metabolism, and the unknown function group (Fig. 3.5). However, the abundances of these groups in oospores were not

significant different from those in hyphae due to too many “outliers” that skewed the statistical models. Here “outliers” are a few proteins in the group with expression levels very different from the group mean expression value that their inclusion in the statistical calculations, led to the standard deviation being increased. Proteins in carbohydrate metabolism, ion and macromolecule trafficking, signal transduction, energy production and conversion, translational regulation, and post-translational modification had approximately the same average expression level in oospores as in hyphae.

Figure 3.4. Distribution of protein functional categories in the global proteomes of the nonsporulating mycelia and oospores of *P. infestans*. Protein categories were clustered based on their functional annotation based on the Broad Institute *P. infestans* and NCBI non-redundant protein sequence database. (A) Number of proteins in functional groups in nonsporulating hyphae. The proportion of the proteins was calculated using the number of the proteins present in one particular functional group divided by the total number of proteins detected. (B) Number of proteins in functional groups in oospores. The proportion of the proteins was calculated using the number of the proteins present in one particular functional group divided by the total number of proteins detected. (C) The relative expression ratio of each functional group in the whole proteome of nonsporulating hyphae (NSH). The ratio of each group was calculated by dividing the sum of the relative expression value of all the proteins belonging to one particular functional group by the sum of the relative expression values of the total protein. (D) The relative expression ratio of each functional group in the whole proteome of oospores.

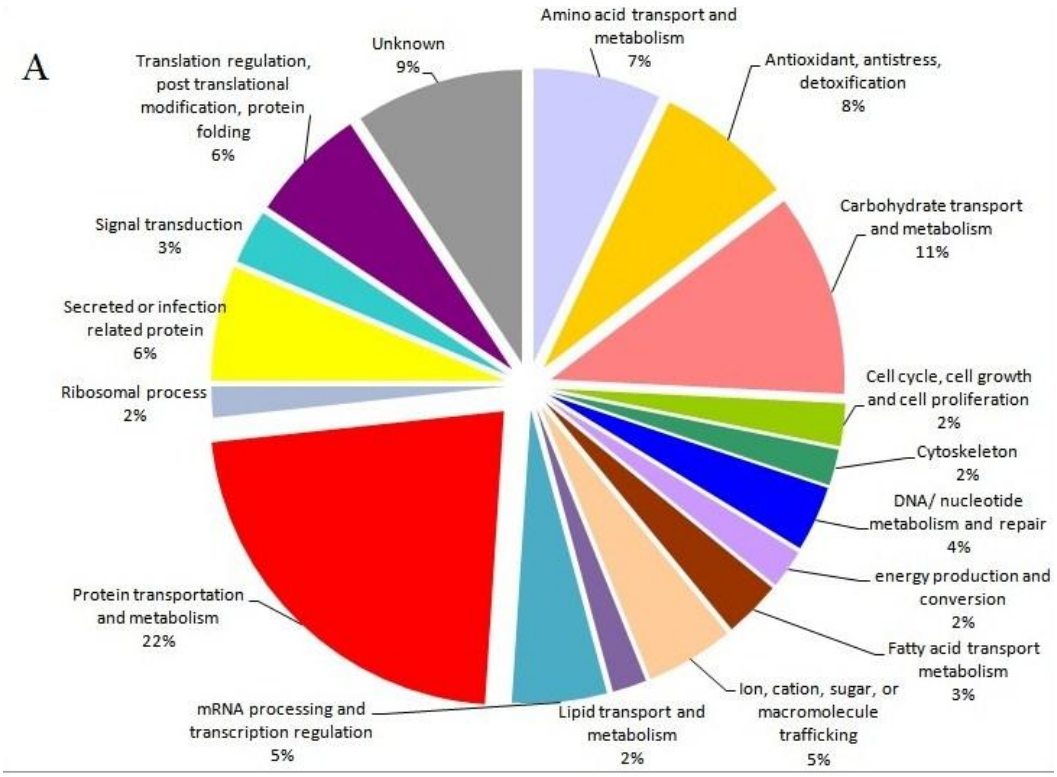
A
Amino acid transport and metabolism 7%
Antioxidant, antistress, detoxification 8%
Carbohydrate transport and metabolism 11%
Cell cycle, cell growth and cell proliferation 2%
Cytoskeleton 2%
DNA/ nucleotide metabolism and repair 4%
energy production and conversion 2%
Fatty acid transport metabolism 3%
Ion, cation, sugar, or macromolecule trafficking 5%
Lipid transport and metabolism 2%
mRNA processing and transcription regulation 5%
Protein transportation and metabolism 22%
Ribosomal process 2%
Secreted or infection related protein 6%
Signal transduction 3%
Translation regulation, post translational modification, protein folding 6%
Unknown 9%

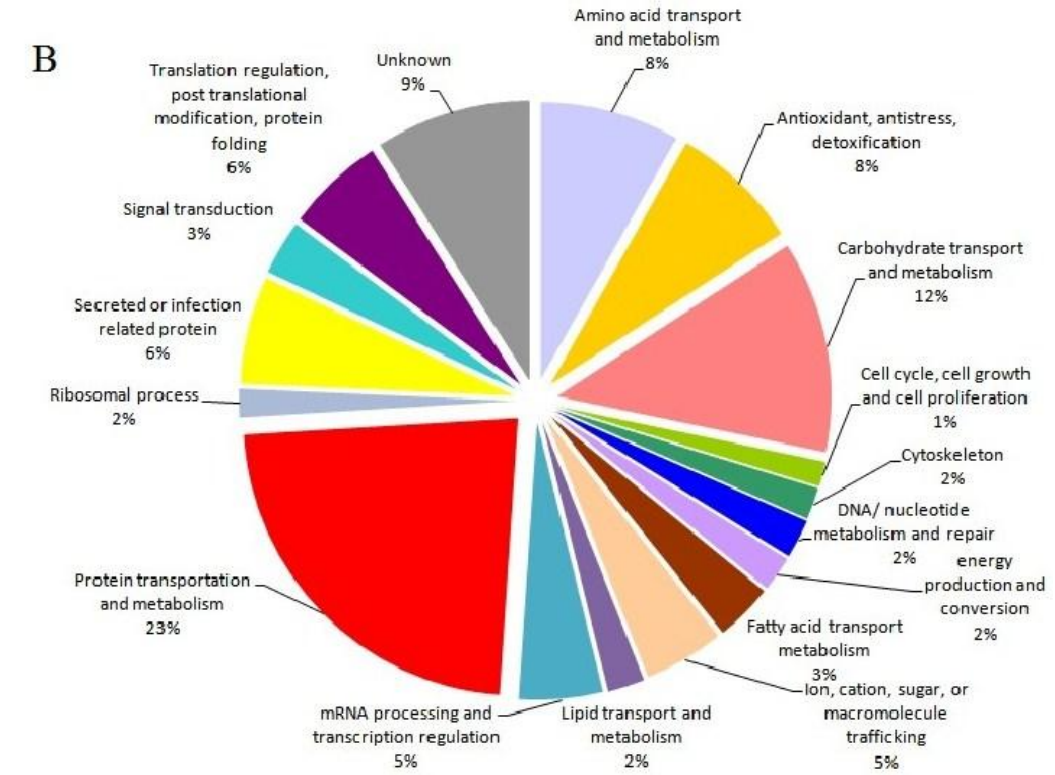
B
Amino acid transport and metabolism 8%
Antioxidant, antistress, detoxification 8%
Carbohydrate transport and metabolism 12%
Cell cycle, cell growth and cell proliferation 1%
Cytoskeleton 2%
DNA/ nucleotide metabolism and repair 2%
energy production and conversion 2%
Fatty acid transport metabolism 3%
Ion, cation, sugar, or macromolecule trafficking 5%
Lipid transport and metabolism 2%
mRNA processing and transcription regulation 5%
Protein transportation and metabolism 23%
Ribosomal process 2%
Secreted or infection related protein 6%
Signal transduction 3%
Translation regulation, post translational modification, protein folding 6%
Unknown 9%

C

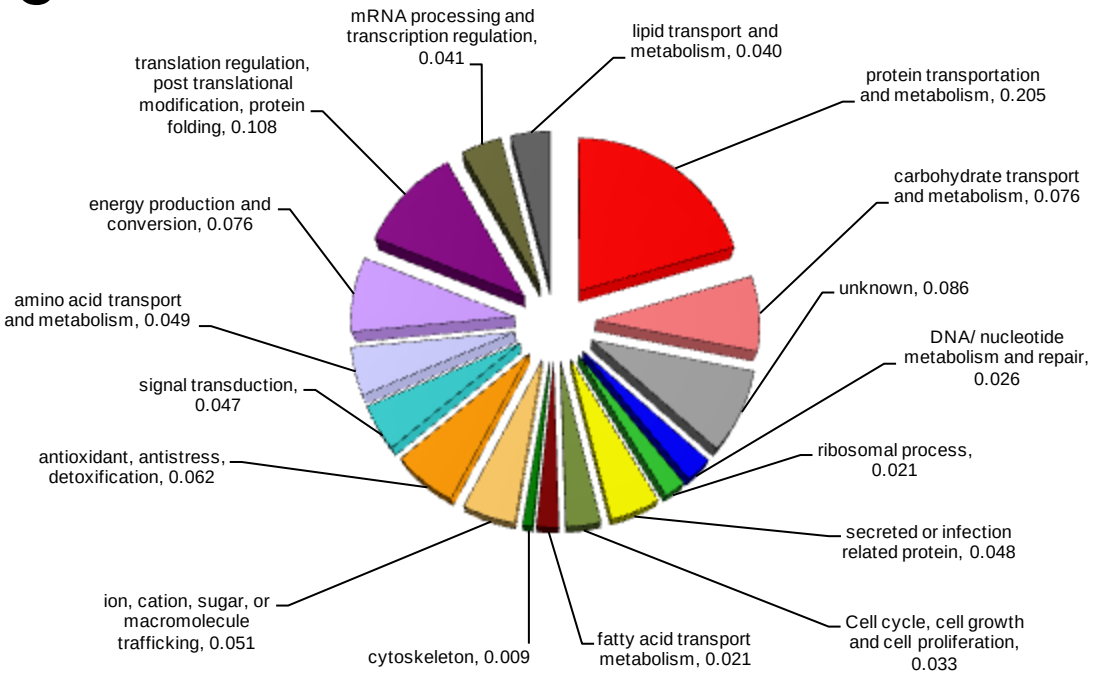
mRNA processing and transcription regulation, 0.041
lipid transport and metabolism, 0.040
translation regulation, post translational modification, protein folding, 0.108
protein transportation and metabolism, 0.205
energy production and conversion, 0.076
carbohydrate transport and metabolism, 0.076
amino acid transport and metabolism, 0.049
unknown, 0.086
signal transduction, 0.047
DNA/ nucleotide metabolism and repair, 0.026
antioxidant, antistress, detoxification, 0.062
ribosomal process, 0.021
secreted or infection related protein, 0.048
ion, cation, sugar, or macromolecule trafficking, 0.051
Cell cycle, cell growth and cell proliferation, 0.033
cytoskeleton, 0.009
fatty acid transport metabolism, 0.021

D

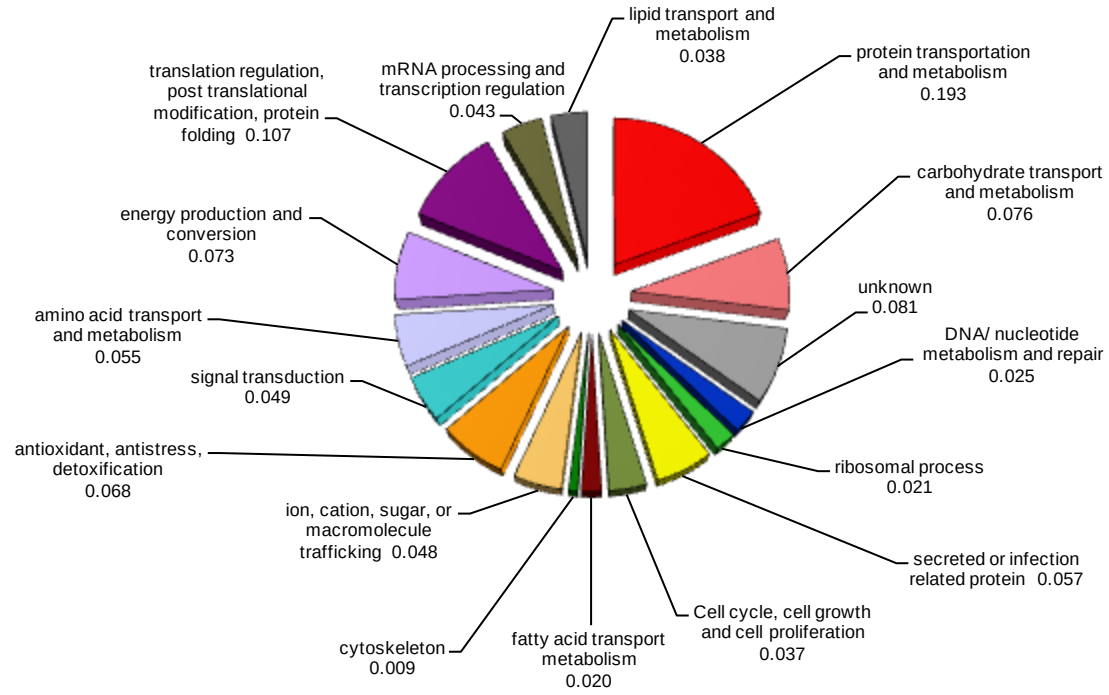
lipid transport and metabolism 0.038
translation regulation, post translational modification, protein folding 0.107
mRNA processing and transcription regulation 0.043
protein transportation and metabolism 0.193
energy production and conversion 0.073
carbohydrate transport and metabolism 0.076
amino acid transport and metabolism 0.055
unknown 0.081
signal transduction 0.049
DNA/ nucleotide metabolism and repair 0.025
antioxidant, antistress, detoxification 0.068
ribosomal process 0.021
ion, cation, sugar, or macromolecule trafficking 0.048
secreted or infection related protein 0.057
cytoskeleton 0.009
fatty acid transport metabolism 0.020
Cell cycle, cell growth and cell proliferation 0.037

Figure 3.5. Differential abundance of protein functional groups during the oospore stage compared to nonsporulating hyphae. The log protein expression ratio of oospore to hyphae was subjected to Student's *t*-test. Protein functional group expression level was calculated based on the sum of the relative expression value of each protein presented in the group. The ratio of the protein functional group expression values in two stages was log transformed. A ratio of 1 means no differential expression between the two stages. Error bars indicate standard deviations of the means of the log relative expression values of proteins in functional groups.

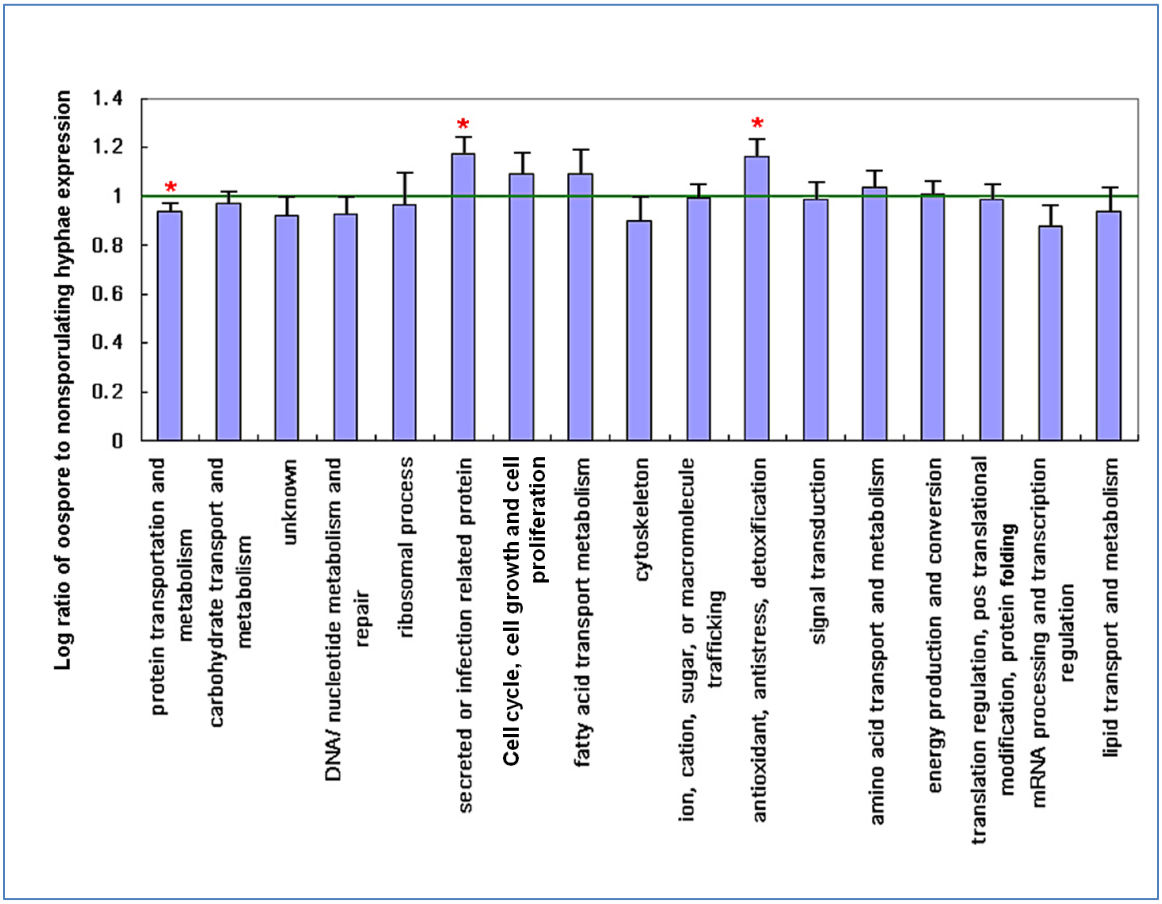

* Students *t* test indicated that the marked groups are significantly up or downregulated (higher or lower than 1) in oospores.

The functional group having the most members identified in both stages was protein metabolism and transport. More than 20% of the proteins were in this category (Fig. 3.4.A), and were mostly predicted to be ribosomal RNAs, importins, and exportins. This was consistent with results from in *P. sojae* and *P. ramorum* (Savidor et al., 2008). Combining this group with the 9% involved in protein folding and maturation, one third of the total proteins in the two life stages of *P. infestans* participate in protein metabolism pathways. By calculating the log ratio of proteins present in the protein metabolism and transportation pathways during the oospore and nonsporulating hypha stages, the average expression of proteins in this functional group is significantly less (*t*-test, $p<0.05$) at the oospore stage (Fig. 3.5). Three out of nine of the most decreased individual proteins were in this functional category (Table 3.3). In the study of *P. sojae* and *P. ramorum* proteomics, the expression level of this functional group was also found to be significantly lower in germinating cysts, temporary dormant structures, than in hyphae (Savidor,et al., 2008). This result suggested that the cellular activities in mature oospores are much lower than those in the vegetative stages. This finding could be supported by the study on the ultrastructural features of dormant oospores, which revealed that the cytoplasm of the mature oospore contains abundant fragments of disrupted organelle membranes and probably has no cell activities (Drenth et al., 1995). This result further reinforced the hypothesis that most of the proteins that are needed for the sustainability of the oospores and for the next step, germination, may have been already synthesized and stored at the desired locations. The cell cycle could start immediately without having to make new proteins first.

The amino acid processing and transportation group has a similar expression level in oospores and hyphae. Amino acid metabolism also links with the citric acid cycle and glyoxylate cycle, and with carbohydrate metabolism.

About a quarter of proteins identified contribute to energy production through different pathways, such as carbohydrate metabolism and lipid or fatty acid metabolism. In a previous study of proteomes of nonsporulating hypahe and germinating cysts of *P. sojae* and *P. ramorum*, proteins that are involved in the energy production pathways were grouped into carbohydrate transport and metabolism, energy production and conversion, and lipid (fatty acid) transport and metabolism (Savidor et al., 2008). In order to be able to compare our data with these results, proteins identified here were grouped in a similar fashion. In *P. sojae* and *P. ramorum*, 19% of the proteins identified were in pathways of carbohydrate transport and metabolism, lipid transport and metabolism, and energy production, which could all contribute to energy production. We observed a similar distribution, with 16% of the total proteins identified, being involved with the same pathways.

Almost all the enzymes involved in carbohydrate metabolism pathways were identified in both life stages, and their relationships are described in the diagram in Fig. 3.6. According to the ultrastructural features of germinating oospores, the oospore walls are thinned during germination, especially at the position where germ tubes develop (Drenth et al., 1995). Since the major component of the oospore wall are β-glucans (80%, Lippman et al., 1974), glycolysis is probably one of the main pathways to generate energy and enable the development of the germ tubes through digesting the oospore walls.

When glucose is at a low level or not present, pentose sugars and fructose can also be used to enter glycolysis and the downstream citric acid cycle (Fig. 3.6). A bidirectional enzyme that is involved in glycolysis/gluconeogenesis, phophoglycerate mutase encoded by PITG_03792 was increased significantly (Table 3.4). Identification of a few other enzymes indicated that oospores have other sidetracks to enter citric acid cycle without going through glycolysis. PITG_01966, PITG_11901, and PITG_10600 all encode a phosphoenolpyruvate carboxykinase enzyme and were all found to have a higher concentration in oospores than in NSH for 0.7-1.02 fold. These enzymes could generate acetyle-CoA to enter the citric acid cycle by converting oxaloacetate to phosphoenolpyruvate. Another one of the most abundant proteins in oospore was a gluconolactonase, encoded by PITG_17257 (Table 3.2). Gluconolactonase was found to be up-regulated in INF1-treated tomato leaves (Kavamura et al., 2009), and in brown algae when it is under stress (Dittami et al. 2010). This enzyme participates pentose phosphate pathway, which is an alternative to glycolysis for generating energy.

Another 10% of the oospore walls is comprised of cellulose and small amounts of mannose and glucosamine. Cellulose degradation enzymes would be another possible way of degrading the oospore walls for energy production and germination. One of the examples of these proteins is a glycosyl hydrolase, which was encoded by PITG_02335. Its expression level was increased 2.4 times in oospores than in NSH and it is one of the most abundant proteins in oospores (Table 3.2, Lippman et al., 1974; Beakers & Bartnicki-Garcia, 1989).

About 37% of the dry weight of the oospore is lipid (Fox et al., 1983). Oospores store large amounts of lipids as an energy supply. For the same mass, lipid oxidation yields twice energy as much as carbohydrates. In our study, we found that the concentration of PITG_06430 and PITG_05542, which respectively encode acyl-coA synthase and 3-hydroxacyl-CoA-dehydrogenase that both participate in fatty acid β-oxidation, were increased in oospores 2-fold (Fig. 3.6, Table 3.6). This might be because this is a fast and efficient way to generate energy from stored lipid when germination begins. While fatty acid β-oxidation occurs in peroxisomes and mitochondria of mammals and some algae, it occurs exclusively in peroxisomes of plants and fungi (Kunau et al., 1999; Poirier et al., 2006). In this study, proteins that are specific to both peroxisome and mitochondrion were identified, suggesting the occurrence of β -oxidation in both organelles. Thus, it suggested that the evolutionary relationship between *Phytophthora* and animals might be closer than the one between *Phytophthora* and plants or fungi (Savidor et al., 2008).

In this study, approximately 7% of the proteins identified were predicted to be secreted proteins, which is consistent with the prediction of 6% of all the genes in the genome being secreted (Jiang et al., 2006; Haas et al., 2009). According to Student's *t*-test, this group of proteins was expressed significantly higher in oospores than in mycelia. Across the four MudPIT experiments performed, for unknown reasons, only three of the proteins identified possess RxLR motifs, PITG_10347, PITG_22922 and PITG_22925 (Table 3.2 and 3.5). The protein encoded by PITG_10347 was significantly enriched in oospores with a 2.5-fold induction relative to hyphae, while the latter two genes were

hyphae specific. The RxLR motif has been shown to deliver pathogen effector proteins into plant cells, and manipulate host defense responses (Dou et al., 2008). Considering the 563 RxLR proteins that *P. infestans* is predicted to possess (Haas et al., 2009), the identification of only one RxLR protein was unusual. In oospores, this presynthesized RxLR protein could be Secreted during germination without delay in order to establish the infection. This particular RxLR protein might be the most important one for establishing the host-pathogen interaction so that it was the only RxLR made and stored in the oospores.

The majority of the secreted proteins we observed belong to the crinkler (CRN) protein family (45 out of 50). This is a group of poorly studied effector proteins that activate defense responses in the plant cytoplasm and trigger necrosis *in planta* (Haas et al., 2009). This study revealed that there are 196 predicted CRN proteins in the *P. infestans* genome and they shared highly conserved N-termini, an approximately 50 amino acid LFLAK domain and a DWL domain, and have very diverse C-termini. CRN proteins usually contain a predicted signal peptide. Experiments have shown that the C-terminal effector domains are sufficient for eliciting a necrosis response in the host plant. However, many CRN proteins identified in this study were conserved at their C-termini and more diverse on the N-termini, such as PITG_16614, PITG_20172, and PITG_16597. It indicated that a group of very closely related proteins that share the same C-terminal effector domains were identified in the proteome.

Three elicitin-like proteins were identified. Among them, a putative elicitin-like protein 2 (ELL2) encoded by PITG_04378 was concentrated 3.3-fold higher in oospores

than in hyphae, while INF4 encoded by PITG_21410 and an INF5 like protein encoded by PITG_12562were more abundant by 1.5-fold. Elicitins are effector proteins that can induce a necrotic and systemic hypersensitive response (HR) and some of them were proved to have sterol-binding activity, such as INF1. These 3 elicitin and elicitin-like proteins identified in this study all showed relatively high conservation with INF1 (Jianag et al., 2005), so their potential role in oospores is probably being sterol carriers as well.

It was not expected that oospores would have more abundant secreted/ effector proteins since it was the dormant oospores that were analyzed. It is possible that the elicitin/elicitin-like proteins, RxLR protein and CRNs were made during the early stage of oosporogenesis and stored to facilitate pathogen-host infection relationship. This result might again prove our hypothesis that proteins that are needed for the current stage were made in the previous step. Even though the spores are inactive at this stage, they are fully prepared to infect and manipulate a host as soon as they encounter one.

As mentioned previously, oospores serve as a survival structure for *P. infestans*. An oospore can persist through severe drought, heat, and even UV radiation. Naturally, we expected to see anti-stress and antioxidant proteins being one of the highly expressed protein groups, and this hypothesis was supported by the results of this study. The functional group of antioxidant and anti-stress proteins was significantly enriched in oospores compared hyphae (Fig. 3.5). Three out of 17 significantly more abundant proteins in oospores were classified in this group (Table 3.2). The glutathione-S-transferase (GST), PITG_15531, was identified to have 1.2-fold induction in oospores. GSTs are a major group of detoxification enzymes. They present in both eukaryotes and

prokaryotes, where they catalyze the reactions of detoxifying a variety of endogenous and xenobiotic toxic substrates to protect the cells. Another group of redox proteins such as thioredoxin and oxireductase were identified and concentrations of many of these proteins were increased by about 0.75 and 1.3-fold. Product of PITG_15292, a catalase that catalyzes decomposition of hydrogen peroxide to water and oxygen, was concentrated by 1.9-fold in oospores. These proteins are very likely to be involved in the preparations for the beginning of the germination. At that stage, thick oospore walls will be thinned down for both the production of energy through cell wall degradation and also the formation of the germination tube. At this point cells are will be much more sensitive to environmental factors. These antioxidant and anti-stress proteins that are already stored in the oospore will be able to protect the germ tubes or sporangia before the pathogen finds its way into the host.

The post-transcriptional modification group was expressed at the same level in both stages. However, in this group there is one protein whose abundance was significantly increased in oospores, PITG_19199, an arginine N-methyltransferase (Table. 3.2). This enzyme participates in transcriptional regulation by methylating arginine residues in histones and other chromatin proteins (Kleinschmidt et al., 2008). Its function in oospores could be to facilitate the synthesis of new RNAs for germination.

Apart from the significantly concentrated proteins, we also identified 44 proteins unique to oospores from the unlabeled oospore samples 1, 2 and 3. They are listed in Table 3.4. These were involved in the majority of the cellular functions that have been described above, and are potentially candidates for direct involvement in oospore

germination. Curiously, there is an argonaute 1 protein encoded by PITG_04470. An RNAi-like mechanism has been described previously in *P. Infestans* (Ah-Fong et al., 2008), so the identification of argonaute was not surprising. It might be involved in some translational repression pathways that enable only the synthesis of essential proteins during germination.

Nine genes that were significantly less concentrated in oospores (*t*-test, $p<0.05$) were also identified in our study (Table 3.3). Together with 200 proteins unique to hyphae (Table 3.4), they were proposed to be the candidates for vegetative growth. Besides the proteins involved in protein production, enzymes that are responsible for signal transduction, cell cycle regulation, and DNA repair were also detected. Calmodulin, PITG_06514, an important Ca^{2+} binding protein, was absent in oospores across all four oospore samples, and detected in both of the hyphae samples. However, Western analysis using a human calmodulin antibody did not show binding activity to the *P. infestans* calmodulin probably due to the low sequence conservation of calmodulin proteins in the two organisms. A nucleolar protein encoded by PITG_14730, was another that was unique to hyphae, and its homologs are responsible for ribosomal RNA synthesis (Ahmad et al., 2009). The downregulation and the lack of presence of these proteins in oospores suggested that oospores have very low cellular activity and metabolic rate, and are possibly less influenced by outside environment stresses.

This study was the first global profiling study on *Phytophthora* oospore proteomes. Oospore protein compositions and their differences to nonsporulating hyphae proteomes were identified and new insights were brought in understanding the biology of

oospores at a molecular level. The results proved our hypothesis that proteins needed for a current stage of life cycle are synthesized and stored in the previous stage. In our case, since there are minimal cell activities in oospores, proteins stored in the oospores were probably made at the beginning of oosporogenesis, when large quantities of cell organelles could still be observed (Ruben & Stanghellini, 1978; Beakes et al., 1986). The proteins that we detected in oospores from this study are probably mainly prepared for maintaining the dormant status and the germination process.

Proteins involved in protein metabolism and transportation were found to be significantly less abundant in the oospores supported the theory that being the dormant structures, oospores do not actively synthesize proteins. The identification of varieties of abundant antistress and oxidoreduction proteins suggested that oospores are truly the survival structures of the pathogen. Equipped with these proteins, germinating oospores are prepared to overcome unfavorable conditions such as drought, heat, and UV radiationwhen they start to germinate and lose the physical protection afforded by oospore walls. The present of complete set of fatty acid oxidation enzymes and carbohydrate metabolism enzymes enable the energy production from stored lipids and β-glucans in oospore walls to begin immediately when necessary. New pesticides could be deigned that to manipulate these enzymes to disrupt the energy supply to the germtube or to systematically impair the thick cell wall of oospores, to achieve the goal of better controlling this pathogen.

Table 3.2. Proteins that are significantly more abundant (ratio>0.82, *t*-test, $p<0.05$) in *P. infestans* oospores compared to nonsporulating hyphae. Ratios are calculated by relative expression values in oospores divided by the relative expression values in hyphae.

Broad database accession number	Predicted function	Functional category	Ratio
PITG_19199	Arginine N-methyltransferase, putative	mRNA processing and transcription regulation	3.16
PITG_08044	Conserved hypothetical protein with Protein kinase C conserved region 2	Signal transduction	2.49
PITG_10347	Secreted RxLR effector peptide, putative	Secreted or infection related protein	2.45
PITG_02335	Glycosyl hydrolases family 17	Energy production and conversion	2.38
PITG_04937	Conserved hypothetical protein	Unknown	2.04
PITG_15292	Catalase	Antioxidant, antistress, detoxification	1.93
PITG_19162	Alcohol dehydrogenase, putative	Carbohydrate transport and metabolism	1.63
PITG_17257	Gluconolactonase	Carbohydrate transport and metabolism	1.63
PITG_10881	Kinesin-like protein	Cell cycle, cell growthth and cell proliferation	1.43
PITG_15531	Glutathione S-transferase, putative	Antioxidant, antistress, detoxification	1.15
PITG_18306	Conserved hypothetical protein	Unknown	1.14
PITG_00164	Conserved hypothetical protein with RNA recognition site	mRNA processing and transcriptional regulation	1.03
PITG_07155	Conserved hypothetical protein	Unknown	0.98
PITG_22265	NADH:Flavin oxidoreductase	Antioxidant, antistress, detoxification	0.96
PITG_21186	Unknown protein	Unknown	0.91
PITG_00251	Nucleotidyltransferase (NT) domain of DNA polymerase beta	DNA/nucleotide metabolism and repair	0.90
PITG_15321	Aminomethyltransferase	Amino acid transport and metabolism	0.86

Table 3.3. Proteins that are significantly less concentrated (ratio<0.24, *t*-test, $p<0.05$) in *P. infestans* oospores compared to nonsporulating hyphae. Ratios are calculated by relative expression values in oospores divided by the relative expression values in hyphae. A ratio of 0 indicates that the protein is absent in oospores.

Broad Institute database accession number	Predicted function	Functional category	Ratio
PITG_06514	Calmodulin	Signal transduction	0.00
PITG_14730	Nucleolar protein	Ribosomal process	0.00
PITG_08810	Conserved hypothetical protein with calcium binding domain	Signal transduction	0.13
PITG_09563	40S ribosomal protein S9-1	Ribosomal process	0.19
PITG_06203	Conserved hypothetical protein	Cell cycle, cell growthth and cell proliferation	0.21
PITG_07567	Brefeldin A-inhibited guanine nucleotide-exchange protein	Protein transportation and metabolism	0.22
PITG_11071	Unknown protein	Unknown	0.24
PITG_15398	Conserved hypothetical protein with FYVE domain; Zinc-binding domain; targets proteins to membrane lipids via interaction with phosphatidylinositol-3-phosphate	Protein transportation and metabolism	0.24
PITG_08696	Iron-sulfur cluster scaffold protein Nfu-like protein	Translation regulation, post translational modification, protein folding	0.24

Figure. 3.6. Carbohydrate and fatty acid β-oxidation pathways**.** All the enzymes shown in the diagram were identified in both hyphae and oospore samples. Enzymes in bold red were found to be significantly more concentrated in the oospores than in nonsporulating hyphae.

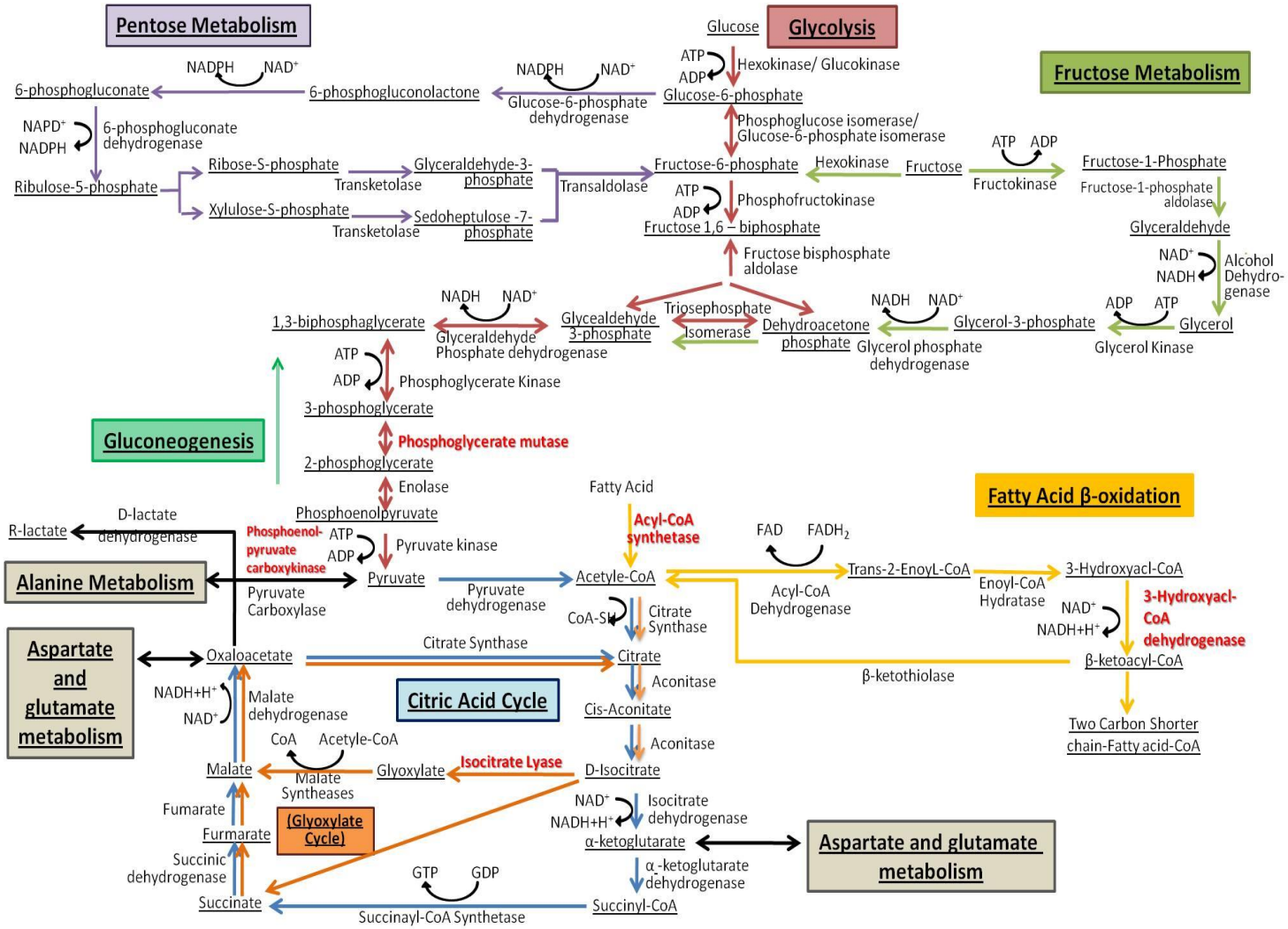
Pentose Metabolism
Glycolysis
Fructose Metabolism
Gluconeogenesis
Alanine Metabolism
Aspartate and glutamate metabolism
Citric Acid Cycle
Fatty Acid β-oxidation
(Glyoxylate Cycle)
Aspartate and glutamate metabolism
Glucose
Hexokinase/ Glucokinase
Glucose-6-phosphate
Glucose-6-phosphate dehydrogenase
6-phosphogluconolactone
6-phosphogluconate
6-phosphogluconate dehydrogenase
Ribulose-5-phosphate
Ribose-5-phosphate
Xylulose-5-phosphate
Transketolase
Glyceraldehyde-3-phosphate
Sedoheptulose -7-phosphate
Transaldolase
Phosphoglucose isomerase/ Glucose-6-phosphate isomerase
Fructose-6-phosphate
Hexokinase
Fructose
Fructokinase
Fructose-1-Phosphate
Fructose-1-phosphate aldolase
Glyceraldehyde
Alcohol Dehydro-genase
Glycerol
Glycerol Kinase
Phosphofructokinase
Fructose 1,6 – biphosphate
Fructose bisphosphate aldolase
Triosephosphate Isomerase
Glycealdehyde 3-phosphate
Dehydroacetone phosphate
Glycerol phosphate dehydrogenase
Glycerol-3-phosphate
1,3-biphosphaglycerate
Glyceraldehyde Phosphate dehydrogenase
Phosphoglycerate Kinase
3-phosphoglycerate
Phosphoglycerate mutase
2-phosphoglycerate
Enolase
Phosphoenolpyruvate
Phosphoenol-pyruvate carboxykinase
Pyruvate kinase
Pyruvate
Pyruvate Carboxylase
Pyruvate dehydrogenase
D-lactate dehydrogenase
R-lactate
Oxaloacetate
Citrate Synthase
Citrate
Aconitase
Cis-Aconitate
D-Isocitrate
Isocitrate dehydrogenase
α-ketoglutarate
α-ketoglutarate dehydrogenase
Succinyl-CoA
Succinayl-CoA Synthetase
Succinate
Succinic dehydrogenase
Fumarate
Furmarate
Malate
Malate dehydrogenase
Malate Syntheases
Glyoxylate
Isocitrate Lyase
Acetyle-CoA
CoA-SH
Fatty Acid
Acyl-CoA synthetase
Acetyle-CoA
Acyl-CoA Dehydrogenase
Trans-2-EnoyL-CoA
Enoyl-CoA Hydratase
3-Hydroxyacl-CoA
3-Hydroxyacl-CoA dehydrogenase
β-ketoacyl-CoA
β-ketothiolase
Two Carbon Shorter chain-Fatty acid-CoA

Table 3.4. Proteins uniquely found in oospores with their annotation and the functional group that they were classified into.

Broad Institute database accession number	Predicted function	Functional category
PITG_00544	Conserved hypothetical protein	Unknown
PITG_01186	Lipase	Lipid transport and metabolism
PITG_01938	Glyceraldehyde-3-phosphate dehydrogenase	Carbohydrate metabolism
PITG_02068	GTP-binding protein SAR1	Signal transduction
PITG_02615	Conserved hypothetical protein	Unknown
PITG_03685	2-amino-3-ketobutyrate coenzyme A ligase,	Amino acid transport and metabolism
PITG_04470	Argonaute 1 (AGO1)	mRNA processing and transcription regulation
PITG_04538	Splicing factor 3 subunit, putative	mRNA processing and transcription regulation
PITG_04573	Conserved hypothetical protein	Unknown
PITG_04766	Crinkler (CRN) family protein, putative	Secreted or infection related protein
PITG_05295	Conserved hypothetical protein	Unknown
PITG_05850	Pterin-4-alpha-carbinolamine dehydratase	Amino acid transport and metabolism
PITG_06514	Calmodulin	Signal transduction
PITG_06908	Elicitin-like protein	Secreted or infection related protein
PITG_07598	Conserved hypothetical protein with B23D domain	Unknown
PITG_07938	Conserved hypothetical protein	Unknown
PITG_08120	Conserved hypothetical protein	Unknown
PITG_08188	Conserved hypothetical protein	Unknown
PITG_08832	Conserved hypothetical protein	Unknown

Table 3.4. continued

PITG_09297	Conserved hypothetical protein	Unknown
PITG_09716	NPP1-like protein	Secreted or infection related protein
PITG_10819	Midasin-like protein	Protein transportation and metabolism
PITG_11676	Conserved hypothetical protein	Unknown
PITG_11996	Conserved hypothetical protein	Unknown
PITG_12090	Crinkler (CRN) family protein	Secreted or infection related protein
PITG_12884	Conserved hypothetical protein	Unknown
PITG_13122	ATP-binding Cassette (ABC) Superfamily	Lipid transport and metabolism
PITG_13204	Conserved hypothetical protein	Unknown
PITG_13834	Vacuolar protein, putative	Protein transportation and metabolism
PITG_14131	Conserved hypothetical protein	Unknown
PITG_14730	Nucleolar protein	Ribosomal process
PITG_14818	Guanylate-binding protein, putative	Signal transduction
PITG_16169	Carbohydrate-binding protein, putative	Carbohydrate transport and metabolism
PITG_16720	Conserved hypothetical protein	Unknown
PITG_17037	Calcineurin-like phosphoesterase	DNA/nucleotide metabolism and repair
PITG_18746	Conserved hypothetical protein	Unknown

Table 3.4. continued

PITG_19604	Elicitin-like protein	Secreted or infection related protein
PITG_19767	ATP-dependent Clp protease proteolytic subunit, putative	Protein transportation and metabolism
PITG_20599	26S protease regulatory subunit 8	Protein transportation and metabolism
PITG_21187	Myoferlin-like protein	Lipid transport and metabolism
PITG_21271	Conserved hypothetical protein	Unknown
PITG_21451	Conserved hypothetical protein	Unknown
PITG_22065	Conserved hypothetical protein	Unknown

Table 3.5. Proteins unique to nonsporulating hyphae with their annotation and the functional group that they were classified into.

Broad Institute database accession number	Predicted function	Functional category
PITG_00054	Mitochondrial protein translocase (MPT) Family	Protein metabolism and transportation
PITG_00219	Glucan 1,3-beta-glucosidase	Carbohydrate transport and metabolism
PITG_00397	Eukaryotic translation initiation factor 3 subunit C,	Protein transportation and metabolism
PITG_00442	Cytochrome c/c1 heme lyase	Translation regulation, post translational modification, protein folding
PITG_00492	Cytochrome c peroxidase	Antioxidant, antistress, detoxification
PITG_00654	DNA damage inducible protein 1	Protein transportation and metabolism
PITG_00663	rRNA methyltransferase	Ribosomal process
PITG_00665	Vesicle transport v-SNARE protein N-terminal	Protein metabolism and transportation
PITG_00695	Importin	Protein metabolism and transportation
PITG_00914	Nuclear transcription factor Y subunit	mRNA and transcriptional regulation
PITG_00930	Mitochondrial glycoprotein	Translation regulation, post translational modification, protein folding
PITG_01019	U3 small nucleolar RNA-associated protein	Ribosomal process
PITG_01171	Signal recognition particle	Protein metabolism and transportation
PITG_01246	Signal recognition particle	Protein metabolism and transportation
PITG_01255	Eukaryotic translation initiation factor 5	Protein metabolism and transportation
PITG_01300	DNA topoisomerase 2 DNA gyrase B	DNA/nucleotide metabolism and repair
PITG_01470	Syntaxin-like protein	Protein metabolism and transportation
PITG_01535	Myosin-like protein	Cell cycle, cell growthth and cell proliferation
PITG_01591	Unknown protein	Unknown
PITG_01616	Metalloprotease family M01	Protein metabolism and tansportation
PITG_01839	4-coumarate-CoA ligase	Antioxidant, antistress, detoxification

Table 3.5. continued

PITG_01950	Protein kinase	Translation regulation, post translational modification, protein folding
PITG_01982	Conserved hypothetical protein with ENTH domain	Cell cycle, cell growthth and cell proliferation
PITG_01997	Dynein 1 light intermediate chain	Cell cycle, cell growthth and cell proliferation
PITG_02327	Conserved hypothetical protein	Unknown
PITG_02347	Signal recognition particle receptor beta subunit	Protein metabolism and transportation
PITG_02546	Ubiquitin carboxyl-terminal hydrolase	Protein metabolism and transportation
PITG_02686	Conserved hypothetical protein	Unknown
PITG_02917	Puromycin-sensitive aminopeptidase	Protein metabolism and transportation
PITG_03112	Importin-like protein	Protein metabolism and transportation
PITG_03336	GTP-binding protein TypA/BipA	Signal transduction
PITG_03347	Ribonucleoside-diphosphate reductase small chain	DNA/nucleotide metabolism and repair
PITG_03360	AP-4 complex subunit epsilon	Protein metabolism and transportation
PITG_03388	Lectin	Carbohydrate metabolism
PITG_03462	Cysteine protease family C26	Protein metabolism and transportation
PITG_03493	Amidophosphoribosyltransferase	DNA/nucleotide metabolism and repair
PITG_03577	Vacuolar protein sorting-associated protein VTA1	Protein metabolism and transportation
PITG_03596	Histidine acid phosphatase	Amino acid transport and metabolism
PITG_03653	Protein phosphatase 2	Protein metabolism and transportation
PITG_03711	Serine/threonine-protein phosphatase 2A regulatory subunit B	Cell cycle, cell growth and cell proliferation
PITG_03828	Conserved hypothetical protein	Unknown
PITG_03846	Conserved hypothetical protein	Unknown
PITG_03855	DNA-directed RNA polymerase I subunit RPA1	mRNA processing and transcription regulation
PITG_03955	U3 small nucleolar RNA-associated protein	Ribosomal process
PITG_03971	Acetyltransferase (GNAT) family	mRNA processing and transcription regulation
PITG_03987	DEAD/DEAH box RNA helicase	mRNA and transcriptional regulation
PITG_04025	Nuclease	DNA/nucleotide metabolism and repair
PITG_04294	NADH:Flavin oxidoreductase	Antioxidant, antistress, detoxification
PITG_04441	3-isopropylmalate dehydrogenase	Antioxidant, antistress, detoxification

Table 3.5. continued

PITG_04452	H^+ - or Na^+ -translocating F-type, V-type and A-type ATPase (F-ATPase) Superfamily	Ion, cation, sugar, or macromolecule trafficking
PITG_04547	Conserved hypothetical protein	Unknown
PITG_04603	Flagellar protein FliS	Cytoskeleton
PITG_04774	Mitochondrial small ribosomal subunit Rsm22	Protein metabolism and transportation
PITG_04781	Conserved hypothetical protein	Unknown
PITG_04792	Conserved hypothetical protein	Unknown
PITG_04831	Regulator of chromosome condensation (RCC1)-like protein	Protein metabolism and transportation
PITG_04845	Conserved hypothetical protein	Unknown
PITG_04958	Coatomer subunit beta. Protein transportation	Protein metabolism and transportation
PITG_05226	KRI1-like family	Ribosomal process
PITG_05240	Casein kinase	Protein metabolism and transportation
PITG_05366	Branchpoint-bridging protein	mRNA and transcriptional regulation
PITG_05367	Translational activator GCN1	Protein metabolism and transportation
PITG_05391	Histone H1	mRNA and transcriptional regulation
PITG_05408	Transmembrane protein	Protein metabolism and transportation
PITG_05480	Conserved hypothetical protein	Unknown
PITG_05551	Ribose-phosphate pyrophosphokinase	DNA/nucleotide metabolism and repair
PITG_05556	D-lactate dehydrogenase	Amino acid transport and metabolism
PITG_05569	Conserved hypothetical protein	Unknown
PITG_05601	Cytokine-induced anti-apoptosis inhibitor 1	Cell cycle, cell growth and cell proliferation
PITG_05685	Transcription elongation factor SPT5	mRNA and transcriptional regulation
PITG_05861	Conserved hypothetical protein with peptidase dimerisation domain	Protein metabolism and transportation
PITG_05953	Ectoine synthase	Amino acid transport and metabolism
PITG_05990	Myb-like DNA-binding protein	mRNA and transcriptional regulation
PITG_06260	Dihydroxyacetone kinase	Carbohydrate transport and metabolism
PITG_06427	Serine hydroxymethyltransferase	Amino acid transport and metabolism
PITG_06772	ATP-binding cassette sub-family F member 1	Protein metabolism and transportation

Table 3.5. continued

PITG_06815	NADH dehydrogenase flavoprotein 1	Antioxidant, antistress, detoxification
PITG_07162	Sideroflexin-1-like protein	Ion, cation, sugar, or macromolecule trafficking
PITG_07790	Peroxisomal (S)-2-hydroxy-acid oxidase	Fatty acid transport, metabolism
PITG_07846	Glycylpeptide N-tetradecanoyltransferase 2	Protein metabolism and transportation
PITG_07865	Autophagy-related protein	Protein metabolism and transportation
PITG_07955	Xaa-Pro dipeptidase, metalloprotease family M24B	Protein metabolism and transportation
PITG_07985	Myosin-like protein	Cell cycle, cell growth and cell proliferation
PITG_08048	Conserved hypothetical protein	Unknown
PITG_08326	DNA synthesis. DNA polymerase alpha catalytic subunit	DNA/nucleotide metabolism and repair
PITG_08601	Conserved hypothetical protein with RPEL repeat	Unknown
PITG_08653	Mitochondrial import inner membrane translocase subunit TIM50	Protein metabolism and transportation
PITG_08660	Prefoldin, beta subunit	Translation regulation, post translational modification, protein folding
PITG_08693	Hook domain-containing protein	Protein metabolism and transportation
PITG_08740	FYVE zinc finger domain	Protein metabolism and transportation
PITG_08804	Metalloprotease family M01	Protein metabolism and transportation
PITG_08844	Mannitol dehydrogenase	Carbohydrate transport and metabolism
PITG_09004	Conserved hypothetical protein	Unknown
PITG_09041	Conserved hypothetical protein	Unknown
PITG_09367	Sterol 3-beta-glucosyltransferase, putative	Lipid transport and metabolism
PITG_09378	Conserved hypothetical protein	Unknown
PITG_09394	Glycolysis--pyruvate kinase	Carbohydrate metabolism
PITG_09419	Gamma-soluble NSF attachment protein	Protein metabolism and transportation
PITG_09533	Phosphoribosylaminoimidazole-succinocarboxamide synthase	DNA/nucleotide metabolism and repair
PITG_09566	Inositol monophosphatase	Signal transduction
PITG_09576	Orotidine 5'-phosphate decarboxylase	DNA/nucleotide metabolism and repair
PITG_09702	RNA splicing factor	mRNA and transcriptional regulation

Table 3.5. continued

PITG_09807	4-hydroxyphenylpyruvate dioxygenase	Amino acid transport and metabolism
PITG_10195	Acyl-CoA desaturase	Fatty acid transport metabolism
PITG_10324	Atlastin-like protein	Cytoskeleton
PITG_10443	Peroxisomal acyl-coenzyme A oxidase	Fatty acid transport metabolism
PITG_10463	Conserved hypothetical protein	Unknown
PITG_10573	Succinyl-CoA:3-ketoacid-coenzyme A transferase subunit A	Fatty acid transport metabolism
PITG_10777	Imidazoleglycerol-phosphate dehydratase	Amino acid transport and metabolism
PITG_10822	Mitochondrial protein translocase	Protein metabolism and transportation
PITG_10858	Glycine cleavage system H protein	Amino acid transport and metabolism
PITG_11110	Eukaryotic translation initiation factor 2 subunit 3	Protein metabolism and transportation
PITG_11152	Conserved hypothetical protein	Unknown
PITG_11170	Histone-binding protein RBBP4	DNA/nucleotide metabolism and repair
PITG_11197	Myosin-like protein	Cell cycle, cell growth and cell proliferation
PITG_11249	Heat shock 70 kDa protein	Translation regulation, post translational modification, protein folding
PITG_11457	Phosphoribosylformylglycinamidine synthase	DNA/nucleotide metabolism and repair
PITG_11603	Peptidyl-prolyl cis-trans isomerase CYP19-4	Translation regulation, post translational modification, protein folding
PITG_11702	Conserved hypothetical protein	Unknown
PITG_11789	Vacuolar (H^+)-ATPase G subunit	Ion, cation, sugar, or macromolecule trafficking
PITG_11856	C2 domain-containing protein	Lipid transport and metabolism
PITG_11959	Conserved hypothetical protein	Unknown
PITG_12291	RNA metabolism pre-mRNA-processing factor 39	mRNA and transcriptional regulation
PITG_12348	Conserved hypothetical protein	Unknown
PITG_12486	tRNA binding domain	Translation regulation, post translational modification, protein folding
PITG_12514	Bifunctional aspartokinase/homoserine dehydrogenase	Amino acid transport and metabolism
PITG_12528	Conserved hypothetical protein	Unknown
PITG_12682	Electron transport	Ion, cation, sugar, or macromolecule trafficking
PITG_12725	Cysteine synthase	Amino acid transport and metabolism
PITG_13271	Conserved hypothetical protein	Unknown

Table 3.5. continued

PITG_13683	NADH dehydrogenase flavoprotein 2	Antioxidant, antistress, detoxification
PITG_13713	MICAL-like	Cytoskeleton
PITG_13726	Ca^{2+}: Cation Antiporter	Ion, cation, sugar, or macromolecule trafficking
PITG_13738	Conserved hypothetical protein	Unknown
PITG_13889	4-coumarate-CoA ligase	Antioxidant, antistress, detoxification
PITG_14066	CUG-BP- and ETR-3-like factor	mRNA and transcriptional regulation
PITG_14189	Conserved hypothetical protein	Unknown
PITG_14248	rRNA-processing protein EBP2	rRNA processing
PITG_14254	Phosphoenolpyruvate carboxykinase	Carbohydrate metabolism
PITG_14485	Conserved hypothetical protein	Unknown
PITG_14578	Phosducin-like protein	Signal transduction
PITG_14584	Microtubule -associated protein EB1	Cytoskeleton
PITG_14730	Nucleolar protein	Protein metabolism and transportaion
PITG_14768	Double-stranded DNA-binding domain	mRNA and transcriptional regulation
PITG_14918	Riboflavin biosynthesis protein ribBA	Energy production and conversion
PITG_15016	Conserved hypothetical protein	Unknown
PITG_15496	Fatty acid reduction-acyl-coA synthetase	fatty acid transport metabolism
PITG_15568	Conserved hypothetical protein	Unknown
PITG_15784	Polyadenylate-binding protein 2	mRNA and transcriptional regulation
PITG_15998	Phospholipase A2-activating protein	Lipid transport and metabolism
PITG_16058	Conserved hypothetical protein	Unknown
PITG_16580	Crinkler (CRN) family protein	Secreted or infection related protein
PITG_16591	Crinkler (CRN) family protein	Secreted or infection related protein
PITG_16619	Crinkler (CRN) family protein	Secreted or infection related protein
PITG_16623	Crinkler (CRN) family protein	Secreted or infection related protein
PITG_16856	Hypoxanthine-guanine phosphoribosyltransferase	DNA/nucleotide metabolism and repair
PITG_16864	Conserved hypothetical protein	Unknown
PITG_17035	Conserved hypothetical protein	Unknown
PITG_17069	Coatomer protein complex	Protein metabolism and transportation
PITG_17280	Conserved hypothetical protein	Unknown

Table 3.5. continued

PITG_17289	Deoxyuridine 5'-triphosphate nucleotidohydrolase	DNA/nucleotide metabolism and repair
PITG_17708	Translationally controlled tumour protein	Cell cycle, cell growthth and cell proliferation
PITG_17747	H^+ - or Na^+ -translocating F-type, V-type and A-type ATPase (F-ATPase) Superfamily	Ion, cation, sugar, or macromolecule trafficking
PITG_17936	Structural maintenance of chromosomes protein 4	DNA/nucleotide metabolism and repair
PITG_18091	Structural maintenance of chromosomes protein	DNA/nucleotide metabolism and repair
PITG_18170	12-oxophytodienoate reductase	Antioxidant, antistress, detoxification
PITG_18248	Acetate kinase	Energy production and conversion
PITG_18503	Crinkler (CRN) family protein	Secreted or infection related protein
PITG_19063	Conserved hypothetical protein	Unknown
PITG_19164	Mitochondrial protein translocase	Protein metabolism and transportation
PITG_19263	Sulfite reductase [NADPH] flavoprotein component	Amino acid transport and metabolism
PITG_19340	Crinkler (CRN) family protein	Secreted or infection related protein
PITG_19347	Crinkler (CRN) family protein	Secreted or infection related protein
PITG_19493	Triosephosphate isomerase/glyceraldehyde-3-phosphate dehydrogenase	Carbohydrate metabolism
PITG_19590	Conserved hypothetical protein	Unknown
PITG_19668	Biotin-requiring enzyme	Carbohydrate metabolism
PITG_19774	Mannose-6-phosphate isomerase	Carbohydrate metabolism
PITG_19993	GMP synthase [glutamine-hydrolyzing]	DNA/nucleotide metabolism and repair
PITG_20081	Conserved hypothetical protein	Unknown
PITG_20139	Resistance-Nodulation-Cell Division (RND) Superfamily	Cell cycle, cell growthth and cell proliferation
PITG_20141	PpiC-type peptidyl-prolyl cis-trans isomerase	Translation regulation, post translational modification, protein folding
PITG_20386	Eukaryotic translation initiation factor 5B	Protein metabolism and transportation
PITG_20562	RAC family serine/threonine-protein kinase	ion, cation, sugar, or macromolecule trafficking
PITG_20965	Imidazoleglycerol-phosphate dehydratase	Amino acid transport and metabolism
PITG_21010	Eukaryotic translation initiation factor 3 subunit	Protein metabolism and transportation
PITG_21077	DNA-directed RNA polymerase II largest subunit	mRNA and transcriptional regulation

Table 3.5. continued

PITG_21176	Transportin-like protein	Protein metabolism and transportation
PITG_21480	Conserved hypothetical protein	Unknown
PITG_21626	ATP-binding cassette protein	Ion, cation, sugar, or macromolecule trafficking
PITG_21945	NmrA-like family protein	mRNA processing and transcription regulation
PITG_22107	Conserved hypothetical protein	Unknown
PITG_22186	Crinkler (CRN) family protein,	Secreted or infection related protein
PITG_22734	NPP1-like protein	Secreted or infection related protein
PITG_22832	Crinkler (CRN) family protein	Secreted or infection related protein
PITG_22919	Conserved hypothetical protein	Unknown
PITG_22922	Secreted RxLR effector peptide	Secreted or infection related protein
PITG_22925	Secreted RxLR effector peptide,	Secreted or infection related protein
PITG_23055	NPP1-like protein	Secreted or infection related protein
PITG_23056	NPP1-like protein, pseudogene	Protein metabolism and transportation
PITG_23140	Elicitin-like protein, pseudogene	Secreted or infection related protein
PITG_23156	Small cysteine rich protein SCR58	Protein metabolism and transportation

Table 3.6. Proteins shared by oospore and nonsporulating hypahe (NSH). The ratio of oospore/NSH, protein function annotation and functional groups of proteins are listed. When the identified protein came from unlabeled samples, the ratio was set as 0.

Broad institute accession number	Predicted function	Functional category	Ratio
PITG_00034	Aldehyde dehydrogenase	Carbohydrate transport and metabolism	0.46
PITG_00058	Protease inhibitor epic4	Protein transportation and metabolism	0.48
PITG_00070	Conserved hypothetical protein with 2OG-Fe(II) oxygenase domain	Antioxidant, antistress, detoxification	0.54
PITG_00074	Conserved hypothetical protein with Mitochondrial ATP synthase B chain domain	Energy production and conversion	0.35
PITG_00127	Estradiol 17-beta-dehydrogenase	Signal transduction	0.00
PITG_00132	Phosphoglycerate kinase	Carbohydrate transportation and metabolism	0.49
PITG_00133	Phosphoserine aminotransferase	Amino acid transport and metabolism	0.31
PITG_00146	Glucose-6-phosphate 1-dehydrogenase	Carbohydrate transport and metabolism	0.31
PITG_00156	Beta-tubulin	Cytoskeleton	0.41
PITG_00158	Conserved hypothetical protein	Unknown	0.00
PITG_00163	Threonine dehydratase, mitochondrial precursor	Amino acid transport and metabolism	0.53
PITG_00164	Conserved hypothetical protein with RNA recognition site	mRNA processing and transcription regulation	1.03
PITG_00170	Vacuolar-sorting receptor	Protein transportation and metabolism	0.00
PITG_00172	Proteasome subunit alpha	Protein transportation and metabolism	0.43
PITG_00179	40S ribosomal protein S12	Protein transportation and metabolism	0.32
PITG_00183	Dynamin-2	Ion, cation, sugar, or macromolecule trafficking	0.41
PITG_00203	Mitochondrial-processing peptidase subunit beta	Protein transportation and metabolism	0.36
PITG_00212	Conserved hypothetical protein	Unknown	0.55
PITG_00216	Conserved hypothetical protein	Unknown	0.30

Table 3.6. continued

PITG_00221	Tryptophan synthase	Amino acid transport and metabolism	0.00
PITG_00229	26S protease regulatory subunit S10B	Protein transportation and metabolism	0.36
PITG_00251	Conserved hypothetical protein with NT domain of DNA polymerase	DNA/nucleotide metabolism and repair	0.90
PITG_00264	Delta(3,5)-Delta(2,4)-dienoyl-coa isomerase	Fatty acid transport and metabolism	0.34
PITG_00266	40S ribosomal protein S10	Protein transportation and metabolism	0.29
PITG_00279	Ubiquitin carboxyl-terminal hydrolase	Protein transportation and metabolism	0.51
PITG_00380	Sphingosine-1-phosphate lyase	Cell division, cell growthth, and cell proliferation	0.50
PITG_00390	Conserved hypothetical protein with PB1 domain	Protein transportation and metabolism	0.85
PITG_00395	Cathepsin B, cysteine protease family C01A	Protein transportation and metabolism	0.84
PITG_00396	Aspartyl protease family A01B	Protein transportation and metabolism	0.35
PITG_00410	Bystin	Ribosomal process	0.76
PITG_00443	40S ribosomal protein S6	Ribosomal process	0.33
PITG_00448	tRNA (cytosine-5-)-methyltransferase NSUN2	Protein transportation and metabolism	0.39
PITG_00453	Lipoamide acyltransferase component of branched-chain alpha-keto acid dehydrogenase complex	Amino acid transport and metabolism	0.96
PITG_00457	Conserved hypothetical protein with EF-hands--signaling proteins and buffering/transport proteins	Ion, cation, sugar, or macromolecule trafficking	0.39
PITG_00458	Dihydrolipoyllysine-residue acetyltransferase component of pyruvate dehydrogenase complex	Carbohydrate transportation and metabolism	0.38
PITG_00461	Mitochondrial carrier (MC) family	Energy production and conversion	0.43
PITG_00471	Pyridoxal biosynthesis lyase pdxs	Amino acid transport and metabolism	0.56
PITG_00490	Protein phosphatase 2C	Translation regulation, post translational modification, protein folding	0.33

Table 3.6. continued

PITG_00518	Nucleoredoxin	Antioxidant, antistress, detoxification	0.37
PITG_00527	Luminal-binding protein 3 precursor	Translation regulation, post translational modification, protein folding	0.41
PITG_00571	Bifunctional purine biosynthesis protein PURH	DNA/nucleotide metabolism and repair	0.58
PITG_00585	Peroxiredoxin-like protein	Antioxidant, antistress, detoxification	0.34
PITG_00613	26S protease regulatory subunit 8	Protein transportation and metabolism	0.42
PITG_00620	Kinesin-like protein	Cytoskeleton	0.00
PITG_00623	4-aminobutyrate aminotransferase	Amino acid transport and metabolism	0.46
PITG_00631	Conserved hypothetical protein with RNA S14 domain	Protein transportation and metabolism	0.39
PITG_00632	Dolichyl-diphosphooligosaccharide-protein glycosyltransferase subunit STT3A	Protein transportation and metabolism	0.42
PITG_00648	Periodic tryptophan protein	Ribosomal process	0.51
PITG_00682	Carbonic anhydrase	Antioxidant, antistress, detoxification	0.43
PITG_00693	Plasma membrane H^+-ATPase	Ion, cation, sugar, or macromolecule trafficking	0.00
PITG_00701	Conserved hypothetical protein with manganese-dependent ADP-ribose/CDP-alcohol diphosphatase	Signal transduction	0.00
PITG_00702	Conserved hypothetical protein	Unknown	0.27
PITG_00708	Thioredoxin	Antioxidant, antistress, detoxification	0.50
PITG_00715	Thioredoxin	Antioxidant, antistress, detoxification	0.70
PITG_00765	Flagellar adenylate kinase	Energy production and conversion	0.36
PITG_00804	T-complex protein 1 subunit delta	Translation regulation, post translational modification, protein folding	0.42
PITG_00827	Prohibitin	mRNA processing and transcription regulation	0.46
PITG_00850	Thioredoxin-dependent peroxide reductase	Antioxidant, antistress, detoxification	0.56

Table 3.6. continued

PITG_00863	DEAD/DEAH box RNA helicase	mRNA processing and transcription regulation	0.27
PITG_00879	60S ribosomal protein L30	Protein transportation and metabolism	0.37
PITG_00899	Prefoldin subunit 3	Translation regulation, post translational modification, protein folding	0.38
PITG_00910	EF-1 guanine nucleotide exchange domain-containing protein	Protein transportation and metabolism	0.43
PITG_00912	3-hydroxyisobutyrate dehydrogenase	Amino acid transport and metabolism	0.40
PITG_00921	Phospholipase D, Pi-PLD-like-1	Signal transduction	0.39
PITG_00923	Phospholipase D, Pi-PLD-like-3	Signal transduction	0.40
PITG_00931	Conserved hypothetical protein with tetratrico peptide repeat	Protein transportation and metabolism	0.45
PITG_00941	60S ribosomal protein L21-1	Protein transportation and metabolism	0.46
PITG_00967	Methionyl-tRNA synthetase, beta subunit	Protein transportation and metabolism	0.37
PITG_00980	Nuclear cap-binding protein subunit	mRNA processing and transcription regulation	0.37
PITG_00986	Peroxiredoxin-4	Antioxidant, antistress, detoxification	0.68
PITG_01041	60S acidic ribosomal protein P2	Protein transportation and metabolism	0.52
PITG_01042	60S ribosomal protein L22	Protein transportation and metabolism	0.34
PITG_01064	Proteomeasome activitor pa28 beta subunit	Protein transportation and metabolism	0.57
PITG_01072	5-methlytetrahydropteroyltriglutamate -homocysteine methyltransferease	Amino acid transport and metabolism	0.48
PITG_01082	Ran-specific GTPase-activating protein	Signal transduction	0.44
PITG_01094	26S proteasome non-ATPase regulatory subunit 11	Protein transportation and metabolism	0.00
PITG_01110	NADH:Flavin oxidoreductase	Antioxidant, antistress, detoxification	0.46
PITG_01112	UDP-3-O-[3-hydroxymyristoyl] glucosamine N-acyltransferase	Carbohydrate transportation and metabolism	0.00

Table 3.6. continued

PITG_01144	Conserved hypothetical protein with nucleosome assembly protein motif	DNA/nucleotide metabolism and repair	0.52
PITG_01181	Conserved hypothetical protein	Protein transportation and metabolism	0.32
PITG_01184	Eukaryotic translation initiation factor 3 subunit G	Protein transportation and metabolism	0.40
PITG_01203	Mitogen-activated protein kinase	Antioxidant, antistress, detoxification	0.32
PITG_01208	Trifunctional enzyme subunit beta, mitochondrial precursor	Fatty acid transport and metabolism	0.63
PITG_01218	Conserved hypothetical protein	Unknown	0.00
PITG_01223	Conserved hypothetical protein	Unknown	0.43
PITG_01253	Aldehyde dehydrogenase, mitochondrial precursor	Carbohydrate transport and metabolism	0.34
PITG_01260	S-phase kinase-associated protein 1A	Cell cycle, cell growthth and cell proliferation	0.54
PITG_01397	Glycoside hydrolase	Carbohydrate transport and metabolism	0.32
PITG_01398	Beta-glucosidase	Carbohydrate transport and metabolism	0.50
PITG_01408	D-isomer specific 2-hydroxyacid dehydrogenase	Antioxidant, antistress, detoxification	0.42
PITG_01431	Glycoside hydrolase	Carbohydrate transport and metabolism	0.40
PITG_01447	Serine protease family S10	Protein transportation and metabolism	0.59
PITG_01452	Conserved hypothetical protein	Unknown	0.00
PITG_01477	Myosin-like protein	Ion, cation, sugar, or macromolecule trafficking	0.85
PITG_01498	ATP-binding cassette sub-family F member 2	Lipid transport and metabolism	0.72
PITG_01508	Conserved hypothetical protein with GYF domain	Signal transduction	0.00
PITG_01508	Conserved hypothetical protein	Unknown	0.34
PITG_01549	Succinate semialdehyde dehydrogenase, mitochondrial precursor	Amino acid transport and metabolism	0.40
PITG_01599	Coronin-like protein	Cytoskeleton	0.45
PITG_01619	Metalloprotease family M01	Protein transportation and metabolism	0.44

Table 3.6. continued

PITG_01700	Inositol-3-phosphate synthase	Carbohydrate transport and metabolism	0.35
PITG_01752	Transketolase	Carbohydrate transportation and metabolism	0.37
PITG_01762	Glycyl-tRNA synthetase	Protein transportation and metabolism	0.45
PITG_01778	Soluble pyridine nucleotide transhydrogenase	Energy production and conversion	0.43
PITG_01783	Acetyl-coA acetyltransferase/ketothiolase	Fatty acid transport and metabolism	0.50
PITG_01791	Protein disulfide-isomerase	Translation regulation, post translational modification, protein folding	0.66
PITG_01797	26S protease regulatory subunit 6A-A	Protein transportation and metabolism	0.41
PITG_01833	60S ribosomal protein L13	Protein transportation and metabolism	0.44
PITG_01862	Glucose-6-phosphate isomerase	Carbohydrate transportation and metabolism	0.34
PITG_01922	40S ribosomal protein SA	Protein transportation and metabolism	0.30
PITG_01923	Conserved hypothetical protein, Transcription factor S-II	mRNA processing and transcription regulation	0.66
PITG_01939	Glyceraldehyde-3-phosphate dehydrogenase	Carbohydrate transportation and metabolism	0.34
PITG_01940	Triosephosphate isomerase/glyceraldehyde-3-phosphate dehydrogenase	Carbohydrate transportation and metabolism	0.37
PITG_01943	60S ribosomal protein L23	Protein transportation and metabolism	0.33
PITG_01945	Conserved hypothetical protein similar to carbonic anhydrase/acetyltransferase	Carbohydrate transport and metabolism	0.47
PITG_01966	Conserved hypothetical protein with PEPCK domain	Carbohydrate transportation and metabolism	1.02
PITG_01985	Iron/zinc purple acid phosphatase-like protein	Secreted or infection related protein	0.52
PITG_02002	Enhancer of mRNA-decapping protein	mRNA processing and transcription regulation	0.64
PITG_02022	Clathrin heavy chain	Protein transportation and metabolism	0.51

Table 3.6. continued

PITG_02026	Succinyl-coA ligase subunit alpha, mitochondrial precursor	Carbohydrate transportation and metabolism	0.42
PITG_02038	Fructose 1,6 bisphosphatase	Carbohydrate transport and metabolism	0.55
PITG_02039	EF-1 guanine nucleotide exchange domain-containing protein,	Protein transportation and metabolism	0.43
PITG_02049	Citrate synthase, mitochondrial precursor	Carbohydrate transport and metabolism	0.40
PITG_02053	40S ribosomal protein S8-2	Protein transportation and metabolism	0.42
PITG_02112	3-hydroxyisobutyryl-coA hydrolase	Amino acid transport and metabolism	0.45
PITG_02114	Aspartyl aminopeptidase	Protein transportation and metabolism	0.43
PITG_02115	Propionyl-coA carboxylase beta chain, mitochondrial precursor	Carbohydrate transportation and metabolism	0.34
PITG_02122	Glucosamine-fructose-6-phosphate aminotransferase [isomerizing]	Carbohydrate transport and metabolism	0.45
PITG_02137	Serine/threonine-protein phosphatase 2A 65 kDa regulatory subunit A	Cell cycle, cell growthth and cell proliferation	0.40
PITG_02186	FKBP-type peptidyl-prolyl cis-trans isomerase	Translation regulation, post translational modification, protein folding	0.42
PITG_02198	Homoserine kinase	Amino acid transport and metabolism	0.39
PITG_02210	Phenylalanine-4-hydroxylase	Amino acid transport and metabolism	0.55
PITG_02211	UV excision repair protein RAD23	DNA/nucleotide metabolism and repair	0.40
PITG_02239	ATP-dependent hsl protease ATP-binding subunit hslu	Protein transportation and metabolism	0.33
PITG_02255	Histone H1	mRNA processing and transcription regulation	0.33
PITG_02256	Aspartate aminotransferase, mitochondrial precursor	Amino acid transport and metabolism	0.37
PITG_02259	Hsp70-like protein	Translation regulation, post translational modification, protein folding	0.48
PITG_02267	Coatomer subunit beta	Protein transportation and metabolism	0.36

Table 3.6. continued

PITG_02276	Peroxisomal trans-2-enoyl-coA reductase	Fatty acid transport and metabolism	0.52
PITG_02282	Acyl-coA dehydrogenase	Fatty acid transport and metabolism	0.35
PITG_02283	Conserved hypothetical protein	Unknown	0.76
PITG_02302	Crinkler (CRN) family protein	Secreted or infection related protein	0.00
PITG_02305	Conserved hypothetical protein with FKBP-type peptidylprolyl isomerases domain, accelerate protein folding	Translation regulation, post translational modification, protein folding	0.48
PITG_02335	Conserved hypothetical protein with glycoside hydrolase domain	Carbohydrate transport and metabolism	2.38
PITG_02344	5-oxoprolinase	Amino acid transport and metabolism	0.51
PITG_02353	Calcium-transporting ATPase	Ion, cation, sugar, or macromolecule trafficking	0.46
PITG_02458	Conserved hypothetical protein	Unknown	0.39
PITG_02467	Translocation protein SEC63	Protein transportation and metabolism	0.32
PITG_02468	Conserved hypothetical protein	Unknown	0.36
PITG_02475	Conserved hypothetical protein	Unknown	0.33
PITG_02479	T-complex protein 1 subunit theta	Translation regulation, post translational modification, protein folding	0.36
PITG_02502	T-complex protein 1 subunit zeta	Translation regulation, post translational modification, protein folding	0.43
PITG_02510	Conserved hypothetical protein	Unknown	0.38
PITG_02515	LETM1 and EF-hand domain-containing protein 1	Energy production and conversion	0.66
PITG_02532	Ca^{2+} :Cation Antiporter (caca) Family	Ion, cation, sugar, or macromolecule trafficking	0.57
PITG_02557	tRNA-dihydrouridine synthase 3	Protein transportation and metabolism	0.99
PITG_02567	T-complex protein 1 subunit alpha	Translation regulation, post translational modification, protein folding	0.35
PITG_02578	60S ribosomal protein L15-1	Protein transportation and metabolism	0.31
PITG_02586	Conserved hypothetical protein DNAJ domain, FYVE zinc finger	Translation regulation, post translational modification, protein folding	0.43

Table 3.6. continued

PITG_02594	Glutamate decarboxylase	Amino acid transport and metabolism	0.37
PITG_02598	Conserved hypothetical protein DNA with polymerase III subunits gamma and tau	DNA/nucleotide metabolism and repair	0.30
PITG_02599	Conserved hypothetical protein	Unknown	0.42
PITG_02607	Peroxisomal multifunctional enzyme	Fatty acid transport and metabolism	0.78
PITG_02627	Conserved hypothetical protein with major sperm motif	Cell cycle, cell growthth and cell proliferation	0.38
PITG_02629	Nucleolin	Ribosomal process	0.43
PITG_02634	Conserved hypothetical protein with STAR(steroidogenic Acute Regulatory) related domain	Lipid transport and metabolism	0.29
PITG_02642	Pyruvate dehydrogenase [lipoamide]	Carbohydrate transportation and metabolism	0.40
PITG_02694	60S ribosomal protein L23a	Protein transportation and metabolism	0.34
PITG_02740	Acetolactate synthase	Amino acid transport and metabolism	0.40
PITG_02752	Ribosomal RNA methyltransferase nop2-like protein	Ribosomal process	0.43
PITG_02754	Conserved hypothetical protein with VHS, ENTH, and ANTH domain	Ion, cation, sugar, or macromolecule trafficking	0.45
PITG_02785	Fructose-bisphosphate aldolase	Carbohydrate transportation and metabolism	0.44
PITG_02786	Fructose-bisphosphate aldolase	Carbohydrate transportation and metabolism	0.53
PITG_02802	Stomatin-like protein	Lipid transport and metabolism	0.49
PITG_02807	Conserved hypothetical protein	Unknown	0.00
PITG_02853	3,2-trans-enoyl-coa isomerase, mitochondrial precursor	Fatty acid transport and metabolism	0.41
PITG_02854	Aspartate-semialdehyde dehydrogenase	Amino acid transport and metabolism	0.42
PITG_02856	DEAD/DEAH box RNA helicase	mRNA processing and transcription regulation	0.41
PITG_02921	Valyl-tRNA synthetase	Protein transportation and metabolism	0.35
PITG_02925	Ketol-acid reductoisomerase	Amino acid transport and metabolism	0.35

Table 3.6. continued

PITG_02968	Choline dehydrogenase	Antioxidant, antistress, detoxification	0.38
PITG_02998	S-adenosyl-L-methionine-dependent methyltransferase	Ribosomal process	0.29
PITG_03020	Cysteine protease family C01A	Protein transportation and metabolism	0.43
PITG_03028	Pre-mRNA-splicing factor SF2	mRNA processing and transcription regulation	0.27
PITG_03039	Conserved hypothetical protein, Guanylate-binding protein	Signal transduction	0.44
PITG_03065	Conserved hypothetical protein	Unknown	0.40
PITG_03081	26S proteasome non-ATPase regulatory subunit 2	Protein transportation and metabolism	0.50
PITG_03095	Carbohydrate-binding protein	Carbohydrate transport and metabolism	0.48
PITG_03098	Carbamoyl-phosphate synthase	Amino acid transport and metabolism	0.38
PITG_03101	Conserved hypothetical protein with Semialdehyde dehydrogenase	Antioxidant, antistress, detoxification	0.51
PITG_03150	Proteasome subunit alpha type-3	Protein transportation and metabolism	0.43
PITG_03178	60S ribosomal protein L9	Protein transportation and metabolism	0.37
PITG_03221	40S ribosomal protein S18	Protein transportation and metabolism	0.35
PITG_03226	Glutathione S-transferase	Antioxidant, antistress, detoxification	0.42
PITG_03239	60S ribosomal protein L27	Protein transportation and metabolism	0.36
PITG_03246	Conserved hypothetical protein, ribonuclease inhibitor (RI)-like subfamily	mRNA processing and transcription regulation	0.61
PITG_03252	Alpha-soluble NSF attachment protein	Protein transportation and metabolism	0.55
PITG_03277	Pyruvate dehydrogenase E1 component subunit alpha	Carbohydrate transportation and metabolism	0.38
PITG_03294	60S ribosomal protein L6	Protein transportation and metabolism	0.35
PITG_03304	DEAD/DEAH box RNA helicase	mRNA processing and transcription regulation	0.52

Table 3.6. continued

PITG_03333	Hyaluronan (a glucosaminoglycan)/mRNA binding domain	mRNA processing and transcription regulation	0.26
PITG_03341	Conserved hypothetical protein	Unknown	0.00
PITG_03342	Sorting and assembly machinery component 50	Protein transportation and metabolism	0.30
PITG_03353	60S ribosomal protein L17-2	Protein transportation and metabolism	0.39
PITG_03373	Cell division protein FTSZ	Cell cycle, cell growthth and cell proliferation	0.00
PITG_03410	Acetolactate synthase small subunit,	Amino acid transport and metabolism	0.63
PITG_03424	GTPase	Signal transduction	0.44
PITG_03440	Malate synthase	Carbohydrate transportation and metabolism	0.50
PITG_03445	Holliday junction ATP-dependent DNA helicase ruvb	DNA/nucleotide metabolism and repair	1.10
PITG_03477	60S ribosomal protein l7a-2	Protein transportation and metabolism	0.44
PITG_03486	Conserved hypothetical protein with 60s Acidic ribosomal protein domain	Protein transportation and metabolism	1.08
PITG_03530	Alpha-aminoadipic semialdehyde synthase	Amino acid transport and metabolism	0.29
PITG_03532	Conserved hypothetical protein with BAR domain	Ion, cation, sugar, or macromolecule trafficking	0.23
PITG_03546	Hsp70-like protein	Translation regulation, post translational modification, protein folding	0.32
PITG_03549	Coatomer subunit gamma	Protein transportation and metabolism	0.30
PITG_03550	Histone H2B	mRNA processing and transcription regulation	0.37
PITG_03551	Histone H3	mRNA processing and transcription regulation	0.40
PITG_03552	Histone H4	mRNA processing and transcription regulation	0.42
PITG_03555	Importin-like protein	Protein transportation and metabolism	0.38
PITG_03561	COP9 signalosome complex subunit 5	Protein transportation and metabolism	0.70
PITG_03568	DEAD/DEAH box RNA helicase	mRNA processing and transcription regulation	0.64

Table 3.6. continued

PITG_03593	Alanine aminotransferase 2	Amino acid transport and metabolism	0.40
PITG_03594	Protein transporter Sec31A	Protein transportation and metabolism	0.54
PITG_03598	6-phosphofructokinase	Carbohydrate transportation and metabolism	0.37
PITG_03599	Alanine aminotransferase 2	Amino acid transport and metabolism	0.00
PITG_03661	Cysteinyl-tRNA synthetase	Protein transportation and metabolism	0.61
PITG_03694	Disulfide-isomerase	Translation regulation, post translational modification, protein folding	0.47
PITG_03700	Enolase	Carbohydrate transportation and metabolism	0.34
PITG_03712	Elongation factor 3	Protein transportation and metabolism	0.44
PITG_03719	Voltage-gated potassium channel subunit beta	Ion, cation, sugar, or macromolecule trafficking	0.36
PITG_03721	Pyruvate, phosphate dikinase	Carbohydrate transportation and metabolism	0.33
PITG_03724	Pyruvate, phosphate dikinase	Carbohydrate transportation and metabolism	0.33
PITG_03738	2-isopropylmalate synthase	Amino acid transport and metabolism	0.56
PITG_03763	Pre-mRNA-splicing factor SF2-like protein	mRNA processing and transcription regulation	0.36
PITG_03792	2,3-bisphosphoglycerate-independent phosphoglycerate mutase	Carbohydrate transportation and metabolism	0.82
PITG_03802	Eukaryotic translation initiation factor 6	Protein transportation and metabolism	0.60
PITG_03836	Conserved hypothetical protein with ankyrin repeat domain	Translation regulation, post translational modification, protein folding	1.28
PITG_03853	Conserved hypothetical protein	Unknown	0.42
PITG_03856	Peptidyl-prolyl cis-trans isomerase	Translation regulation, post translational modification, protein folding	0.39
PITG_03873	Rab GDP dissociation inhibitor alpha	Protein transportation and metabolism	0.35
PITG_03881	Histone H2A	mRNA processing and transcription regulation	0.35

Table 3.6. continued

PITG_03900	Conserved hypothetical protein with Rossmann-fold NAD(P)H/NAD(P)(+) binding (NADB) domain	Carbohydrate transportation and metabolism	0.00
PITG_03916	Ribosomal protein L28	Ribosomal process	0.00
PITG_03936	Ras protein let-60	Signal transduction	0.00
PITG_04010	APS kinase/ATP sulfurlyase/pyrophosphatase fusion protein	Signal transduction	0.40
PITG_04125	Glycosyl transferase	Secreted or infection related protein	0.45
PITG_04131	Glycoside hydrolase	Carbohydrate transport and metabolism	0.58
PITG_04229	Conserved hypothetical protein	Unknown	0.00
PITG_04376	Conserved hypothetical protein with Splicing factor 1 (SF1) K homology RNA-binding domain (KH)	mRNA processing and transcription regulation	0.00
PITG_04378	Elicitin-like protein	Secreted or infection related protein	1.62
PITG_04457	Tripeptidyl-peptidase	Protein transportation and metabolism	0.52
PITG_04487	Ribosomal protein S6	Protein transportation and metabolism	1.39
PITG_04500	Nucleosome assembly protein 1	DNA/nucleotide metabolism and repair	0.49
PITG_04522	Peptidyl-prolyl cis-trans isomerase	Translation regulation, post translational modification, protein folding	0.39
PITG_04640	Translation elongation factor 1-alpha	Protein transportation and metabolism	0.33
PITG_04658	Methylcrotonoyl-coA carboxylase subunit alpha	Amino acid transport and metabolism	0.46
PITG_04690	Pyridine nucleotide-disulphide oxidoreductase	Antioxidant, antistress, detoxification	0.00
PITG_04690	Pyridine nucleotide-disulphide oxidoreductase	Antioxidant, antistress, detoxification	0.48
PITG_04726	Mitochondrial-processing peptidase subunit alpha	Protein transportation and metabolism	0.41
PITG_04738	Conserved hypothetical protein with CRN domain	Secreted or infection related protein	0.34

Table 3.6. continued

PITG_04755	Conserved hypothetical protein with CRN domain	Secreted or infection related protein	0.43
PITG_04760	Crinkler (CRN) family protein	Secreted or infection related protein	0.43
PITG_04767	Crinkler (CRN) family protein	Secreted or infection related protein	0.43
PITG_04769	Crinkler (CRN) family protein	Secreted or infection related protein	0.48
PITG_04780	CRN domain-containing protein	Secreted or infection related protein	0.35
PITG_04795	CRN domain-containing protein	Secreted or infection related protein	0.46
PITG_04805	Crinkler (CRN) family protein	Secreted or infection related protein	0.86
PITG_04838	Cytosol aminopeptidase	Protein transportation and metabolism	0.45
PITG_04843	60S ribosomal protein L13	Protein transportation and metabolism	0.42
PITG_04861	Conserved hypothetical protein with Rap1 Myb domain	mRNA processing and transcription regulation	0.00
PITG_04862	RNA binding protein	mRNA processing and transcription regulation	0.42
PITG_04868	ADP/ATP translocase	Energy production and conversion	0.57
PITG_04906	Glutaredoxin	Antioxidant, antistress, detoxification	0.41
PITG_04937	Conserved hypothetical protein	Unknown	2.04
PITG_05007	Glutaminyl-tRNA synthetase	Protein transportation and metabolism	0.35
PITG_05045	Crinkler (CRN) family protein	Secreted or infection related protein	0.62
PITG_05049	Crinkler (CRN) family protein	Secreted or infection related protein	0.68
PITG_05115	HECT E3 ubiquitin ligase	Translation regulation, post translational modification, protein folding	0.61
PITG_05117	Glycine amidinotransferase, mitochondrial precursor	Amino acid transport and metabolism	0.74
PITG_05156	Secretory protein OPEL, putative polygalacturonase	Carbohydrate transport and metabolism	0.31
PITG_05264	10 kDa chaperonin	Translation regulation, post translational modification, protein folding	0.29
PITG_05294	Pi-LEA_hypothetical protein	Antioxidant, antistress, detoxification	0.70

Table 3.6. continued

PITG_05307	Phosphoenolpyruvate carboxykinase, putative	Carbohydrate transportation and metabolism	0.77
PITG_05318	N-(5'-phosphoribosyl)anthranilate isomerase indole-3-glycerol-phosphate synthase	Amino acid transport and metabolism	0.43
PITG_05356	Maleylacetoacetate isomerase	Amino acid transport and metabolism	0.00
PITG_05360	Conserved hypothetical protein	Unknown	0.45
PITG_05363	Dihydrodipicolinate synthase	Amino acid transport and metabolism	0.35
PITG_05374	Argininosuccinate synthase	Amino acid transport and metabolism	0.37
PITG_05434	Importin subunit beta	Protein transportation and metabolism	0.28
PITG_05462	Aldehyde dehydrogenase family 7 member A1	Carbohydrate transport and metabolism	0.49
PITG_05464	Putative endo-1,3;1,4-beta-glucanase	Carbohydrate transport and metabolism	0.42
PITG_05465	L-gulonolactone oxidase	Carbohydrate transportation and metabolism	0.54
PITG_05498	Heat shock protein 90	Translation regulation, post translational modification, protein folding	0.38
PITG_05501	Non-selective Cation Channel-2 (NSCC2) Family	Ion, cation, sugar, or macromolecule trafficking	0.55
PITG_05512	Conserved hypothetical protein	Unknown	0.44
PITG_05516	Glutathione S-transferase omega-like protein	Antioxidant, antistress, detoxification	0.43
PITG_05519	Phosphatidylinositol 4-phosphate 5-kinase D3 (PIPK-D3/GPCR-PIPK)	Cytoskeleton	0.32
PITG_05534	Nucleolar protein Nop56	Ribosomal process	0.43
PITG_05539	Carbon-nitrogen hydrolase	Amino acid transport and metabolism	0.39
PITG_05540	Conserved hypothetical protein	Unknown	0.37
PITG_05542	3-hydroxyacyl-coA dehydrogenase	Fatty acid transport and metabolism	0.42
PITG_05552	Heat shock protein 75 kDa, mitochondrial precursor	Translation regulation, post translational modification, protein folding	0.49
PITG_05553	D-lactate dehydrogenase	Amino acid transport and metabolism	0.51
PITG_05561	Conserved hypothetical protein	Unknown	0.48

Table 3.6. continued

PITG_05577	Glutathione S-transferase	Antioxidant, antistress, detoxification	0.33
PITG_05578	Catalase-peroxidase	Antioxidant, antistress, detoxification	0.00
PITG_05580	Glutathione S-transferase	Antioxidant, antistress, detoxification	0.31
PITG_05582	Glutathione S-transferase	Antioxidant, antistress, detoxification	0.32
PITG_05615	Pyrophosphate-energized vacuolar membrane proton pump	Ion, cation, sugar, or macromolecule trafficking	0.49
PITG_05636	Transaldolase	Carbohydrate transportation and metabolism	0.36
PITG_05664	Choline/Carnitine O-acyltransferase	Fatty acid transport and metabolism	0.35
PITG_05675	Histone	mRNA processing and transcription regulation	0.35
PITG_05679	Replication protein A 70 kDa DNA-binding subunit	DNA/nucleotide metabolism and repair	0.47
PITG_05684	Conserved hypothetical protein, ribonuclease inhibitor (RI)-like subfamily	mRNA processing and transcription regulation	0.60
PITG_05689	Conserved hypothetical protein with interferon-related domain	Translation regulation, post translational modification, protein folding	0.40
PITG_05690	Ubiquitin activating enzyme, E1 family	Protein transportation and metabolism	0.00
PITG_05778	Conserved hypothetical protein with WD domain, and G-beta repeat	Signal transduction	0.34
PITG_05929	Conserved hypothetical protein involved in transportation cross ER	Ion, cation, sugar, or macromolecule trafficking	0.00
PITG_05938	Conserved hypothetical protein with 3-carboxy-cis,cis-muconate lactonizing domain	Antioxidant, antistress, detoxification	0.49
PITG_05998	Ribonucleoside-diphosphate reductase large subunit	DNA/nucleotide metabolism and repair	0.37
PITG_06004	ATP-binding Cassette (ABC) Superfamily	Ion, cation, sugar, or macromolecule trafficking	0.00
PITG_06016	Glucokinase	Carbohydrate transportation and metabolism	0.45
PITG_06021	Glucokinase	Carbohydrate transportation and metabolism	0.49

Table 3.6. continued

PITG_06025	Conserved hypothetical protein	Unknown	0.22
PITG_06108	Dihydrolipoyllysine-residue acetyltransferase component of pyruvate dehydrogenase complex	Carbohydrate transportation and metabolism	0.36
PITG_06118	V-type proton ATPase subunit B	Ion, cation, sugar, or macromolecule trafficking	0.47
PITG_06131	Conserved hypothetical protein with preprotein translocase subunite Sec66	Protein transportation and metabolism	0.52
PITG_06203	Conserved hypothetical protein, NaCl-inducible	Antioxidant, antistress, detoxification	0.21
PITG_06237	60S ribosomal protein L8	Protein transportation and metabolism	0.33
PITG_06242	Conserved hypothetical protein	Unknown	0.39
PITG_06257	Conserved hypothetical protein, nuclear pore complex protein Nup205	Ion, cation, sugar, or macromolecule trafficking	0.35
PITG_06320	T-complex protein 1 subunit epsilon	Translation regulation, post translational modification, protein folding	0.38
PITG_06410	Conserved hypothetical protein with importin-beta N-terminal domain	Protein transportation and metabolism	0.23
PITG_06415	Heat shock protein 90	Translation regulation, post translational modification, protein folding	0.41
PITG_06430	Long fatty acyl-coA synthetase	Fatty acid transport and metabolism	0.82
PITG_06440	Eukaryotic translation initiation factor 2A	Protein transportation and metabolism	0.33
PITG_06448	Pyruvate carboxylase, mitochondrial precursor	Carbohydrate transportation and metabolism	0.43
PITG_06449	Pyruvate carboxylase	Carbohydrate transportation and metabolism	0.43
PITG_06482	Eukaryotic translation initiation factor 3 subunit	Protein transportation and metabolism	0.00
PITG_06514	Calmodulin	Signal transduction	0.00
PITG_06566	Long-chain-fatty-acid-coa ligase	Fatty acid transport and metabolism	0.46
PITG_06595	ATP synthase subunit beta	Energy production and conversion	0.33

Table 3.6. continued

PITG_06604	Fumarate hydratase, mitochondrial precursor	Carbohydrate transportation and metabolism	0.41
PITG_06615	H^+ - or Na^+ -translocating F-type, V-type and A-type ATPase (F-ATPase) Superfamily	Ion, cation, sugar, or macromolecule trafficking	0.73
PITG_06635	Signal recognition particle	Protein transportation and metabolism	0.47
PITG_06636	Conserved hypothetical protein with ribosomal protein L19 domain	Protein transportation and metabolism	0.58
PITG_06647	Conserved hypothetical protein with effector domain of the CAP family of transcription factors	mRNA processing and transcription regulation	0.47
PITG_06649	Adenylyl cyclase-associated protein	Signal transduction	0.34
PITG_06657	Thioredoxin-like protein	Antioxidant, antistress, detoxification	0.33
PITG_06674	Acetyl-coA acetyltransferase IB	Fatty acid transport and metabolism	0.56
PITG_06693	Trifunctional enzyme subunit alpha	Fatty acid transport and metabolism	0.37
PITG_06695	Conserved hypothetical protein	Unknown	1.00
PITG_06719	Glycerol-3-phosphate dehydrogenase, mitochondrial precursor	Carbohydrate transportation and metabolism	0.36
PITG_06732	Acyl-coA dehydrogenase	Fatty acid transport and metabolism	0.28
PITG_06771	40S ribosomal protein S24	Protein transportation and metabolism	0.36
PITG_06783	Quinolinate synthetase A protein	DNA/nucleotide metabolism and repair	0.44
PITG_06799	Ribosomal protein L27	Protein transportation and metabolism	0.40
PITG_06889	Peptidase	Protein transportation and metabolism	0.53
PITG_06891	S-formylglutathione hydrolase	Antioxidant, antistress, detoxification	0.46
PITG_06969	Oxidoreductase	Antioxidant, antistress, detoxification	0.00
PITG_06995	60S ribosomal protein L4	Protein transportation and metabolism	0.37
PITG_07024	Inosine-5'-monophosphate dehydrogenase 2	Cell cycle, cell growthth and cell proliferation	0.32
PITG_07027	Isocitrate lyase	Carbohydrate transportation and metabolism	0.66

Table 3.6. continued

PITG_07036	Ubiquitin activating enzyme, E1 family	Protein transportation and metabolism	0.58
PITG_07048	Superoxide dismutase, mitochondrial precursor	Antioxidant, antistress, detoxification	0.55
PITG_07056	Isocitrate dehydrogenase, mitochondrial precursor	Carbohydrate transportation and metabolism	0.42
PITG_07080	Conserved hypothetical protein with phosphoribosyl transferase domain	DNA/nucleotide metabolism and repair	0.35
PITG_07149	Serine protease family S10	Protein transportation and metabolism	0.39
PITG_07153	Serine protease family S10	Protein transportation and metabolism	0.43
PITG_07155	Conserved hypothetical protein	Unknown	0.98
PITG_07173	40S ribosomal protein S15	Protein transportation and metabolism	0.39
PITG_07197	3-ketoacyl-coA thiolase, mitochondrial	Fatty acid transport and metabolism	0.46
PITG_07218	Exportin-4	Protein transportation and metabolism	0.00
PITG_07269	60S ribosomal protein L7	Protein transportation and metabolism	0.35
PITG_07300	60S ribosomal protein L35	Protein transportation and metabolism	0.27
PITG_07308	rRNA 2'-O-methyltransferase fibrillarin	Ribosomal process	0.41
PITG_07328	Manganese superoxide dismutase	Antioxidant, antistress, detoxification	0.47
PITG_07340	Conserved hypothetical protein	Unknown	0.44
PITG_07341	Conserved hypothetical protein with ubiquitin-conjugating enzyme domain	Protein transportation and metabolism	0.42
PITG_07349	Gamma-glutamyl hydrolase	Amino acid transport and metabolism	1.13
PITG_07400	2,3-bisphosphoglycerate-dependent phosphoglycerate mutase	Carbohydrate transportation and metabolism	0.42
PITG_07405	Pyruvate kinase	Carbohydrate transportation and metabolism	0.40
PITG_07534	Conserved hypothetical protein	Unknown	0.76
PITG_07546	Replication protein A 32 kDa subunit	DNA/nucleotide metabolism and repair	0.37

Table 3.6. continued

PITG_07567	Brefeldin A-inhibited guanine nucleotide-exchange protein	Ion, cation, sugar, or macromolecule trafficking	0.22
PITG_07671	NADP-specific glutamate dehydrogenase	Antioxidant, antistress, detoxification	0.44
PITG_07778	Conserved hypothetical protein	Unknown	0.40
PITG_07792	ATP synthase subunit delta	Energy production and conversion	0.32
PITG_07795	Myosin-like protein	Ion, cation, sugar, or macromolecule trafficking	0.41
PITG_07797	Methionyl-tRNA synthetase	Protein transportation and metabolism	0.40
PITG_07829	Exosome complex exonuclease RRP43	mRNA processing and transcription regulation	0.00
PITG_07843	Protein disulfide-isomerase	Translation regulation, post translational modification, protein folding	0.50
PITG_07860	NADH ubiquinone oxidoreductase subunit	Antioxidant, antistress, detoxification	0.33
PITG_07885	Eukaryotic translation initiation factor 2 subunit alpha	Protein transportation and metabolism	0.41
PITG_07887	26S proteasome non-ATPase regulatory subunit 6	Protein transportation and metabolism	0.39
PITG_07903	26S proteasome non-ATPase regulatory subunit	Protein transportation and metabolism	0.42
PITG_07953	3-ketoacyl-coA thiolase A	Fatty acid transport and metabolism	0.37
PITG_07960	Alpha-tubulin	Cytoskeleton	0.43
PITG_07961	Cleavage induced tubulin alpha chain	Cytoskeleton	0.42
PITG_07972	Conserved hypothetical protein, flagellar associated protein	Cytoskeleton	0.50
PITG_07974	Conserved hypothetical protein	Unknown	0.49
PITG_07975	Methylcrotonoyl-coA carboxylase beta chain, mitochondrial precursor	Amino acid transport and metabolism	0.61
PITG_07999	Alpha-tubulin	Cytoskeleton	0.43
PITG_08002	Glucosylceramidase	Carbohydrate transport and metabolism	0.37
PITG_08025	HECT E3 ubiquitin ligase	Translation regulation, post translational modification, protein folding	0.00

Table 3.6. continued

PITG_08044	Conserved hypothetical protein with Ca^{2+}-dependent membrane-targeting module	Signal transduction	2.49
PITG_08061	Hydroxyacyl-coenzyme A dehydrogenase, mitochondrial precursor	Fatty acid transport and metabolism	0.39
PITG_08138	Conserved hypothetical protein	Unknown	0.46
PITG_08234	DnaJ subfamily C member 2 protein	Translation regulation, post translational modification, protein folding	0.62
PITG_08306	Myosin-like protein	Ion, cation, sugar, or macromolecule trafficking	0.74
PITG_08416	Conserved hypothetical protein	Unknown	0.00
PITG_08425	Endothelin-converting enzyme 1, metalloprotease family M13	Protein transportation and metabolism	0.42
PITG_08445	Cystathionine gamma-lyase	Amino acid transport and metabolism	0.40
PITG_08454	Conserved hypothetical protein, large tegument protein UL36	Protein transportation and metabolism	0.67
PITG_08491	NADH:Flavin oxidoreductase	Antioxidant, antistress, detoxification	0.57
PITG_08565	Conserved hypothetical protein with ribosomal protein 60S subunit	Protein transportation and metabolism	0.23
PITG_08579	Isoleucyl-tRNA synthetase	Protein transportation and metabolism	0.58
PITG_08591	Actin-depolymerizing factor	Cytoskeleton	0.34
PITG_08599	Thimet oligopeptidase	Protein transportation and metabolism	0.48
PITG_08657	Conserved hypothetical protein, pleiotropic drug resistance family protein	Ion, cation, sugar, or macromolecule trafficking	0.44
PITG_08659	Conserved hypothetical protein with annexin domain	Lipid transport and metabolism	0.38
PITG_08676	26S proteasome non-ATPase regulatory subunit 14	Protein transportation and metabolism	0.55
PITG_08681	Elongation factor G	Protein transportation and metabolism	0.45
PITG_08696	Iron-sulfur cluster scaffold protein Nfu-like protein	Protein transportation and metabolism	0.24

Table 3.6. continued

PITG_08702	Conserved hypothetical protein with 3'5'-cyclic nucleotide phosphodiesterase domain	Signal transduction	0.63
PITG_08703	Conserved hypothetical protein with ribosomal protein L36e subunit	Protein transportation and metabolism	0.28
PITG_08711	Hsp90-like protein	Translation regulation, post translational modification, protein folding	0.54
PITG_08714	Lysyl-tRNA synthetase	Protein transportation and metabolism	0.50
PITG_08744	Long-chain-fatty-acid-coA ligase	Fatty acid transport and metabolism	0.49
PITG_08761	Nucleoside diphosphate kinase B	mRNA processing and transcription regulation	0.49
PITG_08795	Conserved hypothetical protein with collagen triple helix repeat	Cytoskeleton	0.60
PITG_08802	NAD-specific glutamate dehydrogenase	Antioxidant, antistress, detoxification	0.43
PITG_08808	Calcyphosin-like protein	Signal transduction	0.24
PITG_08809	60S ribosomal protein L12	Protein transportation and metabolism	0.34
PITG_08810	Conserved hypothetical protein, calcyphosin-like protein	Ion, cation, sugar, or macromolecule trafficking	0.13
PITG_08843	Mannitol dehydrogenase	Carbohydrate transport and metabolism	0.45
PITG_08843	Mannitol dehydrogenase	Carbohydrate transport and metabolism	0.58
PITG_08845	Mannitol dehydrogenase	Carbohydrate transportation and metabolism	0.00
PITG_08846	Mannitol dehydrogenase	Carbohydrate transportation and metabolism	0.41
PITG_08881	Succinyl-coA ligase beta-chain, mitochondrial precursor	Carbohydrate transportation and metabolism	0.39
PITG_08959	40S ribosomal protein S3-3	Antioxidant, antistress, detoxification	0.37
PITG_08997	ATP-dependent RNA helicase DBP5	mRNA processing and transcription regulation	0.55
PITG_09006	Conserved hypothetical protein with Mannitol-1-phosphate/altronate dehydrogenases domain	Carbohydrate transportation and metabolism	0.00
PITG_09015	NADH ubiquinone oxidoreductase	Antioxidant, antistress, detoxification	0.30

Table 3.6. continued

PITG_09089	Exportin-6-like protein	Protein transportation and metabolism	0.00
PITG_09235	Crinkler	Secreted or infection related protein	0.00
PITG_09271	Ornithine aminotransferase, mitochondrial precursor	Amino acid transport and metabolism	0.39
PITG_09282	Calcium-transporting ATPase 1, endoplasmic reticulum-type	Ion, cation, sugar, or macromolecule trafficking	0.52
PITG_09289	Eukaryotic translation initiation factor 3 subunit F	Protein transportation and metabolism	0.57
PITG_09304	Conserved hypothetical protein with PEPCK domain	Carbohydrate transportation and metabolism	0.36
PITG_09345	40S ribosomal protein S5-2	Protein transportation and metabolism	0.34
PITG_09348	Glutaredoxin	Antioxidant, antistress, detoxification	0.35
PITG_09393	Pyruvate kinase	Carbohydrate transportation and metabolism	0.57
PITG_09400	Pyruvate kinase	Carbohydrate transportation and metabolism	0.35
PITG_09402	Phosphoglycerate kinase	Carbohydrate transportation and metabolism	0.49
PITG_09404	Myosin-like protein	Ion, cation, sugar, or macromolecule trafficking	0.48
PITG_09431	40S ribosomal protein S19-3	Protein transportation and metabolism	0.37
PITG_09432	Nucleolar protein NOP5	Ribosomal process	0.41
PITG_09440	Conserved hypothetical protein with WWP or rsp5 domain	Signal transduction	0.55
PITG_09472	Conserved hypothetical protein with LYR domain	Protein transportation and metabolism	0.49
PITG_09506	30S ribosomal protein S5	Protein transportation and metabolism	0.00
PITG_09512	Prohibitin-2	mRNA processing and transcription regulation	0.78
PITG_09526	Transcription factor BTF3-like protein	mRNA processing and transcription regulation	0.34
PITG_09540	60S ribosomal protein L19-1	Protein transportation and metabolism	0.33
PITG_09547	Conserved hypothetical protein with ATP synthase D chain domain	Energy production and conversion	0.55

Table 3.6. continued

PITG_09553	Conserved hypothetical protein with ATP synthase D chain domain	Energy production and conversion	0.59
PITG_09555	Ubiquitin-ribosomal fusion protein	Ribosomal process	0.58
PITG_09556	Guanine nucleotide-binding protein subunit beta-2-like protein	Signal transduction	0.30
PITG_09563	40S ribosomal protein S9-1	Ribosomal process	0.19
PITG_09596	Nucleoside diphosphate kinase B	mRNA processing and transcription regulation	0.34
PITG_09600	Conserved hypothetical protein	Unknown	0.38
PITG_09753	Conserved hypothetical protein	Unknown	0.00
PITG_09789	Conserved hypothetical protein with FKBP-type peptidylprolyl cis-trans isomerase	Translation regulation, post translational modification, protein folding	0.50
PITG_09798	Glucan 1,3-beta-glucosidase	Carbohydrate transport and metabolism	0.41
PITG_09817	Ribose-phosphate pyrophosphokinase	DNA/nucleotide metabolism and repair	0.37
PITG_09846	Prolyl-tRNA synthetase	Protein transportation and metabolism	0.47
PITG_09848	Medium-chain specific acyl-coA dehydrogenase, mitochondrial precursor	Fatty acid transport and metabolism	0.48
PITG_09939	Conserved hypothetical protein	Unknown	0.30
PITG_09941	Myosin-like protein	Ion, cation, sugar, or macromolecule trafficking	0.48
PITG_09955	Acyl-coA dehydrogenase family member 9, mitochondrial precursor	Fatty acid transport and metabolism	0.40
PITG_09965	Protein transport Sec23/Sec24-like protein	Protein transportation and metabolism	0.39
PITG_10011	Polyketide hydroxylase	Antioxidant, antistress, detoxification	0.43
PITG_10028	Serine palmitoyltransferase	Lipid transport and metabolism	0.49
PITG_10031	Lysosomal alpha-mannosidase	Carbohydrate transport and metabolism	0.27
PITG_10032	6-phosphogluconate dehydrogenase	Carbohydrate transportation and metabolism	0.41
PITG_10142	Conserved hypothetical protein	Unknown	0.58
PITG_10146	40S ribosomal protein S2	Ribosomal process	0.39
PITG_10147	Cell division protease FTSH	Cell cycle, cell growthth and cell proliferation	0.41

Table 3.6. continued

PITG_10169	26S protease regulatory subunit 7	Protein transportation and metabolism	0.43
PITG_10185	Conserved hypothetical protein with CDP-alcohol phosphatidyltransferase domain	Lipid transport and metabolism	0.47
PITG_10193	Ubiquitin	Protein transportation and metabolism	0.54
PITG_10198	Adenosylhomocysteinase	Amino acid transport and metabolism	0.36
PITG_10203	Conserved hypothetical protein	Unknown	0.38
PITG_10210	Phosphoenolpyruvate carboxykinase	Carbohydrate transportation and metabolism	0.43
PITG_10218	Glucan 1,3-beta-glucosidase	Carbohydrate transport and metabolism	0.40
PITG_10240	Pirin	Ion, cation, sugar, or macromolecule trafficking	0.29
PITG_10290	Alcohol dehydrogenase	Carbohydrate transportation and metabolism	0.49
PITG_10292	Alcohol dehydrogenase	Carbohydrate transportation and metabolism	0.48
PITG_10293	Alcohol dehydrogenase	Carbohydrate transportation and metabolism	0.49
PITG_10300	Electron transfer flavoprotein subunit beta	Energy production and conversion	0.34
PITG_10325	Conserved hypothetical protein	Secreted or infection related protein	0.00
PITG_10347	Secreted RXLR effector peptide	Secreted or infection related protein	2.45
PITG_10416	Nuclear pore glycoprotein	Ion, cation, sugar, or macromolecule trafficking	0.38
PITG_10452	CAD protein	DNA/nucleotide metabolism and repair	0.31
PITG_10454	Carbamoyl-phosphate synthase	Amino acid transport and metabolism	0.32
PITG_10455	Conserved hypothetical protein with mitofilin domain	Cytoskeleton	0.42
PITG_10513	Proteasome subunit alpha type-6	Protein transportation and metabolism	0.44
PITG_10543	Conserved hypothetical protein	Unknown	0.45
PITG_10590	Kynurenine-oxoglutarate transaminase	Amino acid transport and metabolism	0.52
PITG_10600	Conserved hypothetical protein with PEPCK domain	Carbohydrate transportation and metabolism	0.64

Table 3.6. continued

PITG_10707	Ppic-type peptidyl-prolyl cis-trans isomerase	Translation regulation, post translational modification, protein folding	0.68
PITG_10827	Nuclease	DNA/nucleotide metabolism and repair	0.38
PITG_10846	Lysosomal alpha-glucosidase	Carbohydrate transport and metabolism	0.37
PITG_10857	Ubiquitin fusion degradation protein	Protein transportation and metabolism	0.00
PITG_10863	60S ribosomal protein L32-1	Protein transportation and metabolism	0.36
PITG_10881	Kinesin-like protein	Cytoskeleton	1.43
PITG_10883	26S proteasome non-ATPase regulatory subunit	Protein transportation and metabolism	0.65
PITG_10887	40S ribosomal protein S11	Protein transportation and metabolism	0.36
PITG_10922	Fatty acid synthase subunit alpha	Fatty acid transport and metabolism	0.50
PITG_10926	Fatty acid synthase subunit alpha	Fatty acid transport and metabolism	0.32
PITG_10932	Dipeptidyl peptidase	Protein transportation and metabolism	0.39
PITG_10938	Protein phosphatase 2C	Antioxidant, antistress, detoxification	0.00
PITG_10941	Elongation factor 2	Protein transportation and metabolism	0.32
PITG_10951	Succinate dehydrogenase iron-sulfur protein, mitochondrial precursor	Carbohydrate transport and metabolism	0.41
PITG_10967	Ras GTPase-activating protein-binding protein	Signal transduction	0.47
PITG_10972	Thioredoxin-like protein	Antioxidant, antistress, detoxification	0.42
PITG_10974	Elongation factor 1-gamma	Protein transportation and metabolism	0.41
PITG_10979	Elongation factor 1-gamma	Protein transportation and metabolism	0.50
PITG_11009	Conserved hypothetical protein with PWWP domain	Protein transportation and metabolism	0.46
PITG_11017	Conserved hypothetical protein, S-adenosylmethionine-dependent methyltransferases	Protein transportation and metabolism	0.48

Table 3.6. continued

PITG_11036	NADH dehydrogenase [ubiquinone] 1 alpha subcomplex subunit	Antioxidant, antistress, detoxification	0.44
PITG_11046	Creatine kinase B-type	Energy production and conversion	0.38
PITG_11047	T-complex protein 1 subunit eta	Translation regulation, post translational modification, protein folding	0.57
PITG_11060	Conserved hypothetical protein, cysteine-rich secretory protein family, pathogenesis-related 1 proteins	Signal transduction	0.32
PITG_11063	26S proteasome non-ATPase regulatory subunit 7	Protein transportation and metabolism	0.66
PITG_11065	NAD-dependent malic enzyme	Antioxidant, antistress, detoxification	0.37
PITG_11069	Villin-like protein	Cytoskeleton	0.38
PITG_11071	Conserved hypothetical protein	Unknown	0.24
PITG_11093	Phosphoenolpyruvate carboxykinase, putative	Carbohydrate transportation and metabolism	0.34
PITG_11099	60S ribosomal protein L18-2	Protein transportation and metabolism	0.34
PITG_11111	Leucyl-tRNA synthetase	Protein transportation and metabolism	0.40
PITG_11116	NAD-specific glutamate dehydrogenase	Antioxidant, antistress, detoxification	0.34
PITG_11138	Fumarate reductase flavoprotein subunit	Carbohydrate transport and metabolism	0.93
PITG_11143	AP-1 complex subunit gamma-1	Protein transportation and metabolism	0.43
PITG_11207	Conserved hypothetical protein	Unknown	0.00
PITG_11215	DnaJ subfamily C protein	Translation regulation, post translational modification, protein folding	0.48
PITG_11244	Heat shock 70 kDa protein	Translation regulation, post translational modification, protein folding	0.37
PITG_11247	Heat shock 70 kDa protein	Translation regulation, post translational modification, protein folding	0.41
PITG_11252	Heat shock 70 kDa protein	Translation regulation, post translational modification, protein folding	0.38

Table 3.6. continued

PITG_11291	Conserved hypothetical protein with multicopper oxidase domain	Ion, cation, sugar, or macromolecule trafficking	0.47
PITG_11329	Annexin	Lipid transport and metabolism	0.54
PITG_11425	Transcriptional repressor TUP1-like protein	mRNA processing and transcription regulation	0.31
PITG_11569	Metalloprotease family M17	Protein transportation and metabolism	0.40
PITG_11588	Hypothetical cleavage-induced protein	Unknown	0.43
PITG_11592	Serine protease family S15	Protein transportation and metabolism	0.45
PITG_11605	Aldehyde dehydrogenase	Carbohydrate transport and metabolism	0.62
PITG_11615	Homoserine dehydrogenase	Amino acid transport and metabolism	0.51
PITG_11619	FKBP-type peptidyl-prolyl cis-trans isomerase	Translation regulation, post translational modification, protein folding	0.39
PITG_11638	Voltage-gated potassium channel subunit beta	Ion, cation, sugar, or macromolecule trafficking	0.00
PITG_11653	Conserved hypothetical protein with K homology RNA-binding domain	mRNA processing and transcription regulation	0.73
PITG_11689	Putative GPI-anchored serine-rich hypothetical protein	Protein transportation and metabolism	0.64
PITG_11690	Putative GPI-anchored serine-rich hypothetical protein	Protein transportation and metabolism	0.48
PITG_11704	Lectin	Carbohydrate transport and metabolism	0.00
PITG_11712	Neutral alpha-glucosidase	Carbohydrate transport and metabolism	0.48
PITG_11719	4-hydroxyphenylpyruvate dioxygenase	Amino acid transport and metabolism	0.32
PITG_11727	Conserved hypothetical protein	Unknown	0.00
PITG_11729	Phosphate transporter (Pho88) and ankyrin repeat, protein protein interaction motif	Cell cycle, cell growthth and cell proliferation	0.27
PITG_11755	GPI-anchored serine-threonine rich hypothetical protein	Protein transportation and metabolism	0.00
PITG_11766	40S ribosomal protein S3a	Ribosomal process	0.35
PITG_11767	Phosphoacetylglucosamine mutase	Amino acid transport and metabolism	0.47

Table 3.6. continued

PITG_11852	C2 domain-containing protein	Lipid transport and metabolism	0.43
PITG_11853	C2 domain-containing protein	Lipid transport and metabolism	0.30
PITG_11855	C2 domain-containing protein	Lipid transport and metabolism	0.41
PITG_11901	Phosphoenolpyruvate carboxykinase, pseudogene	Carbohydrate transportation and metabolism	0.34
PITG_11913	Heat shock cognate 70 kDa protein	Translation regulation, post translational modification, protein folding	0.35
PITG_11929	Dihydrolipoyllysine-residue acetyltransferase component of pyruvate dehydrogenase complex	Carbohydrate transportation and metabolism	0.62
PITG_11943	Thioredoxin reductase 1	Antioxidant, antistress, detoxification	1.29
PITG_11965	Conserved hypothetical protein with phosphatidylcholine-sterol O-acyltransferase	Lipid transport and metabolism	0.49
PITG_11966	Chaperonin CPN60-1, mitochondrial precursor	Translation regulation, post translational modification, protein folding	0.38
PITG_12041	Cysteine protease family C01A	Protein transportation and metabolism	0.00
PITG_12053	Acetylornithine aminotransferase, mitochondrial precursor	Amino acid transport and metabolism	0.40
PITG_12072	CRN domain-containing protein	Secreted or infection related protein	0.34
PITG_12119	ATPase family AAA domain-containing protein 3A	Energy production and conversion	0.41
PITG_12122	Proteasome subunit alpha type-5	Protein transportation and metabolism	0.49
PITG_12141	H - or Na -translocating F-type, V-type and A-type ATPase (F-ATPase) Superfamily	Ion, cation, sugar, or macromolecule trafficking	0.45
PITG_12151	Aspartyl-tRNA synthetase	Protein transportation and metabolism	0.42
PITG_12154	Conserved hypothetical protein	Unknown	0.57
PITG_12158	Annexin	Lipid transport and metabolism	0.49
PITG_12161	Delta-1-pyrroline-5-carboxylate synthetase	Amino acid transport and metabolism	0.45
PITG_12185	26S protease regulatory subunit 4	Protein transportation and metabolism	0.46
PITG_12191	Conserved hypothetical protein	Unknown	0.41
PITG_12193	50S ribosomal protein L1	Protein transportation and metabolism	0.39

Table 3.6. continued

PITG_12220	Methionine aminopeptidase	Amino acid transport and metabolism	0.42
PITG_12293	cAMP-dependent protein kinase catalytic subunit, putative	Signal transduction	0.35
PITG_12300	Phosphoribosylglycinamide synthetase	DNA/nucleotide metabolism and repair	0.38
PITG_12327	Conserved hypothetical protein with FYVE domain	Protein transportation and metabolism	0.25
PITG_12427	Conserved hypothetical protein with cytochrome c oxidase subunit Vb	Ion, cation, sugar, or macromolecule trafficking	0.34
PITG_12483	Eukaryotic translation initiation factor 3	Protein transportation and metabolism	0.47
PITG_12504	Mitochondrial carrier (MC) family	Energy production and conversion	0.43
PITG_12524	Elongation factor 3	Protein transportation and metabolism	0.00
PITG_12526	Conserved hypothetical protein with Pleckstrin homology domain	Signal transduction	0.54
PITG_12562	Elicitin-like protein	Secreted or infection related protein	0.62
PITG_12575	Autophagocytosis associated protein	Antioxidant, antistress, detoxification	0.00
PITG_12613	Crinkler (CRN) family protein	Secreted or infection related protein	0.32
PITG_12642	Crinkler (CRN) family protein	Secreted or infection related protein	0.44
PITG_12694	Protein transport protein SEC13	Protein transportation and metabolism	0.74
PITG_12697	30S ribosomal protein S9	Protein transportation and metabolism	0.00
PITG_12727	Cysteine synthase	Amino acid transport and metabolism	0.44
PITG_12745	40S ribosomal protein S17	Protein transportation and metabolism	0.41
PITG_12788	NADH:Flavin oxidoreductase	Antioxidant, antistress, detoxification	0.35
PITG_12864	Asparaginyl-tRNA synthetase	Protein transportation and metabolism	0.43
PITG_12882	Electron transfer flavoprotein subunit alpha, mitochondrial precursor	Energy production and conversion	0.55
PITG_12915	Sorting nexin	Protein transportation and metabolism	0.24

Table 3.6. continued

PITG_12948	Conserved hypothetical protein with redox TRV like domain	Antioxidant, antistress, detoxification	0.00
PITG_12961	Alanyl-tRNA synthetase	Protein transportation and metabolism	0.43
PITG_12990	Glutathione transferase, theta class	Antioxidant, antistress, detoxification	0.70
PITG_13007	Conserved hypothetical protein with DnaJ-class molecular chaperone domain	Translation regulation, post translational modification, protein folding	0.37
PITG_13014	Proliferation-associated protein, metalloprotease family M24X	Protein transportation and metabolism	0.37
PITG_13024	Alpha-1,3-mannosyltransferase	Translation regulation, post translational modification, protein folding	0.00
PITG_13112	Conserved hypothetical protein with metallophosphatase domain	Protein transportation and metabolism	0.92
PITG_13116	Triosephosphate isomerase	Carbohydrate transportation and metabolism	0.40
PITG_13139	Threonine synthase	Amino acid transport and metabolism	0.51
PITG_13159	Conserved hypothetical protein, transcription termination factor Rho	mRNA processing and transcription regulation	0.40
PITG_13237	Alpha-actinin-1	Cytoskeleton	0.37
PITG_13242	Conserved hypothetical protein with DnaJ/Hsp40	Translation regulation, post translational modification, protein folding	0.37
PITG_13250	Mitochondrial protein translocase (MPT) family	Protein transportation and metabolism	0.77
PITG_13262	Cystathionine beta-synthase	Amino acid transport and metabolism	0.47
PITG_13265	Adenosine kinase	DNA/nucleotide metabolism and repair	0.47
PITG_13296	Aldose 1-epimerase	Carbohydrate transportation and metabolism	0.61
PITG_13301	H^+ - or Na^+ -translocating F-type, V-type and A-type ATPase (F-ATPase) Superfamily	Ion, cation, sugar, or macromolecule trafficking	0.40
PITG_13307	Conserved hypothetical protein	Unknown	0.55
PITG_13312	40S ribosomal protein S25	Protein transportation and metabolism	0.33

Table 3.6. continued

PITG_13341	2,4-dienoyl-coa reductase, mitochondrial precursor	Fatty acid transport and metabolism	0.54
PITG_13370	Conserved hypothetical protein with DnaJ-class molecular chaperone domain	Translation regulation, post translational modification, protein folding	0.52
PITG_13371	60S ribosomal protein L31	Protein transportation and metabolism	0.43
PITG_13387	Conserved hypothetical protein, nuclear transport factor 2 (NTF2-like) family	Ion, cation, sugar, or macromolecule trafficking	0.98
PITG_13399	Asparagine synthetase	Amino acid transport and metabolism	0.61
PITG_13405	Conserved hypothetical protein with Calponin homology	Signal transduction	0.39
PITG_13407	Serine protease family S33	Protein transportation and metabolism	0.33
PITG_13448	Formate dehydrogenase	Antioxidant, antistress, detoxification	0.41
PITG_13500	40S ribosomal protein S4	Protein transportation and metabolism	0.32
PITG_13614	Malate dehydrogenase, mitochondrial precursor	Carbohydrate transportation and metabolism	0.34
PITG_13686	Sulfate Permease (SulP)	Ion, cation, sugar, or macromolecule trafficking	0.27
PITG_13737	Protoplast secreted protein 2 precursor	mRNA processing and transcription regulation	0.33
PITG_13749	2,3-bisphosphoglycerate-dependent phosphoglycerate mutase	Carbohydrate transportation and metabolism	0.42
PITG_13761	Protoplast secreted protein 2 precursor	mRNA processing and transcription regulation	0.39
PITG_13762	Flavodoxin-like protein	Antioxidant, antistress, detoxification	0.34
PITG_13763	Flavodoxin-like protein	Antioxidant, antistress, detoxification	0.39
PITG_13769	Conserved hypothetical protein	Unknown	0.45
PITG_13809	Rab18 family GTPase	Protein transportation and metabolism	0.00
PITG_13831	Tryptophanyl-tRNA synthetase	Protein transportation and metabolism	0.36
PITG_13832	Delta-aminolevulinic acid dehydratase	Protein transportation and metabolism	0.40

Table 3.6. continued

PITG_14008	Conserved hypothetical protein with streptococcal surface antigen repeat	Lipid transport and metabolism	0.41
PITG_14057	Alcohol dehydrogenase	Carbohydrate transportation and metabolism	0.79
PITG_14083	Glutathione reductase	Antioxidant, antistress, detoxification	0.44
PITG_14108	Conserved hypothetical protein with WW domain, a Calmodulin binding domain; and GCK domain	Signal transduction	0.46
PITG_14110	Endoplasmic reticulum-Golgi intermediate compartment protein	Protein transportation and metabolism	0.46
PITG_14133	Programmed cell death protein	Cell cycle, cell growthth and cell proliferation	0.36
PITG_14173	Endo-1,3(4)-beta-glucanase	Carbohydrate transport and metabolism	0.48
PITG_14180	Glutamine synthetase	Amino acid transport and metabolism	0.62
PITG_14195	Enolase	Carbohydrate transportation and metabolism	0.29
PITG_14278	Eukaryotic translation initiation factor 4 gamma	Protein transportation and metabolism	0.33
PITG_14309	Crinkler (CRN) family protein	Secreted or infection related protein	0.64
PITG_14343	Crinkler (CRN) family protein	Secreted or infection related protein	0.70
PITG_14380	Lon protease	Antioxidant, antistress, detoxification	0.00
PITG_14397	Proliferating cell nuclear antigen	DNA/nucleotide metabolism and repair	0.43
PITG_14441	Cytoskeleton-associated protein	Cytoskeleton	0.00
PITG_14456	Glutamyl-tRNA synthetase	Protein transportation and metabolism	0.42
PITG_14492	Nmra-like family protein	Signal transduction	0.31
PITG_14563	Ubiquinone biosynthesis monooxygenase	Protein transportation and metabolism	0.54
PITG_14598	Prolyl endopeptidase	Protein transportation and metabolism	0.41
PITG_14602	Conserved hypothetical protein	Unknown	0.00
PITG_14609	Eukaryotic translation initiation factor 2 subunit beta	Protein transportation and metabolism	0.61
PITG_14624	Conserved hypothetical protein	Unknown	0.78

Table 3.6. continued

PITG_14639	Aminotransferase	Amino acid transport and metabolism	0.38
PITG_14641	Glutathione peroxidase	Antioxidant, antistress, detoxification	0.78
PITG_14696	Serine hydroxymethyltransferase 1, mitochondrial precursor	Amino acid transport and metabolism	0.40
PITG_14697	Cystathionine beta-synthase	Amino acid transport and metabolism	0.40
PITG_14721	NADH:Flavin oxidoreductase	Antioxidant, antistress, detoxification	0.35
PITG_14722	NADH:Flavin oxidoreductase	Antioxidant, antistress, detoxification	0.57
PITG_14730	Nucleolar protein	Ribosomal process	0.00
PITG_14775	Crinkler (CRN) family protein	Secreted or infection related protein	0.61
PITG_14850	40S ribosomal protein S7	Protein transportation and metabolism	0.29
PITG_14854	Signal recognition particle	Protein transportation and metabolism	0.53
PITG_14888	Conserved hypothetical protein, Mov34/MPN/PAD-1 family	mRNA processing and transcription regulation	0.31
PITG_14936	ATP synthase subunit gamma	Energy production and conversion	0.41
PITG_14941	Conserved hypothetical protein with tetratricopeptide repeat	Protein transportation and metabolism	0.40
PITG_15045	Trans-2-enoyl-coA reductase	Fatty acid transport and metabolism	0.41
PITG_15078	Actin-like protein	Cytoskeleton	0.45
PITG_15111	Heat shock 70 kDa protein II	Translation regulation, post translational modification, protein folding	0.54
PITG_15117	Actin-like protein	Cytoskeleton	0.42
PITG_15242	Phosphate acetyltransferase	Energy production and conversion	0.66
PITG_15243	Phosphate acetyltransferase	Energy production and conversion	0.65
PITG_15250	Conserved hypothetical protein	Unknown	0.41
PITG_15292	Catalase	Antioxidant, antistress, detoxification	1.93
PITG_15294	Histidinol dehydrogenase	Amino acid transport and metabolism	0.00
PITG_15321	Aminomethyltransferase	Amino acid transport and metabolism	0.86

Table 3.6. continued

PITG_15358	Calreticulin precursor	Translation regulation, post translational modification, protein folding	0.51
PITG_15359	Dihydrolipoyl dehydrogenase 1, mitochondrial precursor	Carbohydrate transportation and metabolism	0.44
PITG_15370	Hsp70-like protein	Translation regulation, post translational modification, protein folding	0.52
PITG_15392	Leukotriene A-4 hydrolase-like protein	Amino acid transport and metabolism	0.00
PITG_15393	Eukaryotic translation initiation factor	Protein transportation and metabolism	0.55
PITG_15398	Conserved hypothetical protein with FYVE domain	Protein transportation and metabolism	0.25
PITG_15449	Branched-chain-amino-acid aminotransferase	Amino acid transport and metabolism	0.44
PITG_15476	Malate dehydrogenase	Carbohydrate transportation and metabolism	0.34
PITG_15492	Peroxiredoxin-2	Antioxidant, antistress, detoxification	0.44
PITG_15504	Thioredoxin peroxidase	Antioxidant, antistress, detoxification	0.75
PITG_15526	ATP synthase subunit O	Energy production and conversion	0.42
PITG_15531	Glutathione S-transferase	Antioxidant, antistress, detoxification	1.15
PITG_15553	Inorganic pyrophosphatase	Lipid transport and metabolism	0.32
PITG_15615	Short/branched chain specific acyl-coA dehydrogenase	Fatty acid transport and metabolism	0.40
PITG_15626	Superoxide dismutase 2	Antioxidant, antistress, detoxification	0.00
PITG_15654	Conserved hypothetical protein, multiprotein bridging factor 1	mRNA processing and transcription regulation	0.29
PITG_15697	60S ribosomal protein L11	Protein transportation and metabolism	0.53
PITG_15705	Dihydrolipoamide succinyltransferase	Amino acid transport and metabolism	0.30
PITG_15723	60S ribosomal protein L14	Protein transportation and metabolism	0.37
PITG_15735	Protein kinase	Signal transduction	0.54
PITG_15755	AP-3 complex subunit beta	Protein transportation and metabolism	0.67

Table 3.6. continued

PITG_15771	Heat shock70-like protein	Translation regulation, post translational modification, protein folding	0.45
PITG_15786	Heat shock 70 protein, mitochondrial precursor	Translation regulation, post translational modification, protein folding	0.40
PITG_15791	Glycoside hydrolase	Carbohydrate transport and metabolism	0.40
PITG_15848	Conserved hypothetical protein with ENTH domain	Ion, cation, sugar, or macromolecule trafficking	0.45
PITG_15850	Glycine dehydrogenase, mitochondrial precursor	Amino acid transport and metabolism	0.47
PITG_15866	Conserved hypothetical protein	Unknown	0.69
PITG_16005	Methylmalonate-semialdehyde dehydrogenase, mitochondrial precursor	Amino acid transport and metabolism	0.48
PITG_16008	40S ribosomal protein S27-like protein	Protein transportation and metabolism	0.45
PITG_16016	Cytochrome oxidase assembly protein	Ion, cation, sugar, or macromolecule trafficking	0.47
PITG_16048	Triosephosphate isomerase	Carbohydrate transportation and metabolism	0.57
PITG_16069	Heat shock protein 101	Antioxidant, antistress, detoxification	0.55
PITG_16074	Heat shock protein 101	Antioxidant, antistress, detoxification	0.53
PITG_16117	Conserved hypothetical protein HMG (high mobility group) box-bind single-stranded DNA preferentially and unwind double-stranded DNA	mRNA processing and transcription regulation	0.55
PITG_16144	Crinkler (CRN) family protein	Secreted or infection related protein	0.71
PITG_16144	Crinkler (CRN) family protein	Secreted or infection related protein	0.70
PITG_16183	Adhesin-like protein	Protein transportation and metabolism	0.00
PITG_16198	60S ribosomal protein L18a	Protein transportation and metabolism	0.29
PITG_16328	Tyrosyl-tRNA synthetase	Protein transportation and metabolism	0.54
PITG_16333	ATP-dependent hsl protease ATP-binding subunit hslu	Protein transportation and metabolism	0.64

Table 3.6. continued

PITG_16477	Short-chain specific acyl-coA dehydrogenase, mitochondrial precursor	Fatty acid transport and metabolism	0.53
PITG_16575	Crinkler (CRN) family protein	Secreted or infection related protein	0.38
PITG_16584	Crinkler (CRN) family protein	Secreted or infection related protein	0.42
PITG_16593	Crinkler (CRN) family protein	Secreted or infection related protein	0.41
PITG_16597	Crinkler (CRN) family protein	Secreted or infection related protein	0.42
PITG_16598	Crinkler (CRN) family protein	Secreted or infection related protein	0.40
PITG_16600	Crinkler (CRN) family protein	Secreted or infection related protein	0.45
PITG_16603	Crinkler (CRN) family protein	Secreted or infection related protein	0.46
PITG_16614	Crinkler (CRN) family protein	Secreted or infection related protein	0.45
PITG_16616	Crinkler (CRN) family protein	Secreted or infection related protein	0.47
PITG_16622	Crinkler (CRN) family protein	Secreted or infection related protein	0.41
PITG_16624	Crinkler (CRN) family protein	Secreted or infection related protein	0.38
PITG_16627	Crinkler (CRN) family protein	Secreted or infection related protein	0.42
PITG_16635	Crinkler (CRN) family protein	Secreted or infection related protein	0.40
PITG_16661	Phosphate carrier protein	Protein transportation and metabolism	0.52
PITG_16671	26S proteasome non-ATPase regulatory subunit 3	Protein transportation and metabolism	0.38
PITG_16757	40S ribosomal protein S15a	Protein transportation and metabolism	0.30
PITG_16915	Elongation factor Tu	Protein transportation and metabolism	0.42
PITG_16953	Transglutaminase elicitor	Protein transportation and metabolism	0.86
PITG_16966	2-oxoglutarate dehydrogenase E1 component	Carbohydrate transportation and metabolism	0.40
PITG_17013	Conserved hypothetical protein with tetratricopeptide repeat	Translation regulation, post translational modification, protein folding	0.46
PITG_17033	Annexin	Lipid transport and metabolism	0.45

Table 3.6. continued

PITG_17034	Annexin	Lipid transport and metabolism	0.44
PITG_17045	Mannitol dehydrogenase	Carbohydrate transportation and metabolism	0.37
PITG_17093	60S ribosomal protein L24	Protein transportation and metabolism	0.45
PITG_17123	T-complex protein 1 subunit gamma	Translation regulation, post translational modification, protein folding	0.38
PITG_17139	Conserved hypothetical protein	Unknown	0.00
PITG_17176	Crinkler (CRN) family protein	Secreted or infection related protein	0.70
PITG_17257	Carbohydrate esterase	Carbohydrate metabolism	1.19
PITG_17261	60S acidic ribosomal protein P0	Protein transportation and metabolism	0.37
PITG_17263	Regulator of microtubule dynamics protein	Cell cycle, cell growthth and cell proliferation	0.85
PITG_17273	Conserved hypothetical protein with nucleosome remodeling factor 140 kDa subunit	mRNA processing and transcription regulation	0.33
PITG_17287	AP-1 complex subunit beta	Protein transportation and metabolism	0.38
PITG_17305	Conserved hypothetical protein with rossmann-fold NAD(P)(+)-binding	Antioxidant, antistress, detoxification	0.66
PITG_17346	Conserved hypothetical protein with rossmann-fold NAD(P)($^{+}$)-binding	Antioxidant, antistress, detoxification	0.62
PITG_17406	Enoyl-coA hydratase, mitochondrial precursor	Fatty acid transport and metabolism	0.51
PITG_17445	Glycerol kinase 1	Carbohydrate transportation and metabolism	0.34
PITG_17452	Importin alpha-2 subunit	Protein transportation and metabolism	0.00
PITG_17507	Glucosylceramidase	Carbohydrate transport and metabolism	1.63
PITG_17516	S-adenosylmethionine synthetase 2	Amino acid transport and metabolism	0.48
PITG_17607	Elongation factor Ts	Protein transportation and metabolism	0.79
PITG_17716	Voltage-dependent anion-selective channel protein	Ion, cation, sugar, or macromolecule trafficking	0.52
PITG_17717	Nuclear migration protein NUDC	Ion, cation, sugar, or macromolecule trafficking	0.73
PITG_17753	NADP-dependent malic enzyme	Fatty acid transport and metabolism	0.37

Table 3.6. continued

PITG_17778	Calcium/calmodulin-dependent protein kinase II	Translation regulation, post translational modification, protein folding	0.46
PITG_17786	Argininosuccinate lyase	Amino acid transport and metabolism	0.48
PITG_17787	Arsenite-Antimonite (ArsAB) Efflux Family	Ion, cation, sugar, or macromolecule trafficking	0.35
PITG_17908	Urease accessory protein ureg	Ion, cation, sugar, or macromolecule trafficking	0.00
PITG_17919	P-type ATPase (P-ATPase) Superfamily	Ion, cation, sugar, or macromolecule trafficking	0.38
PITG_17921	P-type ATPase (P-ATPase) Superfamily	Ion, cation, sugar, or macromolecule trafficking	0.69
PITG_17958	Heme/steroid binding domain-containing protein	Lipid transport and metabolism	0.41
PITG_17983	Adenylosuccinate lyase	DNA/nucleotide metabolism and repair	0.27
PITG_17993	Conserved hypothetical protein, GTP cyclohydrolase II (RibA)	Antioxidant, antistress, detoxification	0.54
PITG_17995	Conserved hypothetical protein with armadillo/beta-catenin-like repeats	Protein transportation and metabolism	0.53
PITG_18025	Fatty acid synthase subunit alpha	Fatty acid transport and metabolism	0.35
PITG_18048	Aconitate hydratase, mitochondrial precursor	Carbohydrate transportation and metabolism	0.35
PITG_18052	60S ribosomal protein L3	Protein transportation and metabolism	0.51
PITG_18053	Dolichyl-diphosphooligosaccharide-protein glycosyltransferase subunit	Protein transportation and metabolism	0.25
PITG_18054	50S ribosomal protein L7/L12	Protein transportation and metabolism	0.49
PITG_18100	Conserved hypothetical protein	Unknown	0.57
PITG_18104	Conserved hypothetical protein with RNA binding motif	mRNA processing and transcription regulation	0.31
PITG_18119	Conserved hypothetical protein with PAN/APPLE-like domains	Protein transportation and metabolism	0.48
PITG_18161	Conserved hypothetical protein with TAP42-like domain	Cell cycle, cell growthth and cell proliferation	0.51
PITG_18164	Conserved hypothetical protein with TAP42-like domain	Cell cycle, cell growthth and cell proliferation	0.86

Table 3.6. continued

PITG_18187	Sulfite reductase [NADPH] subunit beta	Amino acid transport and metabolism	0.33
PITG_18305	Conserved hypothetical protein	Unknown	0.94
PITG_18306	Conserved hypothetical protein	Unknown	1.14
PITG_18312	Conserved hypothetical protein	Unknown	0.93
PITG_18316	Phospholipid hydroperoxide glutathione peroxidase	Antioxidant, antistress, detoxification	0.61
PITG_18317	Phospholipid hydroperoxide glutathione peroxidase	Antioxidant, antistress, detoxification	0.40
PITG_18334	Alcohol dehydrogenase	Carbohydrate transportation and metabolism	0.44
PITG_18354	Succinate dehydrogenase flavoprotein subunit, mitochondrial precursor	Carbohydrate transport and metabolism	0.34
PITG_18375	UDP-glucose 6-dehydrogenase	Carbohydrate transport and metabolism	0.40
PITG_18392	T-complex protein 1 subunit beta	Translation regulation, post translational modification, protein folding	0.38
PITG_18414	Phosphoglucomutase	Carbohydrate transport and metabolism	0.39
PITG_18420	Protein kinase	Signal transduction	0.35
PITG_18446	26S protease regulatory subunit 6B	Protein transportation and metabolism	0.49
PITG_18497	Crinkler	Secreted or infection related protein	0.00
PITG_18546	Crinkler (CRN) family protein	Secreted or infection related protein	0.62
PITG_18554	Crinkler (CRN) family protein	Secreted or infection related protein	0.61
PITG_18650	Proteasomal ubiquitin receptor ADRM1-like protein	Protein transportation and metabolism	0.78
PITG_18706	Acetyl-coA carboxylase	Fatty acid transport and metabolism	0.41
PITG_18707	Glycerol-3-phosphate O-acyltransferase	Fatty acid transport and metabolism	0.45
PITG_18718	GTP-binding nuclear protein spi1	Protein transportation and metabolism	0.40
PITG_18720	ATP-citrate synthase	Carbohydrate transportation and metabolism	0.48
PITG_18731	26S proteasome non-ATPase regulatory subunit	Protein transportation and metabolism	0.34

Table 3.6. continued

PITG_18776	Cytochrome c1, mitochondrial precursor	Ion, cation, sugar, or macromolecule trafficking	0.34
PITG_18821	Crinkler (CRN) family protein	Secreted or infection related protein	0.41
PITG_18847	Crinkler (CRN) family protein	Secreted or infection related protein	0.47
PITG_18934	Calreticulin precursor	Translation regulation, post translational modification, protein folding	0.52
PITG_18991	Conserved hypothetical protein with selenoprotein domain	Antioxidant, antistress, detoxification	0.43
PITG_18998	tRNA nucleotidyltransferase	Protein transportation and metabolism	0.00
PITG_19008	Nascent polypeptide-associated complex subunit alpha-like protein	Protein transportation and metabolism	0.34
PITG_19017	14-3-3 protein epsilon	Signal transduction	0.46
PITG_19054	Peroxisomal multifunctional enzyme	Fatty acid transport and metabolism	2.05
PITG_19121	60S ribosomal protein L10	Protein transportation and metabolism	0.38
PITG_19129	ATP-dependent RNA helicase EIF4a	mRNA processing and transcription regulation	0.44
PITG_19161	Pyruvate dehydrogenase E1 component subunit beta	Carbohydrate transportation and metabolism	0.41
PITG_19162	Alcohol dehydrogenase	Carbohydrate transportation and metabolism	1.63
PITG_19179	Mitochondrial import receptor subunit TOM70	Protein transportation and metabolism	0.75
PITG_19199	Arginine N-methyltransferase	Amino acid transport and metabolism	3.16
PITG_19234	Choline/Carnitine O-acyltransferase	Fatty acid transport and metabolism	0.38
PITG_19247	Atlastin-like protein	Cytoskeleton	0.58
PITG_19281	ATP-binding cassette sub-family E member 1	Lipid transport and metabolism	0.32
PITG_19282	Conserved hypothetical protein similar to mitochondrial NADH:ubiquinone oxidoreductase 32 kDa subunit	Carbohydrate transport and metabolism	0.42
PITG_19300	Conserved hypothetical protein	Unknown	0.89
PITG_19320	Crinkler (CRN) family protein	Secreted or infection related protein	0.42

Table 3.6. continued

PITG_19373	Crinkler (CRN) family protein	Secreted or infection related protein	0.70
PITG_19394	Crinkler (CRN) family protein	Secreted or infection related protein	0.70
PITG_19531	50S ribosomal protein L25	Protein transportation and metabolism	0.33
PITG_19537	Calnexin	Translation regulation, post translational modification, protein folding	0.43
PITG_19551	Conserved hypothetical protein with translation initiation factor EIF3 subunit motif	Protein transportation and metabolism	0.38
PITG_19557	Putative dolichyl-diphosphooligosaccharide-protein glycosyltransferase 48kDa subunit	Translation regulation, post translational modification, protein folding	0.57
PITG_19579	Crinkler (CRN) family protein	Secreted or infection related protein	0.38
PITG_19690	Conserved hypothetical protein with biotin-requiring enzyme domain	Carbohydrate transportation and metabolism	0.34
PITG_19814	Conserved hypothetical protein	Unknown	0.44
PITG_19851	Myb-like DNA-binding protein	mRNA processing and transcription regulation	0.44
PITG_19854	Conserved hypothetical protein	Unknown	0.70
PITG_19871	Cell division control protein 48	Cell cycle, cell growthth and cell proliferation	0.38
PITG_19877	Guanylate-binding protein, GTPase activity	Signal transduction	0.00
PITG_19999	40S ribosomal protein S14	Protein transportation and metabolism	0.39
PITG_20170	Crinkler (CRN) family protein	Secreted or infection related protein	0.43
PITG_20171	Crinkler (CRN) family protein	Secreted or infection related protein	0.41
PITG_20172	Crinkler (CRN) family protein	Secreted or infection related protein	0.44
PITG_20188	60S ribosomal protein L5	Protein transportation and metabolism	0.50
PITG_20264	40S ribosomal protein S13	Protein transportation and metabolism	0.35
PITG_20384	Conserved hypothetical protein	Unknown	0.41
PITG_20388	Conserved hypothetical protein	Unknown	0.63
PITG_20463	Vacuolar protein sorting-associated protein 33A	Protein transportation and metabolism	0.00
PITG_20465	Fructokinase	Carbohydrate transport and metabolism	0.43
PITG_20585	Ahpc/TSA family Redoxin	Antioxidant, antistress, detoxification	0.35

Table 3.6. continued

PITG_20607	Phosphoenolpyruvate carboxykinase	Carbohydrate transportation and metabolism	0.50
PITG_20689	Eukaryotic translation initiation factor 3 subunit H	Protein transportation and metabolism	0.00
PITG_20718	Conserved hypothetical protein	Unknown	0.53
PITG_20743	Nuclear transport factor	Ion, cation, sugar, or macromolecule trafficking	0.49
PITG_20775	Adenylate kinase	DNA/nucleotide metabolism and repair	0.42
PITG_20790	DEAD/DEAH box RNA helicase	mRNA processing and transcription regulation	0.00
PITG_20795	Ribosomal protein	Protein transportation and metabolism	0.27
PITG_20824	Aspartyl-tRNA synthetase	Protein transportation and metabolism	0.33
PITG_20849	Alcohol dehydrogenase	Carbohydrate transport and metabolism	0.64
PITG_20901	Voltage-dependent anion-selective channel protein	Ion, cation, sugar, or macromolecule trafficking	0.60
PITG_20970	Triosephosphate isomerase/glyceraldehyde-3-phosphate dehydrogenase	Carbohydrate transportation and metabolism	0.35
PITG_20994	Conserved hypothetical protein with argininosuccinate lyase	Amino acid transport and metabolism	0.00
PITG_21033	Conserved hypothetical protein with monooxygenase domain	Antioxidant, antistress, detoxification	0.45
PITG_21071	Threonyl-tRNA synthetase	Protein transportation and metabolism	0.65
PITG_21128	Succinyl coA transferase	Carbohydrate transport and metabolism	0.41
PITG_21151	Annexin	Lipid transport and metabolism	0.49
PITG_21153	Hypothetical protein	Unknown	0.37
PITG_21182	Apoptosis-inducing factor 1	Antioxidant, antistress, detoxification	0.61
PITG_21186	Conserved hypothetical protein	Unknown	0.91
PITG_21277	Conserved hypothetical protein	Carbohydrate transport and metabolism	0.85
PITG_21295	NADH:Flavin oxidoreductase	Antioxidant, antistress, detoxification	0.34
PITG_21378	Protein disulfide-isomerase	Translation regulation, post translational modification, protein folding	0.47
PITG_21393	Eukaryotic translation initiation factor 3 subunit A	Protein transportation and metabolism	0.45
PITG_21398	DEAD/DEAH box RNA helicase	mRNA processing and transcription regulation	0.26

Table 3.6. continued

PITG_21410	Elicitin-like protein INF4	Secreted or infection related protein	0.00
PITG_21488	Annexin	Lipid transport and metabolism	0.45
PITG_21568	Histone H1	mRNA processing and transcription regulation	0.69
PITG_21620	Fumarylacetoacetate (FAA) hydrolase	Amino acid transport and metabolism	0.49
PITG_21806	Fumarylacetoacetase	Amino acid transport and metabolism	0.46
PITG_21963	Crinkler (CRN) family protein	Secreted or infection related protein	0.48
PITG_22103	Triosephosphate isomerase/glyceraldehyde-3-phosphate dehydrogenase	Carbohydrate transportation and metabolism	0.37
PITG_22135	60S ribosomal protein l10a-1	Protein transportation and metabolism	0.46
PITG_22200	Conserved hypothetical protein with Proteasome activator pa28 beta subunit	Protein transportation and metabolism	0.57
PITG_22265	NADH:Flavin oxidoreductase	Antioxidant, antistress, detoxification	0.96
PITG_22286	Crinkler (CRN) family protein	Secreted or infection related protein	0.49
PITG_22406	Conserved hypothetical protein	Unknown	1.08
PITG_22434	Polyadenylate-binding protein	mRNA processing and transcription regulation	0.36
PITG_22568	Nuclease	DNA/nucleotide metabolism and repair	0.40
PITG_22657	Elongation factor 1-alpha	Protein transportation and metabolism	0.32
PITG_22743	Dihydrolipoyllysine-residue succinyltransferase component of 2-oxoglutarate dehydrogenase complex	Carbohydrate transportation and metabolism	0.00
PITG_22839	Nuclear mitotic apparatus protein	Cell cycle, cell growthth and cell proliferation	0.00
PITG_22958	Conserved hypothetical proteinwith ZPR1 zinc finger domain	Ribosomal process	0.00
PITG_23158	Isocitrate dehydrogenase	Carbohydrate transportation and metabolism	0.43
PITG_23164	Crinkler (CRN) family protein	Secreted or infection related protein	0.48
PITG_23283	Conserved hypothetical protein with Crinkler (CRN) domain	Secreted or infection related protein	0.38

References

Ah-Fong, A. M., C. A. Bormann-Chung, and H. S. Judelson (2008). "Optimization of transgene-mediated silencing in *Phytophthora infestans* and its association with small-interfering RNAs." Fungal Genet Biol **45**: 1197-205.

Ahmad, Y., F.-M. Boisvert, P. Gregor, A. Cobley, A. I. Lamond (2009). "NOPdb: Nucleolar Proteome Database--2008 update." Nucl Acids Res **37**: D181-184.

Andersson, B., M. Sandstrom, and A. Strömberg (1998). "Indications of soil borne inoculum of *Phytophthora infestans*." Potato Res **41**: 305-310.

Ann, P. J. and W. H. Ko (1987). "Induction of Oospore Germination of *Phytophthora parasitica*." Phytopathology **78**: 335-338.

Avrova, A. O., E. Venter, P. R. Birch, and S. C. Whisson (2003). "Profiling and quantifying differential gene transcription in *Phytophthora infestans* prior to and during the early stages of potato infection." Fungal Genet and Biol **40**: 4-14.

Baudouin-Cornu, P., G. Lagniel, S. Chedin, J. Labarre (2009). "Development of a new method for absolute protein quantification on 2-D gels." Proteomics **9**: 4606-4615.

Beakes, G. W. and S. Bartnicki-Garcia (1989). "Ultrastructure of mature oogonium-oospore wall complexes in *Phytophthora megasperma*: a comparison of *in vivo* and *in vitro* dissolution of the oospore wall." Mycol Res **93**: 321-334.

Beakes, G. W., Z. A. El-Hamalawi, and D. C. Erwin (1986). "Ultrastructure of mature oospores of *Phytophthora megasperma* f.sp. *medicaginis*: Preparation protocols and effects of MTT vital staining and permanganate pre-treatment." Trans Br Mycol Soc **86**: 195-206.

Beakes, G. W. and J. L. Gay (1978). "Light and electron microscopy of oospore maturation in *Saprolegnia furcata*: I. Cytoplasmic changes." Trans Br Mycol Soc **71**: 11-24.

Bhadauria, V., S. Banniza, L. X. Wang, Y. D. Wei, and Y. L. Peng (2010). "Proteomic studies of phytopathogenic fungi, oomycetes and their interactions with hosts." Eur J Plant Pathol **126**: 81-95.

Bohmer, M., T. Colby, C. Bohmer, A. Brautigam, J. Schmidt, and M. Bolker (2007). "Proteomic analysis of dimorphic transition in the phytopathogenic fungus *Ustilago maydis*." Proteomics **7**: 675-685.

Brasier, C. M. (1992). "Evolutionary biology of *Phytophthora* Part I. Genetic system sexuality and the generation of variation." Annu Rev Phytopathol **30**: 153-171.

Bruce, C. R., P. van West, and L. J. Grenville-Briggs (2006). "Proteomic studies of plant-pathogenic oomycetes and fungi." Methods Biochem Anal **49**: 271-283.

Chang, T. T. and W. H. Ko (1991). "Factors affecting germination of oospores of *Phytophthora infestans*." J Phytopathol **133**: 29-35.

Dou, D., S. D. Kale, X. Wang, R. H. Y. Jiang, N. A. Bruce, F. D. Arredondo, et al. (2008). "RXLR-Mediated entry of *Phytophthora sojae* effector Avr1b into soybean cells does not require pathogen-encoded machinery." Plant Cell **20**: 1930-1947.

Drenth, A., E. M. Janssen, and F. Govers (1995). "Formation and survival of oospores of *Phytophthora infestans* under natural conditions." Plant Pathol **44**: 86-94.

Ebstrup, T., G. Saalbach, and H. Egsgaard (2005). "A proteomics study of in vitro cyst germination and appressoria formation in *Phytophthora infestans*." Proteomics **5**: 2839-2848.

Elliott, C. G. (1983). Physiology of sexual reproduction in *Phytophthora*. Phytophthora, its Biology, Taxonomy, Ecology, and Pathology, APS Press**:** 71-80.

Flier, W. G., L. P. N. M. Kroon, A. Hermansen, H. M. G. van Raaij, B. Speiser, L. Tamm, et al. (2007). "Genetic struture and pathogenicity of populations of *Phytophthora infestans* from organic potato crops in France, Norway, Switzerland, and the United Kingdom." Plant Pathol **56**: 562-572.

Fox, N. C., J. G. Coniglio, and F. T. Wolf (1983). "Lipid composition and metabolism in oospores and oospheres of *Achlya americana*." Exp Mycol **7**: 216-226.

Fukutomi, M., S. Akai, and M. Shiraishi (1971). "Fine structure of antheridia and oogonia of *Phytophthora macrospora*, the downy mildew fungus of rice plants." Mycopathologia **43**: 249-258.

Grenville-Briggs, L. J. (2005). "Elevated amino acid biosynthesis in *Phytophthora infestans* during appressorium formation and potato infection." Fungal Genet Biol **42**: 244-256.

Haas, B. J., S. Kamoun, M. C. Zody, R. H. Y. Jiang, R. E. Handsaker, L. M. Cano, et al. (2009). "Genome sequence and analysis of the Irish potato famine pathogen *Phytophthora infestans*." Nature **461**: 393-398.

Islam, M. A., R. N. Sturrock, and A. K. Ekramoddoullah (2008). "A proteomics approach to identify proteins differentially expressed in Douglas-fir seedlings infected by *Phellinus sulphurascens*." J Proteomics **71**: 425-438.

Jiang, J., L. W. Stephenson, D. C. Erwin, and J. V. Leary (1989). "Nuclear changes in *Phytophthora* during oospore maturation and germination." Mycol Res **92**: 463-469.

Jiang, R. H. Y., B. M. Tyler, and F. Govers (2006). "Comparative analysis of *Phytophthora* genes encoding secreted proteins reveals conserved synteny and lineage-Specific gene duplications and deletions." Mol Plant Microbe Interact **19**: 1311-1321.

Judelson, H. S., B. M. Tyler, and R. W. Michelmore (1991). "Transformation of the oomycete pathogen, *Phytophthora infestans*." Mol Plant Microbe Interact **4**: 602-607.

Kawamura, Y., S. Hase, S. Takenaka, Y. Kanayama, H, Yoshioka, S. Kamoun, et al. (2009). "INF1 elicitin activates jasmonic acid- and ethylene-mediated singalling pathways and induces resistance of bacterial wilt disase in tomato." J Phytopathol **157**: 287-297

Kleinschmidt, M. A., G. Streubel, B. Samans, M. Krause, and U. Bauer (2008). "The protein arginine methyltransferases CARM1 and PRMT1 cooperate in gene regulation." Nucleic Acids Res **36**: 3202-3213.

Kunau, W. H., V. Dommes, and H. Schulz (1995). "β-Oxidation of fatty acids in mitochondria, peroxisomes, and bacteria: a century of continued progress." Prog Lipid Res **34**: 267–342

Link, A. J., J. Eng, D. M. Schieltz, E. Carmack, G. J. Mize, D. R. Morris, et al. (1999). "Direct analysis of protein complexes using mass spectrometry." Nat Biotech **17**: 676-682.

Lippman, E., D. C. Erwin, and S. Bartnicki-Garcia (1974). "Isolation of chemical composition of oospore-oogonium walls of *Phytophthora megasperma* var. *sojae*." J Gen Microbiol **80**: 131-141.

Medina, M. L., P. A. Haynes, L. Breci, and W. A. Francisco (2005). "Analysis of secreted proteins from *Aspergillus flav*us." Proteomics **5**: 3153-3161.

Medina, M. V. and H. W. Platt (1999). "Viability of oospores of *Phytophthora infestans* under field conditions in northeastern North America." Can J Plant Pathol **21**: 137-143.

Miike, K., M. Aoki, Y. Ryo, T. Yumiko, S. Hideyuki, M. Teruhisa, et al. (2010). "Proteome profiling reveals gender differences in the composition of human serum." Proteomics **10**: 2678-2691.

O'Brien, R. N., Z. Shen, T. Kiyoshi, P. J. Lee, S. P. Briggs (2010). "Quantitative proteome analysis of pluripotent cells by iTRAQ mass tagging reveals post-transcriptional regulation of proteins required for ES cell self-renewal." Mol Cell Proteomics **9**(5) Epub

Pittis, J. E. and R. C. Shattock (1994). "Viability, germination and infection potential of oospores of *Phytophthora infestans*." Plant Pathol **43**: 387-396.

Poirier, Y., Y. D. Antonenkov, T. Glumoff, and J. K. Hiltunen (2006). "Peroxisomal β-oxidation—a metabolic pathway with multiple functions." Biochim Biophys Acta **1763**: 1413–1426

Prakob, W. and H. S. Judelson (2007). "Gene expression during oosporogenesis in heterothallic and homothallic *Phytophthora*." Fungal Genet Biol **44**: 726-739.

Ruben, D. M. and M. E. Stanghellini (1978). "Ultrastructure of oospore germination in *Pythium aphanidermatum*." Am J Bot **65**: 491-501.

Ruben, D. M., Z. R. Frank, I. Chet, and D. Sklan (1981). "Changes in the chemical composition of oospores of *Pythium aphanidermatum* during bimodal germination." Can J Microbiol **27**: 536-543.

Savidor, A., R. S. Donahoo, O. Hurtado-Gonzales, M. L. Land, M. B. Shah, K. H. Lamour, et al. (2008). "Cross-species global proteomics reveals conserved and unique processes in *Phytophthora sojae* and *Phytophthora ramorum*." Mol Cell Proteomics **7**: 1501-1516.

Shan, W. X., J. S. Marshall, and A. R. Hardham (2004). "Gene expression in germinated cysts of *Phytophthora nicotianae*." Mol Plant Pathol **5**: 317-330.

Shepherd, S. J., P. van West, and N. A. R. Gow (2003). "Proteomic analysis of asexual development of *Phytophthora palmivora*." Mycol Res **107**: 395-400.

Smirnov, A. N., S. A. Kuznetsov, N. Y. Kvasnyuk, and K. L. Deahl (2008). "Formation and germination of *Phytophthora infestans* oospores in different regions of Russia." Commun Agric Appl Biol Sci **73**: 109-118.

Sutherland, E. D. and S. D. Cohen (1983). "Evaluation of tetrazolium bromide as a vital stain for fungal oospores." Phytopathology **73**: 1532-1535.

Zahedi, R. P., C. Meisinger, and A. Sickmann (2005). "Two-dimensional benzyldimethyl-n-hexadecylammonium chloride/SDS-PAGE for membrane proteomics." Proteomics **5**: 3581-3588.

Conclusions

Oomycetes are a large collection of species that include important pathogens of plants, vertebrates, insects, fish and microbes. The most important morphological feature of the group is the production of sexual spores, oospores, by the union of two gametangia, the oogonium and antheridium, in which meiosis occurs before fertilization (Erwin & Ribeiro, 1996). Unlike true fungi, oomycetes are diploid during the vegetative stage while true fungi are haploid. The cell wall of oomycetes is primarily composed of cellulose instead of chitin, and generally does not have septations. Oomycota and fungi also have different metabolic pathways for synthesizing a number of enzymes, distinct rRNA sequences, storage compounds and ultra structural characteristics (Bartnicki-Garcia & Wang, 1983; Alexopoulos et al., 1996; Forster et al., 2000).

The genus *Phytophthora,* the "plant destroyer", is one of the most important groups in the oomycetes. In *Phytophthora*, *P. infestans* is the most notorious plant pathogen. Though it was the first member identified in the oomycete group, and although many studies have been done on its physiology and morphology (Lucas et al., 1991; Erwin & Ribeiro, 1996), knowledge of the molecular biology, genetics, and regulatory pathways are still very much lacking compared to many of the true fungi. Even less is known about its featured structure, the oospore.

In order to better understand sexual reproduction in *P. infestans* at the molecular and biochemical level, it is essential to acquire information on gene expression regulation mechanisms, and protein composition and interactions. This knowledge would lead us to an improved understanding of the pathway components and necessary factors to enter and

manipulate the sexual stage, in order to design improved specific strategies to combat this pathogen. For example, since *pum* seems to be essential for the mating process in our silencing study, if a chemical is developed to target this gene, then the sexual reproduction is very likely to be interrupted. Another potential target would be the oospore wall degradating enzymes. If some systematic pesticide is able to abort the synthesis of these enzymes, the oospores may never germinate because the germ tubes cannot be produced. These would be beneficial to the regions where oospores serve as primary inoculums and delay or limit the diease epidemics.

The research presented in this dissertation focuses on the regulation of gene expression and the proteomics of the sexual reproduction stage. It provides valuable knowledge that will contribute to unraveling the signaling network involved in the mating process of *P. infestans.*

Chapter I describes the characterization of the transcriptional regulatory components in the promoters of two mating-induced genes, PITG_02525 and PITG_00483. Studies within this chapter provided information on the transcriptional regulation of mating-induced genes and will eventually help in revealing inducers or repressors of the signaling pathway cascades during *P. infestans* sexual reproduction.

PITG_02525 encodes an elicitin-like protein whose expression was only detected during the mating stage and might possess sterol/lipid binding function, and gene PITG_00483 was identified as pumilio, an RNA-binding protein that functions as a post-transcriptional repressor, which is induced both during asexual sporulation and oosporogenesis. To identify the *cis*-elements regulating the temporal and spatial

expression of these genes, sequentially deleted promoters were fused with a β-glucuronidase (GUS) reporter gene to study their GUS activity. Full length PITG_02525 promoter had mating structure-specific expression. All the 5' and 3' promoter deletion analysis increased the expression eventually to constitutive, unless its 24 nt core promoter region (transcription start site (TSS), flanking promoter region (FPR), SAAS (Roy & Judelson, unpublished)) was removed. This indicated that the expression of this gene is usually being repressed under normal conditions and some repressor element(s) is regulating the transcription. A potential repressor element (TCTTCTAA) was then fused with a sporulating specific chimeric construct. However, the motif did not appear to be able to suppress transcription in this setting. It is possible that downstream elements or the proper context within the promoter are needed to interact with the motif to accomplish the suppression.

The PITG_00483 promoter was more complicated. While its full length promoter exhibited the same patterns during mating as PITG_02525's, it also conferred expression during asexual sporulation. Deletion analysis suggested the presence of an activator located around 200 bp upstream of ATG. The GUS reporter expression was almost completely diminished after the removal of this element. The activating function of this motif needs to be confirmed in the future by fusing it in front of the Nifs minimal promoter and GUS to see if GUS expression is induced. Interestingly, further deletions turned expression pattern back to constitutive. It is very possible that the gene may have switched its transcription start site to compensate the loss of the activator. A 5'RACE experiment could be done to confirm this structure change. Inr and FPR elements did not

reside immediately downstream of the TSS, but at 60 bp upstream of it. Interestingly, Inr and FPR still seemed to be critical for expression even they were not around TSS. A region of sequence containing Inr, FPR and the TSS was cloned into the Nifs-minimal promoter and proved to be the essential region for the expression of the gene during sporulation, but not mating. Maybe the upstream potential activator can be added to the construct later to test if the mating-associated expression could be resumed. EMSA (electrophoresis mobility shift assay) can be employed to confirm the transcription factor binding activity of the core promoter elements identified.

Chapter II focuses on developing tools for protein interaction assays using the Pum RNA-binding-domain (RBD). The system will provide valuable tools for future studies of protein interactions in *P. infestans* and was designed with an option for either N or C terminus tagging. The *in vitro* binding assay was performed as binding maltose-tagged RBD and total RNA *in vitro*, and then the purified RNA was attempted to be recovered by differential display method and cDNA library construction. A tandem affinity purification (TAP) tag was designed according to *P. infestans* codon bias and fused at the C-terminus of the RBD, under the control of the native pumilio promoter. The system successfully purified RBD and a potential binding partner from the affinity columns. Future work could be focused on purification of the RNA that is bound to Pum RBD and further characterization of the regulatory pathways that Pum is involved.

To directly observe the loss of function phenotype of *pum*, constructs for producing silencing mutants were generated and transformed into *P. infestans*. However, no stable transformants with silenced *pum* could be generated, so *pum* could be essential

of *P. infestans*. As discussed previously in Chapter II, an inducible promoter system could be adapted to study the function of the gene without completely silencing it.

Chapter III presents a global protein profiling study comparing the proteomes of oospores and nonsporulating hyphae (NSH) to identify proteins that are potentially important for oospore germination. This is the first large scale proteomics study done to understand the biology of oospores at the protein level. Proteins extracted from oospores and NSH of mating type A1 and A2 were analyzed by multidimensional protein identification technology (MuDPIT), and iTRAQ labeling was used for protein quantification. A total of 1115 proteins were identified in NSH and 959 in oospores. Among them, 202 proteins were unique to NSH and 44 proteins were unique to oospores. Besides these 44 oospore specific genes, our study also revealed that many proteins or protein functional groups that are important to germination were more abundant in oospores, such as carbohydrate and fatty acid oxidation enzymes for immediate energy production, and antioxidant and anti-stress proteins for protecting the fragile germ tubes, as well as secreted proteins that could be involved in infecting the host. After identifying stage-specific proteins or proteins that are significantly more concentrated in oospores than in hyphae, selected proteins could be subjected to detailed studies to confirm their presence by Western analysis. Some of the genes that encode these proteins could be tested by loss of function analysis.

In conclusion, the research in this dissertation focuses on the biology and biochemical composition of the sexual spores of *P. infestans*, the oospores. This information can provide insights into the control of gene expression during

oosporogenesis, and allow the manipulation of the specific molecular components that are important for oospore germination to disrupt the pathogen's life cycle. With the increased information accumulated on this pathogen, environmental friendly control strategies will hopefully soon be developed to reduce the ecological and economic losses due to *P. infestans*.

Reference:

Alexopoulos, C. J., C. W. Mims, and M. Blackwell (1996). Introductory Mycology. Wiley, New York.

Bartnicki-Garcia, S. and M. C. Wang (1983). Biochemical aspects of morphogenesis in *Phytophthora*. *Phytophthora*, its biology, taxonomy, ecology, and pathology. D. C. Erwin, S. Bartnicki-Garcia and P. H. Tsao. St. Paul, Minnesota, APS Press**:** 121-137.

Erwin, D. C. and O. K. Ribeiro (1996). *Phytophthora* diseases worldwide. American Phytopathological Society.

Forster, H., M. P. Cummings, and M. D. Coffey (2000). "Phylogenetic relationships of *Phytophthora* species based on ribosomal ITS1 DNA sequence analysis with emhpasis on Waterhouse groups V and VI." Mycol Res **104**: 1055-1061.

Lucas, J. A., R. C. Shattock, D. S. Shaw, and L. R. Cooke (1991). *Phytophthora*. Cambridge, Press Syndicate of the University of Cambridge.